JULY 2017

Ph. D. in Civil Engineering

YAHYA RESAN ATEWI

UNIVERSITY OF GAZİANTEP
GRADUATE SCHOOL OF
NATURAL AND APPLIED SCIENCES

PROPERTIES OF GLASS FIBER REINFORCED SCC AND STRUCTURAL PERFORMANCE OF SHORT COMPOSITE COLUMNS HAVING SUCH CONCRETE CORE

Ph. D. THESIS
IN
CIVIL ENGINEERING

BY
YAHYA RESAN ATEWI
JULY 2017

Properties of Glass Fiber Reinforced SCC and Structural Performance of Short Composite Columns having such Concrete Core

Ph. D. Thesis
in
Civil Engineering
University of Gaziantep

Supervisor
Assoc. Prof. Dr. Esra METE GÜNEYİSİ

by
Yahya Resan ATEWI
July 2017

REPUBLIC OF TURKEY
UNIVERSITY OF GAZİANTEP
GRADUATE SCHOOL OF NATURAL & APPLIED SCIENCES
CIVIL ENGINEERING DEPARTMENT

Name of the thesis: Properties of Glass Fiber Reinforced SCC and Structural Performance of Short Composite Columns having such Concrete Core

Name of the student: Yahya Resan ATEWI
Exam date: July 10, 2017

Approval of the Graduate School of Natural and Applied Sciences.

Prof. Dr. A. Necmeddin YAZICI
Director

I certify that this thesis satisfies all the requirements as a thesis for the degree of Doctor of Philosophy.

Prof. Dr. Abdulkadir ÇEVİK
Head of Department

This is to certify that we have read this thesis and that in our opinion it is fully adequate, in scope and quality, as a thesis for the degree of Doctor of Philosophy.

Assoc. Prof. Dr. Esra METE GÜNEYİSİ
Supervisor

Examining Committee Members:	Signature
Prof. Dr. Hanifi ÇANAKCI	....
Assoc. Prof. Dr. Esra METE GÜNEYİSİ	....
Assoc. Prof. Dr. Kasım MERMERDAŞ	....
Asst. Prof. Dr. Hatice Öznur ÖZ	....
Asst. Prof. Dr. Ayşe Y. GÜNAL	....

I hereby declare that all information in this document has been obtained and presented in accordance with academic rules and ethical conduct. I also declare that, as required by these rules and conduct, I have fully cited and referenced all material and results that are not original to this work.

Yahya Resan ATEWI

ABSTRACT

PROPERTIES OF GLASS FIBER REINFORCED SCC AND STRUCTURAL PERFORMANCE OF SHORT COMPOSITE COLUMNS HAVING SUCH CONCRETE CORE

ATEWI, Yahya Resan

Ph. D. in Civil Engineering

Supervisor: Assoc. Prof. Dr. Esra METE GÜNEYİSİ

July 2017

149 pages

Research on the structural behavior of confined glass fiber reinforced self-compacting concrete (GFRSCC) in tubes as composite member is rare. Similarly, there is limited research on the use of glass fiber in such structural concrete. In this thesis, two scientific programs have been described in detail. To the first program, an experimental study was introduced to evaluate the behavior of GFRSCC. To this hope, a total of 15 fiber reinforced mixtures were designed at various nano silica contents. They were tested for the fresh and mechanical performances. The second phase of this thesis was interested in the structural performance of steel tubular column infilled with GFRSCC. For this, the engineering properties of the column were numerically investigated by considering three different diameter to wall thickness ratios and steel yield strengths. The experimental results on core concrete strength were employed to assess the performance of the columns in accordance to Eurocode 4, ACI, AIJ and DL/T codes. A total of 1080 different cases on the column strength were evaluated. It was concluded that the designed GFRSCC had satisfactory engineering performance. Additionally, the present numerical study showed that the codes predicted a proper capacity for the composite columns integrated GFRSCC.

Keywords: Composite column; Design code; Glass fiber; Nano silica; Self compacting concrete; Ultimate axial capacity

ÖZET

CAM FİBER TAKVİYELİ KYB'UN ÖZELLİKLERİ VE BU BETON KORA SAHİP KISA KOMPOZİT KOLONLARIN YAPISAL PERFORMANSI

ATEWI, Yahya Resan
Doktora Tezi, İnşaat Mühendisliği Bölümü
Tez Yöneticisi: Doç. Dr. Esra METE GÜNEYİSİ
Temmuz 2017
149 sayfa

Tüpler içerisine yerleştirilerek sargılanan cam fiber takviyeli kendiğinden yerleşen betonun (CFTKYB) yapısal davranışı üzerine yapılmış çalışmalar oldukça azdır. Benzer olarak, yapısal betonlarda cam fiber takviyesi de sınırlıdır. Bu tez kapsamında, iki bilimsel program detaylı olarak tanımlanmıştır. Birincisi, CFTKYB’un davranışını incelemek amacıyla deneysel çalışmalar yapılmıştır. Toplam 15 fiber takviyeli karışım farklı nano silika içeriğinde hazırlanmıştır. Bu karışımların taze ve mekanik performansları test edilmiştir. Tezin ikinci kısmında CFTKYB dolgulu çelik tüplerin yapısal performansları incelenmiştir. Kolonların mühendislik özellikleri, 3 farklı çap-cidar kalınlığı oranında ve çelik akma dayanımında kabul edilerek nümerik olarak değerlendirilmiştir. Beton çekirdek dayanımı üzerine yapılan deneysel çalışmalar, kolonların performansının Eurocode 4, ACI, AIJ ve DL/T standartlarına göre belirlenmesinde kulanılmıştır. Toplam 1080 farklı durum değerlendirilmiştir. Sonuç olarak, CFTKYB’nun tatmin edici mühendislik performansına sahip olduğu görülmüştür. Buna ek olarak, mevcut nümerik çalışma, tasarım yönetmeliklerinin bu yapısal betonlar ile entegre edilmiş kompozit kolonların kapasitelerini makul ölçüde tahmin ettiğini göstermiştir.

Anahtar Kelimeler: Kompozit kolon, Tasarım standartları, Cam fiber, Nano silika, Kendiliğinden yerleşen beton, Maksimum eksenel kapasite.

To my family…….

ACKNOWLEDGEMENTS

I am using this opportunity to express my gratitude and deepest appreciation to Assoc. Prof. Dr. Erhan GÜNEYİSİ, who is the main supervisor of the first six semesters of this thesis and Assoc. Prof. Dr. Esra METE GÜNEYİSİ, who is the primary supervisor of the following two semesters. In this regard, I am thankful for their aspiring guidance, invaluably constructive criticism, and friendly advice during the scientific work. I am honestly grateful to them for sharing their truthful and illuminating views on a number of matters related to my thesis.

I express my warm thanks to Assoc. Prof. Dr. Mehmet GESOĞLU, Assoc. Prof. Dr. Kasım MERMERDAŞ, Asst. Prof. Dr. Hatice Öznur ÖZ, Prof. Dr. Hanifi ÇANAKÇI and Asst. Prof. Dr. Ayşe Y. GÜNAL, for their support, guidance, and suggestions to improve thesis quality.

I would like to extend my thanks to my friends for their precious helps in experimental phase of the study and my sincere thanks also goes to Res. Assist. Süleyman İPEK who gave access to the laboratory and research facilities. Without they precious support it would not be possible to conduct this research.

I would also like to express my very profound gratitude to my parents and to my wife and my daughters Zainab, Fatimah, and Zahra and to my brothers and sisters for providing me with unfailing support and continuous encouragement throughout my years of study and through the process of researching and writing this thesis. This accomplishment would not have been possible without them.

TABLE OF CONTENTS

Page

LIST OF TABLES

Page

LIST OF FIGURES

Page

LIST OF SYMBOLS/ABBREVIATIONS

$(EI)_{eff^2}$	Effective flexural stiffness of CFST
A_c	Cross-sectional area of the concrete specimen core
A_s	Cross sectional area of steel
N_{cr}	Euler buckling load of the pin-ended CFST column
N_{pIR}	Cross-section plastic resistance of the CFST column
f_c'	Compressive strength of concrete cylinders (150×300 mm),
f_{cu}	Compressive strength of 150 mm cube,
f_y	Yield stress of steel
$\bar{\lambda}$	Relative slenderness of the CFST column
A	Cross-sectional area of the sample
a	The notch depth of beam
A_{sc}	area of composite section
CFST	Concrete filled steel tube
D	Outer diameter of concrete filled steel tube
E_{c2}	Elastic modulus of concrete
E_s	Elastic modulus of steel
f_{ck}	Characteristic concrete strength
f_{flex}	Net flexural strength
f_{scy}	Nominal yielding strength of the composite section
g	Gravitational acceleration.
G_F	Fracture energy
HRWRA	High range water reducing admixture
l_{ch}	Characteristics length
m	Mass of individual pellet

N	Rotational speed
nS	Nano silica
P_{max}	Fracture load
SCC	Self compacting concrete
t	Thickness of steel tube
T	Torque
$T_{500\ mm}$	Time required to reach 500 mm slump-flow
U	The length of beam
V	The slope of the line
W	The depth of beam
X	Distance between loading points
Y	The intercept of the line with the torque axis
B	Angle of the disc's plane to normal
γ'	Shear rate
δ_s	The specified deflection of the beam
μ	Plastic viscosity
τ	Shear stress
τ_o	Yield stress
ξ	Confinement factor

CHAPTER 1

INTRODUCTION

1.1 General

In different structure kinds like multi-storey buildings, towers, tunnels and bridges, it is known that concrete is one of the most widely used structural product thought our world. It has superior workability, mechanical and durability properties. Besides, the use of concrete in building industry lessens the cost of construction projects. It has been the significant division of civil engineering substructure for the last century and well-designed concrete can likewise be a durable building material. However, the high weight of conventional concrete and high qualified workmanship accompanying the use of concrete restricts the utilization of conventional concrete in some structural elements. Due to this, recently there has been an effort to introduce new building materials possess special performance such as self-compacting concrete (SCC) to offer the requirements of the construction industry (Bentur et al., 2001; Kılıç, 2003; Kim et al., 2010).

SCC was first advanced in the early 1990s so as to develop new concretes having high durability. After that, investigators worked to establish methodologies for designing aspects comparable to normal concrete. In this regard, we can define SCC as a concrete which deform and resist segregation in its fresh state. Moreover, with the scope of SCC no vibration required to compact concrete during placing stage. Indeed, such type of smart concrete behaves to compact itself only as a result of its self-weight and is placed exactly totally whereas flowing in the sections. The presence of dense reinforcement bars in members represents an obstacle for casting concretes. The use of SCC gives a solution for such problems while SCC flows easily and files all holes. However, SCC can be produced with the same raw materials that those of conventional vibrated concrete. SCC needs too much quantity of superplasticizer so as to reduce water concrete and increase workability as much as possible. Moreover, SCC must envelope high content of powder to reduce the frictional effect of coarse aggregate. Additionally, viscosity agents normally used to enhance concrete viscosity. However, the requirements of SCC in terms of fresh and hardened properties remarkably depend on the mix design used (Okamura, 1997; Dehn et al., 2000).

The accelerated application of SCC in Europe was made possible partly because of the huge potential benefits derived from its use and partly a result of collaborative research in 1996 between academic and industry partners with funding supported from the European Union. Research developed the necessary know-how and information for SCC production, thus generating confidence to the user. For site and precast concrete work, SCC has now been projected with enthusiasm through the world. In the United State, SCC is still a relatively new technology that is well suited for precast application. Currently, the utilization of SCC is being strongly accepted in building sectors for the structural applications (Ho et al., 2001).

The mineral admixtures lower the expenditure in terms of SCC usage. The admixtures such as fly ash, limestone filler and slag can be harnessed to raise the concrete mix slump. For example to these materials, fly ash, which is a derivative of thermal power industrial units, is noted for its ability to enhance the mechanical features and resilience of concrete when utilized as a cementitious materials. The integration of fly ash also lowers the requirement for chemical admixtures to regulate the level of viscosity (Bilodeau et al., 1994).

This revelation was achieved through an investigation involving the utilization of nano-silica (nS) as a synthetic pozzolan to fortify the contact region. Nanotechnology has significantly spread its influence into the realm concrete related technology. Nanoparticles with a dimension measuring less than 100 nm have been observed to be most favourable for improving the durability of concrete. The durability of a hydrated structure of cement with nano scale pores is maintained through the plugging of these pores by nanoparticles. nS is an artificial manufactured item with sphere shaped particles in the size range of 1 to 50 nanometres. This product has been effectively introduced into Portland cement materials in a laboratory setting (Li, 2004).

Exhaustive investigations have revealed that the structural characteristics of concrete including compressive, flexural, impact and tensile strengths and ductility and durability are significantly enhanced with the utilization of fibers (RILEM TC 188-CSC, 2006; Alonso et al., 2008). Among the fibers, glass fibers (GF) come with the benefits of being cost-effective, light and highly resilient in terms of tensile strength. Studies have revealed that the curbing of shrinkage cracking and the enhancement of the flexural and tensile strength in structural members can be realized with the inclusion of these fibers (Barluenga and Hernández-Olivares, 2007; Mirza and Soroushian, 2002). The utilization of fibers also serves to control the tendency of concrete to bleed by raising its capacity for absorptivity (Khaleel et al., 2011). In order to increase the possible use of GF in structural operations, several studies have delved into the relationship between the fiber-fortified concrete and its performance properties (RILEM TC162-TDF, 2002; Pereira et al., 2004). It also worthy to notation that the addition of fibers to the mixture needs to be a gradual process and the total volume of the mixture and fiber merging is termed the size fraction (Vf). Moreover the content and aspect ratio (l/d) of the fiber as well as its mechanical properties govern the quality and performance of the end products. (Pereira et al., 2004).

As a summary, the stability of SCC can be improved by integrating supplementary cementing materials (SCMs), for instance, limestone powder, fly ash, slag and silica fume. The utilization of such SCMs provides significant reduction in the cement content; thus, higher cost and the side effect of extreme cement quantities such as heat stress and contraction can be avoided (Güneyisi and Gesoğlu, 2008). Using SCMs might offer bigger cohesiveness by enhancing the distribution of size and packing of the grain particle. However, recent investigators believe that the filling property and pozzolanic activity can remarkably be increased with small replacement level of nano-materials (i.e. nS) in compared to the use of conventional SCMs (Li, 2004; Qing et al., 2007). From the aforementioned information, nowadays, considerable research activities on the utilization of several nano-materials in different types of concrete for the structural purposes (except for SCC incorporating glass fiber) have been detected in the technical literature.

1.2 Composite buildings

The use of steel and concrete together is the most significant and commonly combination of building material in the construction industry. Like such strategies frequently encountered in high multi-storey constructions as well as bridges and factories projects. Composite members are designed such that the concrete and the structural steel shape act composed to resist axial compression and /or bending. It is well known that the cost of concrete lower than steel, thus in composite systems the concrete provides a cost saving for composite sections. The composite constructions are utilized to take the benefits of both concrete and steel properties; that is the following main advantages from the use of composite structures can be summarized as follows (Tao and Han, 2006; Lu et al., 2007):

- Faster construction and therefore rapid profit of the invested capital.
- More usable space area.
- High steel and concrete efficiency can be achieved as the steel joist is in tension and the reinforced concrete slab in compression.
- Enhanced the seismic resistance.
- Comparing to the steel structure, the composite members have higher stiffness and hence deflection and bending stress are slighter.
- For some types of composite members the formwork cost considerably lower than reinforced concrete construction.
- Decreases in the total weight of structure and thereby saving in foundation costs.

Typically, in multi-storey buildings the steel frame structure is utilized beside concrete, for instance, steel beam with concrete floor slab. The designers are progressively designing mixed building arrangements of steel and concrete to yield further effectual structural performance. Figure 1.1 indicates an impression of using composite construction for multi-storey building (Şamhâl, 2005).

Figure 1.1 A typical composite commercial building in London (Şamhâl, 2005)

During the 1980's, building with composite elements experienced a renaissance, yeilding in an abundance of different novel construction conceptions. Particular composite components, such as beam, column and slab are presented in Figure 1.2 (Şamhâl, 2005).

Composite girder Steel-beam composite slab or reinforced concrete	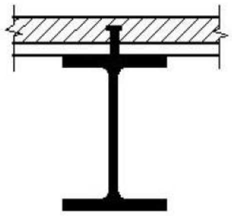
Composite column Steel profile embedded in or filled with concrete	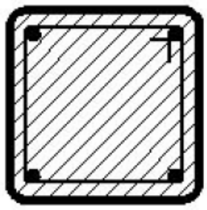
Composite slab Holorib, sheeting and concrete	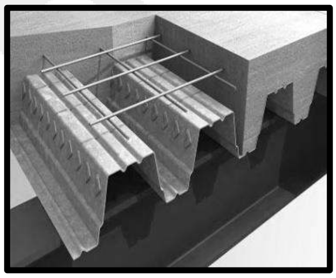

Figure 1.2 Composite structural elements in buildings (McGraw-Hill Concise Engineering, 2002; Şamhâl, 2005)

In general there are mainly two different kinds of composite column; steel-reinforcement concrete (SRC) column and concrete-filled steel tubular (CFST) column. The SRC column comprises of a steel section encased in unreinforced or reinforced concrete, as can be understood in Figure 1.3. The CFST column as presented in Figure 1.4 consist of a steel tube filled with concrete (Giakoumelis and Lam, 2004). CFST column is a compression member and usually they are used as load-bearing members in a composite framed structure. The CFST columns offer significant structural benefits such as; high fire resistances, high strength, favourable ability of energy absorption, favourable ductility, etc. (Han et al., 2014). Practically, the CFST column is favorable over the conventional reinforced concrete columns because the steel tube in the CFST column behaves as a formwork during the casting of concrete. The concrete inside the steel tube prevents the steel tube from locally buckling and at the same time the tube of CFST column improves the ductility of concrete by giving confinement and preventing concrete spalling. Moreover, the presence of high strength concrete and ultra-high strength concrete made the CFST column stronger and stiffer without the need to increase the cross section of the column (Elremaily and Azizinamini, 2002; Giakoumelis and Lam, 2004).

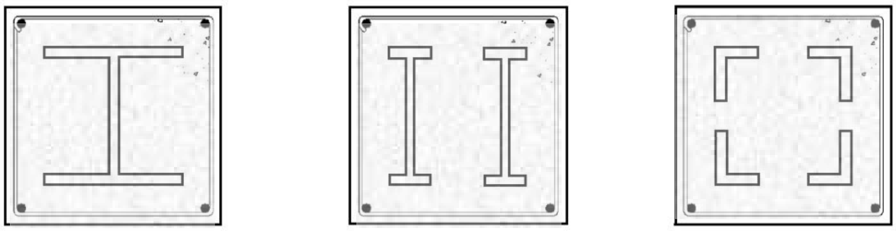

Figure 1.3 Steel-reinforcement concrete columns (Giakoumelis and Lam, 2004)

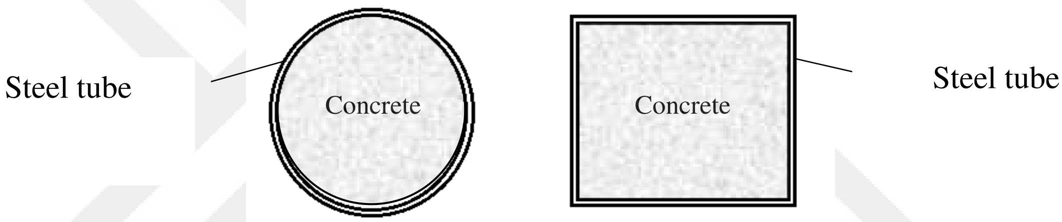

Figure 1.4 Concrete-filled steel tubular columns (Giakoumelis and Lam, 2004)

The use of CFST columns in building construction has been received a great attention in the recent years due to its superior structural performance. Normally, it was utilized in different composite frame constructions such as buildings, bridges, subway stations, workshops, electricity pylons and poles. For example, the CFST can be utilized as a composite member in various bridge structures as depicted in Figure 1.5 (Han et al., 2014).

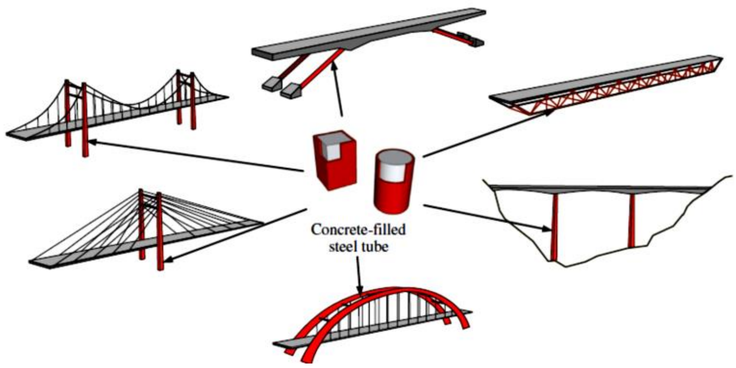

Figure 1.5 Using of CFST column in bridges (Han et al., 2014)

The concrete material inside CFST column is necessary to be of high quality as to increase ductility and strength of composite members, many type of in-fill materials were available to increase ductility of CFST columns. Typically, there are different fiber types can be used to achieve such purpose. This is due to the fact that the addition of fiber can enhance the ductility of fiber reinforced CFST column, increases the absorption energy capacity and delays the deformation of bulge. There are limited scientific researches about the incorporation of glass fiber in concrete-filled tubular members (Lu et al., 2014).

As we know, SCC is a new concrete type and there is a limited experience for its appropriate composition. In fact, there is a dearth of conformation concerning in-place properties and structure performance of SCC is one of the most barriers to recognition of SCC in the construction engineering (Khairallah, 2013). However, due to its favorable rheological properties, new structural applications can be realized and numerous benefits can be stated. In the particular case of CFST columns, the main benefit from a practical point of view in the utilization of SCC involves in employing the steel tube as a formwork to cast concrete without the need of vibration directly inside it. Besides the absence of vibration process, other factors such as dense reinforcement, complex sections, cost saving (i.e reduced labor cost) and environmental conditions encourage the use of SCC instead of ordinary concrete (Muciaccia et al., 2011). In the literature there are some research related to this issue, for example, Han et al. (2005) reported that the use of SCC yields several benefits over the vibrated concrete and it is especially beneficial for CFST columns. Therefore, from the above information it can be stated that the expected high performance of fiber reinforced self-compacting concrete filled steel tube structural member is a motivation for further investigations in this study.

1.3 Research objective

The first objective of this thesis was to make the performance assessment of glass fiber reinforced SCC (GFRSCC) incorporating nS. To achieve the purposes of the first stage, a comprehensive experimental program was conducted by designing a total of 15 mixtures considering five volume fractions for GF and three replacement levels of nS. The properties of GFRSCC with and without nS were examined through fresh and mechanical properties. The second aim of the present thesis was involved the numerical investigation of the structural responses of the composite CFST columns made with GF reinforced SCCs with and without nS under the action of compressive loading. To this objective, three diameter to thickness (D/t) ratios and three yield strengths of the steel tube were considered. A special procedure was adopted to take the benefit of compressive strength results of SCCs from the experimental work on the behavior of CFST column. The axial capacity of the composite columns were estimated and analyzed by using four design codes, namely, Eurocode 4 (EC4), American Concrete Institute (ACI), Japanese Code (AIJ) and Chines Design Code for Steel Concrete Composite Structures (DL/T). The findings from the investigation were discussed comparatively.

1.4 Structure of the thesis

The thesis includes 6 chapters. **Chapter 1** gives an introduction, composite structures and research objectives. **Chapter 2** illustrates a literature review and background which deals with the general information about SCC and GFRSCC as well as the recent study conducted on the SCC. The definition, classification and structural performance of the CFST column as well as the main differences between such composite column and conventional reinforced concrete column and its practical applications are depicted in the same chapter.

Chapter 3 presents in the first part the details of the experiments conducted to satisfy the objectives of current thesis. Materials properties used in the production of mixtures and test procedure are briefly presented. Thereafter, the part of the numerical study which comprises the design code procedures and formulas for calculating the ultimate capacity of the CFST columns having GFRSCC with and without nS are given in this chapter.

Chapter 4 demonstrates the results of experimental program. Moreover, the effect of experimental parameters on fresh and mechanical properties of compressive and split tensile strengths, modulus of elasticity and fracture properties are discussed through tables and figures.

Chapter 5 presents the results of analytical study to examine the behavior of GFRSCC filled steel tube short circular columns subjected to compressive load. The design provision of comparisons on the calculated axial capacity of such structural members were made by using of four international provisions of EC4, ACI, AIJ and DL/T.

Chapter 6 comprises the conclusions of the thesis.

CHAPTER 2

LITERATURE REVIEW AND BACKGROUND

2.1 Self-compacting concrete

New generation of tall and complicated composite building systems can be achieved by considering the latest development in the structural materials and elements, efficient design option, sustainability and construction techniques. In recent decades, there has been a significant interest in the development of new generation of structural concretes. One of these developments is self-compacting concretes (SCC). It is one of the newest innovations in concrete production and concrete engineering. SCCs are composed of mixes that possess properties that ensure compaction under their weight even without any additional treatment. In other words, they are capable of filling the formwork even without segregation and de- aeration. These products serve as suitable components for complex steel-concrete structure shapes (shapes with dense reinforcement). At the same time, the provided properties of such products allow for reducing installation time and further transportation time. Additionally, SCC is very well-suited for architectural projects that require a smooth surface for constructed elements (Shi, 2004).

SCC is responsible for the revolution of improving concrete quality in 1980's in Japan. This is because SCC treated the disadvantages of conventional concrete in terms of removing vibration process required to compact fresh concretes. (Okamura and Ouchi, 2003). SCC was first offered in the end of 1980s through Japanese researchers. SCC does not need any outside vibration for compaction, which flows under its own weight, and it has converted concrete placement. Although, it will not arise bleeding and segregation under own weight through regulated sections, and it has highly workable. This type of concrete must have to be low in yield value for attaining high flowability. On the other hand, an adequate viscosity is required for bleeding beside segregation resistance, in addition, should preserve the similarity through transportation. However, for having moderate structure performance besides long term durability can be obtained in SCC by placing and curing process. Good steadiness between stability besides deformation resistance caused to successful improvement (Aggarwal et al., 2008).

European federation dedicates to specialist construction chemicals, and concrete system abbreviates to EFNARC. According to this requirement, SCC defined as the construction of concrete for numerous decades has a highest innovative improvement. Generally, it was established to equipoise an increasing skilful work shortage. Thus, SCC materials have spatial requirements as per of EFNARC (2005), which include applications and compositions, and it's also suitable manual to contractors, concrete industrial, designer, and identifying authorities with trying administrations.

2.1.1. Development of structural SCC

Typically, SCC cannot be considered new. Some of construction works like applications under water need concrete to be placed without vibration, thus the use of SCC can serve such application. The SCC in its early form required high cement content. In this context, the use of high cement content yields system tend to shrike and generate high temperature during the first days of hydration process. The overall costs were very high and applications remained very limited.

The historical information about the SCC in 1990 revealed there is no much knowledge in Japan. This is because the commercial purposes of large corporations were used fundamental and practical of SCC in a secret situation. For example, NVC (non vibrated concrete) is one of the common commercial name of SCC in Japan (Beissel and Lim, 2001).

As the development of SCC in Japan proceeded, adopted scientific research was continued to optimize mix design and shaping of placing concrete under water by employing novel admixtures for producing SCC with proper performance matching the requirement of concrete industry in Japan (e.g. University of Paisley / Scotland, University of Sherbrooke / Canada etc.). Since then, this technology created worldwide interest, but it was in Europe that SCC was extensively exploited and implemented (Naik et al., 2004).

As a result of excellent workability, mechanical property and confusing projects recently. In the meantime, structural SCC has developed an significant research and request aspect of high performance concrete. In recent years, a number of research and request on SCC have been accepted out (Corinaldesi and Moricini, 2004).

2.1.2 Advantages and disadvantages

The usage of SCC can yield several advantages over conventionally located and compacted concrete. Naik et al. (2012) presented some advantages and disadvantages of SCC such as: admixtures that can be further to improve the concrete slump and to reduce the effective cost of SCC; Although not use vibrators in concrete, low clamor level in the plants and building positions; SCC can be located at a closer rate with no mechanical vibration and a smaller amount screening, subsequent in reserves in location charges; Improvement and uniformity of concrete surface can be achieved with ease efforts; simplicity in filling complex sections and hard to stretch areas. Conventional concrete does not provide chances to create complex architectural forms as well as the hardness of finishing its surface; the uniformity of in-place concrete can be significantly improved as the efforts of consolidation stage dismissed; reduces pumping problems; using of lower labour in compared to those used in conventional concrete; cost saving and reduces time of construction; no or little noise due to the eliminate of vibrators; diminishes movement of ready mixed trucks and pumps throughout placement; increased jobsite protection by removing the necessity for consolidation.

The common disadvantages of SCC can be collected as follows: the selection of raw material is harder than of conventional concrete; accurate precise measurement and further monitoring required for the constituent materials. The slight moisture content that can be found in fine aggregate significantly affects rheology of SCC; in comparison to conventional concrete, further trial mix usually are needed for SCC production (Naik et al., 2012).

2.1.3 Materials for the mixture

A number of mineral and chemical products can be used for manufacturing SCC. Among them, fly ash (FA) and nano silica (nS) are explained in detail. For example, FA is the by-product of the incineration of pulverized coal and is composed by special separators such as mechanical and electrostatic from the fuel gases of power plants where coal is used as a fuel. This is perhaps the most recurrently functional constraint overriding the use of FA in a concrete requirement. When FA formerly applied in concrete application in the 1970s, there was a particular foundation for controlling its use. However, after widespread research and more than a few periods of positive application of FA, there is no foundation for a constraint on the quantity of FA that should be acceptable to be used in concrete application. There are two main classes of FA as identified by ASTM C 618 (2012) based on the sources of their chemical composition resulted from the kind of coal burned; these are designated Class F and Class C. Class F is FA ordinarily formed from burning anthracite or bituminous coal, and Class C is usually produced from the burning of subbituminous coal. Class C FA frequently has cementitious properties as well as pozzolanic properties as a result of free lime, while Class F is infrequently cementitious once mixed with water alone. The cost of SCC reduced with the incorporation of mineral admixtures, which is economical for SCC mixtures. (Uysal and Yilmaz, 2011).

FA in SCC contributes to decrease cracking at early age in SCC which reduces with an improvement in strength. The addition of 30-40% FA reduces permeability, increases freeze-thaw resistance minimizing drying shrinkage. FA had a comparable consequence to VMA on fresh properties of SCC: enhancing the fresh concrete viscosity and keeping consistence constant; 28-day compressive strength of such SCC could attain 70 MPa (Xi et al., 2002).

The splitting tensile, compressive strength, modulus of elasticity, and flexural strength were reduced with replacement of cement with 40%, 45%, and 50% of fly ash, but there was a continuous and significant improvement of strength properties beyond 28 days (Siddique, 2004).

FA mainly consists of amorphous glassy materials, including different oxides such as silica, alumina and iron. Moreover, other metallic oxide also can be found. The chemical composition of FA differs significantly between plants. On the other hand, SiO_2 occupies the greatest of the volume of FA. The forms and comparative quantities of incombustible material in the coal utilized to estimate the chemical configuration of FA. In general different chemical and glasses constituents occupy about 80% of FA. These compounds can be found as aluminum, calcium, magnesium, silicon and iron. Subbituminous and bituminous coals during combustion yields calcium and iron, but for subbituminous coal higher calcium and lower iron produced. Beside FA, unburned coal also exists in combustion process. Commonly, combustion of subbituminous coals produces FA with slight concentration of unburned carbon. However, at early age of hydration process, FA tends to perform a weak pozzolanic reaction as well as slightly as a filler, fundamentally serves as centers for precipitation of $Ca(OH)_2$ and C-S-H from the hydration of cement so contributing to the strength (Fraay et al., 1989).

ASTM C618 (2012) based on coal type and the mainly oxides normally found in FA; SiO_2, Al_2O_3 and Fe_2O_3 to classified FA into two kinds. These two kinds are F and C. The main differences between them are the content of CaO, MgO and SO_3. FA class C has higher oxides comparing to class F. Class F is a pozzolanic material at the same time Class C shows direct cementations activity.

Temperature has a big effect on rate of the pozzolanic reaction, and so increasing temperature leads to develop strength of FA concrete. Thus, it can be stated that the heat curing is favorable. The fineness of the glassy silica and alumina significantly related to the degree of reactivity of FA (Helmuth, 1987). In general, the typical comparison between FA with calcium oxide higher than 15% (high-calcium FA) and FA with calcium oxide lower than 15% (low-calcium FA) reveal that the former characterized by an alumina silicate-type glass and no crystalline compounds of calcium, whereas the latter contains of a calcium alumina silicate glass and crystalline calcium compounds like C_4A_3S, C_3A, CaO and CS. As it is well known, Class C and because its contain higher CaO, such class displays cementations properties without the incorporation of calcium hydroxide (Manz, 1999).

Because of the pozzolanic effect consumes some amount of lime, it has been demanded that the use FA in concrete leads to higher rate of carbonation (Neville, 1995). On the other hand, This finding to some extent depend on enhanced carbonation examining which does not duplicate the actual activity of FA of slight hydration, which decreases the permeability for a long period and therefore lowering the accessibility of CO_2 to the ambient of concrete. In the study of Sear (2005) 50% FA used in the production of several concrete types to examine the exposure of concrete for indoors and outdoors conditions. The study showed that FA contributes for reducing CO_2 ingression. However, other studies showed no significant role for FA on carbonation process comparing to conditions of exposure, strength of concrete and age of curing (Thomas and Mathews, 2004). In spite of all advantages of FA, the lower strength and other concrete performance at early ages due to the incorporation of FA instead of cement can be clearly observed (Liu, 2009).

The main properties of SCC are affected by the fineness, densities, particle size distribution, shape and composite of FA particles. As a result of accumulation of FA molecules in the softened face, the position of grain size spreading for the FA and the pulverized coal varies during the combustion process. Different particles of FA were ranged in size from below 1 µm to more than 1 mm. Furthermore, fineness is one of the physical properties of FA that relates to its pozzolanic activity. Fineness can be evaluated through the use of sieve No. 325 (0.044 mm) as a retained percentage. Very fine particles have the highest specific area. The superficial section for FA is capable to be measured by the Blain apparatuses. The blain fineness of FA differs from 2500 to 5500 cm^2/g. FA solid particles have little specific gravity, which is ranged from 1.9 to 2.9 g/cm^3, as a result of FA high in iron it tends to have higher specific gravity. A typical FA specification for concrete is described in BS EN 450 (2005) and BS EN 12620 (2002) with respect to the purpose of using (cementitious and filler, respectively). Also, BS EN 450 (2005) introduced two types of FA in according to fineness as the finer one yields higher strength.

In the study of Cao et al. (2000) cement was replaced by 50% FA. They concluded that such addition significantly reduced the unfavorable pores (pores larger than 100 nm) as well as the reduction in the volume of total pore in the system. In another study which had been adopted by Jiang and Malhotra (2000) the addition of 55% FA caused to reduce the required water by about 20% so they believed in when FA used its possible to eliminate the amount of superplasticizer to attain the same consistence.

In the regard of nano technology, nano silica (nS) is defined as a nano particles having spherical shape and a diameter in the range of 1-100 nm. It is a synthetic products and can be successfully used to enhance the properties of concrete (Li, 2004). In general, incorporating of ultra-fine material –for example nS- in concrete as cementitious materials significantly affects concrete properties. Such additives possess the ability to serve as a filler in the structural system of cement paste. With the proper composition it is possible to decrease water quantity (due to the packing effect) and consequently improve concrete strengths due to the decrease capillary porosity. Moreover, unlike conventional pozzolanic material such as silica fume, nS has a higher pozzolanic reactivity. For this, the use of nS to improve SCC may be lead to introduce concretes with new performances (Hou and Kawashima, 2013; Hou et al., 2013; Choolaei et al., 2012).

The usage of great amounts of cement products, increasing CO_2 productions, and as a importance the green house influence. A technique to decrease the cement quantity in concrete mixtures is the usage of silica fines. nS is one of the silica fines through great potential as cement replacement and as concrete chemical addition. The main chemical reaction occurs between silica and $Ca(OH)_2$ and produce C-S-H gel. The production of silicon metals and ferro-silicon alloys is the source of nS. It is collected by resulting concentration to fine particles in a cyclone (Jonckbloedt, 1997). The production of nS by this method yields ultra nano spherical or microspheres particles with a diameter particle of 15 nm and a large specific surface area (150 to 250 m^2/g). In fact the specific surface area of nS is responsible to the rate of nS chemical reaction. This is because it works as a nucleation place for the precipitation of C-S-H (Qing et al., 2007). The nS used at SCC contains over 99% with a mean diameter of 15 nm with surface-volume ratio 160 m^2/g and the density < 0.15 g/cm^3 (Nik and Orman, 2013).

2.1.4 Engineering properties of SCC

The analysis of the performance of SCC with FA and nS is mainly given. In a recent study, SCC can be produced with acceptable fresh properties by replacing cement by high volume FA. It was reported that, the splitting tensile strength, compressive strength and modulus of elasticity increased by a reduction in the percentage of FA and the water-binder ratio. The study showed that the use of a high volume of FA in SCC mixes decreased significantly chloride permeability than those free of fly ash (Pathak and Siddique, 2012). The compressive strength of SCC containing different percentages of FA was found to increase with increasing in the percentage of FA up to 30%, but the increase in the ratio of FA (over 30%) caused to decrease compressive strength (Mohamed, 2011). In most situations, the addition of FA to concrete causes to decrease the required amount of superplasticizer. In addition, the use of FA with marble powder and limestone filler in SCC lead to decrease viscosities of the mixtures (Gesoğlu et al., 2012). The use of class F FA in SCC reducing the micro cracking width due to the pozzolanic action of fly ash. However the increase in the replacement of cement by fly ash lead to decrease chloride permeability of concrete and water sorptivity of concrete (Guru et al., 2013; Güneyisi et al., 2014).

The improvement in mechanical properties when the usage of mineral admixtures in different blends, the increased in compressive strengths of concrete mixtures when using pozzolanic materials such as FA and granulated blast furnace slag. The study showed, replacement cement by 25% FA the compressive strength reach to more than 105 MPa at 400 days (Uysal and Sumer, 2011).Replacing cement by 40% of FA lead to increase in compressive strength above of 65 MPa at 56 days, as well as increasing in quantity of FA lead to increase absorption values of concrete and reduction in shrinkage, showed when the replacement cement by 80% of FA lead to reduce in shrinkage by two third compared with the control at 56 days and have 2% absorption (Khatib, 2008). The adding of FA did not significantly affect the chloride permeability of the rubberized SCC at 28 days, but at 90 days the entrance of chloride ions decreased significantly because the long-standing of FA improves the pore structure of concrete (Gesoğlu and Güneyisi, 2011). Prepared SCC with two types of filler having important differences generally in chemical and physical properties. In their study, the charge of SCC reduced by a compressive strength grade 50-60 MPa by using 33% from total binder by limestone powder or FA replacement because of smaller quantities of superplasticizer to satisfied the consistency requirements of the SCC, further that It appears that the filler kind had no effect on the nature of the porosity of the SCC at 28 days (Mohammed et al., 2013).

The increase in FA as a replacement of cement lead to reduce the flowability of mortars. Nevertheless, the usage of ternary cementitious blends of FA and silica fume minimize this influence. In the other hand decreasing in dry unit weight of the mortar with an increase the quantity of the mineral admixtures because their little unit weight compared with cement. Further that the increase in FA and silica fume quantity lead to a reduction in the dynamic modulus of elasticity of the mortars (Turk, 2012). The estimation of the effect of mineral additives on the durability of SCC. The result show that the type of additives had effect on the depth of the carbonation, where to use FA in SCC be carbonation depth less compared with the depth of carbonation if used limestone powder or slag, whereas the surface of concrete become more absorption of water and water penetration compared with normal surface without carbonation (Owsiak and Grzmil, 2015). The effect of various proportions of FA from 30 to 60% a replacement of cement and the effect of silica fume which used by 10% a replacement of cement too on the durability properties such as chloride penetration and freezing, and thawing also mechanical properties. The results of study indicate that, the use high volume of FA with 10% silica fume replacement to obtain the high performance SCC. This type of SCC has a good resistance to freezing and thawing, and chloride penetration, also this concrete had great environmental and economical aids. It is noticeable that the hydration heat is lower and lead to low shrinkage compared with SCC made with high volume cement. Besides that the result showed the replacement of cement by FA without silica fume produced a reduction in compressive strength at all content of FA (Yazıcı, 2008).

Great flow ability condition of SCC can result from the use of mineral admixtures such as FA. FA units are sphere-shaped important to minimize friction through flow of the mortar portion in the concrete. Usage of mineral admixtures such as FA, slag and limestone powder rises the fine ingredients in the concrete mix (Okamura, 1997). The usage of high quantity of Class C FA in the industrial of SCC decreases the price of the SCC production through meaningfully reducing the quantity of superplasticizer and viscosity modifying agent associated with the typical dosage for such admixtures in SCC, since reduced friction between paste and large aggregate particles resulting from ball bearing effects of spherical particles of FA (Naik et al., 1992). The use of FA and dolomite in SCC can be ordered as SF1 in expressions of slump flow, as well as using dolomite and FA to produce SCC with suitable hardened and fresh properties (Barbhuiya, 2011).

Typically, the most generally used test methods for SCC is the slump flow test. It is well recognized later that the usage of mineral admixtures such as FA and slag can increase the slump of the concrete mixture without increasing its cost, although decreasing the quantity of superplasticiser required to acquire alike slump flow compared to concrete made with Portland cement only (Skarendahl et al., 1999). The greatest significant principle of flowing concretes similar SCC is the usage of superplasticizer combined with a comparatively great content of powder materials in terms of Portland cement, mineral fillers, fine aggregates etc. Furthermore, the use of FA develops rheological properties and decreases the cracking potential of concrete as it drops the heat of hydration of the cement. More than, the usage of FA decreases the demand for fine filler, cement and sand, which are necessary in high amounts in SCC. When the FA quantity rises the slump flow too increases up to 50%, and after that there was a drop in the flow at 70% replacement (Dinakar et al., 2013).

Bingöl and Tohumcu (2013) reported the behavior of SCC that includes silica fume and FA to make an evaluation of their utilization potential for SCC. It was observed that FA improved the fresh properties by improving the dispersion of solids in the plastic state. In addition, FA reduces the viscous behavior of SCC.

The characteristics of concrete resulted due to the basic processes are greatly influenced by the quality of material on nanoscale. In fact the products of hydration process and C-S-H gel represent the nano structure phase of cement paste (Sanchez and Sobolev, 2010). Nili et al. (2010) stated that the hardened propertied which defined by durability and mechanical performance of concrete significantly based on the degree of microstructure refinement and the quality of paste-aggregate interface zone of hardened cement past. The application of nano range of amorphous silica particles have not been completely agreed yet. The pozzolanic activity of these materials significantly enhances the compressive strength and permeability of hardened concrete. In this regard the addition of nS yields in finer hydrated C-S-H gel and densified (nano filler and anti-Ca(OH)2 leaching effect) microstructure (Quercia and Brouwers, 2010).

The use of 1% of nS in cement paste lead to accelerated the rate of hydration for cement with high volumes of FA or slag. When increased the percentage of cement replacement by nS to 2% the results refer to reduced initial and final setting times, in addition to increased compressive strength of high volume FA concrete (25%, 30%) at 3 and 7 days compressive strengths of high-volume FA concrete also at 28 and 90 days, the use of nS improve the compressive strength of high volume FA concrete. Nevertheless, nS increased early strengths and reduced the setting time of the high volume FA or slag concrete (Zhang et al., 2012). The use of nS in concrete mixtures and cement paste would cause an increase in compressive strength at early ages, also the strength of concrete at later ages was a more significant effect when used nS by 3%. As well as, the use of nS above 3% was improving the cement paste aggregate interfaces (Nili and Ehsani, 2015). In the light of previous scientific works, mortars and cement paste made with nS have been extensively investigated, while the use of nS to study the mechanical and permeability of concrete have been found in some researches. Several durability properties to present time does not investigated in details. Critical point about the effect of ultra-fine materials on the shrinkage behavior of concrete could be studied. Additionally, carbonation, acid resistance, corrosion, etc. are to be evaluated (Singh et al., 2013). Increasing in nS content to 4% lead to increase the values of chemically combined water contents at all curing ages, as well as the compressive strength of OPC-nS or slag mixture increased (Heikal et al., 2014).

The usage of up to 4% nS, 3% nano-Cu and 2% Fe_2O_3 result in increasing of compressive strength, and then the compressive strength is decreased when used above the percentage of nanomaterials. Whereas, increasing in the quantity of nanoparticales leads to decreased in water absorption and chloride permeability of the specimens. As stated by the micrographs, smaller pores achieved by adding of nanoparticles, which can develop the durability, mechanical and microstructural properties of the mixes. Further than, the results show that nS can improve the microstructure and reduce the water permeability of hardened concrete (Madandoust et al., 2015). The nS addition increases the bond between cement matrix and aggregates, decreases porosity, and increases the density (Qing et al., 2007). The use of nS and Al_2O_3 nano additions have a negative effect on the fresh properties of SCC while the use of nS with amount ranging from 0.5 to 4 %, lead to increase at 28-day compressive strength (Niewiadomski et al., 2015). Increasing in compressive strength when the use of nS up to 4%, while it decreases above 4% (Nik and Orman, 2013). The increase in the quantity of nS in SCC results in an increment in the dosages of superplasticizer to maintain the acceptable levels of flowability. Furthermore, the cohesiveness improvement of mortar due to the incorporation of nS allows to reduce plastic shrinkage of concrete (Sonebi et al., 2015).

The use of nS in SCC has an effect on the fresh properties of concrete as observed by recent studies. The nS can reduce the slump flow of SCC due to the higher viscosity of such concrete (Beigi et al., 2013). In a study by Jalal et al. (2012), twelve mixtures containing 2% nS content as a partial binder substitution. They reported that the addition of micro silica and nS particles developed the consistency of the high performance SCC and reduced the possibility of bleeding and segregation. Ghafari et al.(2014) reported the addition of nS to SCC decreases the spread on flow table. Guneyisi et al. (2015) showed that the use nS and FA in SCC lead to change the diameter of the slump flow between 700 and 800 mm. In addition to decrease in slump flow diameter when using nS, while increase it if used FA. Furthermore, the employment of nS in SCC lead to increase in slump flow and V-funnel time, but the decrease in slump flow and V-funnel time when used FA, the study also showed that the increase in nS content would be decreased in L-box height ratio while increased in L-box height ratio when increasing in FA content. On the other hand, the result of rheology test showed that increasing in the shear-thickening of SCC when nS has been incorporated, while incorporation of FA contributes to decrease it. Nazari and Riahi (2011) observed that the use of nS up to 4% lead to increase in compressive, split tensile, and flexural strengths of SCC. Tangpagasit et al. (2005) reported that the use pozzolanic materials in cement paste and mortar lead to enhance its mechanical characteristics along with densification of microstructure.

2.2 Glass fiber reinforced SCC

To produce fiber reinforced SCC, several types of fiber used such as glass, steel, and polypropylene fibers can be utilized (Aydin, 2007). Among them, glass fiber (GF) is relatively new for the structural SCC mixtures. Conventional borosilicate GF (E-glass) and soda-lime-silica GF (A-glass), this type of GF affected by the alkalinity of the cement-based matrix. So that, those kinds of fiber were unsuitable for use in concrete. Researchers turned to find a solution to this problem by using a new type of fiber is called alkali resistant fiber (AR-GF) that providing developed long-term durability. AR-glass was introduced in the United Kingdom in 1971. The other type of alkali resistant glass produced by Nippon Electric Glass (NEG) Company in 1975, containing 20% zirconia (ACI 544.1R, 1996). Result to loss of the original resistance of GF when put it in cement. It has been resorting to the use of AR fibers because of its high-role to other types, it has tensile strength reach to 1000-1200 N/mm^2 at ambient temperatures in cement (Majumdar, 1974). The chemical properties of these types of GFs are shown in Table 2.1.

The physical properties of GF are important because of its fundamental role in improving the properties of concrete. Table 2.2 shows the physical properties of GF (ACI 544.1R, 1996).

Table 2.1 Composition of selected GF (Majumdar, 1974)

Component (%)	A-glass	E-glass	Cem-FIL AR-glass	NEG AR-glass
SiO_2	73	54	62	61
Na_2O	13	-	14.8	15
CaO	8	22	-	-
MgO	4	0.5	-	-
K_2O	0.5	0.8	-	2
Al_2O_3	1	15	0.8	-
Fe_2O_3	0.1	0.3	-	-
B_2O_3	-	7	-	-
ZrO_2	-	-	16.7	20
TiO_2	-	-	0.1	-
Li_2O	-	-	-	1

Table 2.2 Physical properties of selected GF (ACI 544.1 R, 1996)

Property	A-Glass	E-Glass	Cem-FIL AR-Glass	NEG AR-Glass
Specific gravity	2.46	2.54	2.7	2.74
Tensile strength (ksi)	450	500	360	355
Modulus of elasticity (ksi)	9400	10,400	11,600	11,400
Strain at break (%)	4.7	4.8	3.6	2.5

2.2.1 Engineering properties of glass fiber reinforced SCC

It is well known that the low tensile strength is the reason for generating shrinkage in concrete. In the market there are different types of fibers can be used to prevent cracking propagation and shrinkage (Park et al., 2012). When concrete has reinforced with fiber, higher energy absorption, resistance to shocks and formability could be attained. Such properties support fiber reinforced concrete to improve concrete technology and for saving cost in structural industry (Kang et al., 2010). Among different fiber types, GF are relatively cheap, proper tensile strength and lightweight. The addition of GF have been found to reduce shrinkage cracking (Barluerg and Olivares, 2007), improve energy absorption (Mirza and Soroushian, 2002) and rise the ductility index in compression (Fanella and Naaman, 1985). Numerous factors can be remarkably influence the properties of fiber reinforced concrete, from those foctors; physical properties of the fibers and the bond strength between fiber and concrete components (Hughes and Dougill, 1975).

The ultimate load behavior of steel FRC deep beams and found that the addition of steel fibers results an increased failure loads and change in failure modes (Shanmugam and Swaddiwudhipong, 1988). Much of the credit for the initial development of dispersed glass-fiber as reinforcement for cement must undoubtedly be given to the Russians (Aveston, 1971). FRC is often used in the structures to restrict cracks that originate from stresses caused by volume changes in combination with structural restraint, cracking is a problem especially when high strength concrete, which is in inherently brittle is used. Fiber in concrete provide a means of arresting crack growth and improving the load carrying capacity (Majumdar, 1974). Fiber act as cracks arresters through the initial loading stages, and increase the energy required for crack propagation what provides an increase in the strength. During the later stages of straining the fiber distribute the micro cracking thus increasing toughness and apparent strength (Kurtz and Balaguru, 2002). Fiber in concrete, has found to improve several properties like tensile strength, cracking resistance, impact and wear resistance, ductility and fatigue resistance. Future development in the field of FRC was due to introduction of high strength fiber like glass and carbon fibers. The initial studies showed deterioration of GF due to corrosive alkali environment of the cement paste. The alkali resistant GF, which is developed recently has overcome this defect and can be effectively used in concrete.

The production of FRC should always be considered in two well defined phases, the fresh and the hardened phases (Neville, 1995). The use of GF in SCC lead to reduce concrete cracking due to restrained shrinkage. To prevent the expansion of micro-cracks and to improve tensile strength of concrete, various fibers are used (Park et al., 2012). It was noted that increasing in compressive strength and enhanced the fresh properties of SCC by using the fibers (Kamal et al., 2014). Basheerudeen and Anandan (2015) have observed increase in compressive strength with the addition of fibers. Furthermore, the inclusion of fibers transformed the failure type of concrete from a sudden failure to more ductile failure in which the specimen remainders intact after failure. The study also showed an increase in modulus of elasticity of SCC with fibers as compared to plain SCC is nearly 10%. Ahmed et al. (2015) have reported the use of GF with various percentage between 0.1 and 0.3% in SCC lead to enhance in the engineering properties of SCC.

2.3 Concrete filled steel tubular composite columns

In general, composite columns have superior strength and ductility performance and nowadays they are more widely accepted in the engineering applications. In practice different types of composite columns can be used, those are illustrated in Figure 2.1. As can be seen in the figure, the first type of composite columns require full form-work during the stage of casting fresh concrete, like this type commonly known as fully encased profile composite column, Figure 2.1a. In the second type, the composite column consists of I or H shaped steel section with concrete between the flanges. They are known as partially encased profile composite columns because the formwork require for two sides only as presented in Figure 2.1b. In the third type, (concrete filled steel tubular (CFST) column), the steel tube filled with fresh concrete in such a manner that the steel section works as a formwork during casing process, Figure 2.1c. Concrete filled sections, therefore, offer the advantage to erect the steel frame of a building and subsequently fill the hollow column by pumping in the concrete. By so doing the erection time can be lessened.

Typically, there are significant differences in structural properties like ductility and energy absorption capacity between the CFST column types and conventional reinforced concrete columns. Although no one can deny the favorable performance of conventional reinforced concrete columns, but recently with a sharp increase in labor costs, the on-site temporary works involving formworks of concrete require high costs in construction market. Particularly for the projects like building with high story heights, the time of construction and costs for the temporary works have considerably increased, and thus the competitiveness of the reinforced concrete construction method has been adversely affected. Obviously, construction process of columns in typical reinforced concrete frame constructions is one of the challenges, therefore, absolutely advantageous to minimize the on-site temporary works for reduction of the construction time (Oh et al., 2002). Figure 2.2 depicts the available types of composite cross-sections of CFST column. The most usability CFST column cross-sections are regular shapes, i.e., rectangular, square and circular. For the functional and architectural purposes special cross-section shapes can be used, for example elliptical and polygonal sections. Usually, plain concrete is used to fill the hollow steel tubes. Nowadays, advanced concrete technology allows reinforcing concrete core by fibers or steel bars so as to improve the structural performance and fire resistance of CFST columns, Figure 2.3a. In order to gain further enhancement of compression resistance, special profiles can be inserted into concrete such as solid steel section or H-section, Figure 2.3b. This process will be contributes to reduce the size of column. For columns subjected to high flexural loading, concrete filled double skin steel tubular sections can be used to increase the flexural stiffness with less material used, Figure 2.3c (Liew et al., 2016).

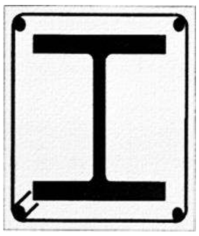

a) Concrete encased profiles

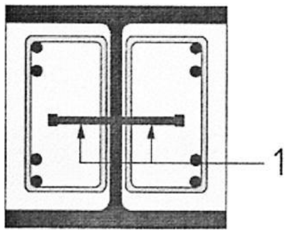

b) Partially encased profiles 1: shear connectors welded to web of profile

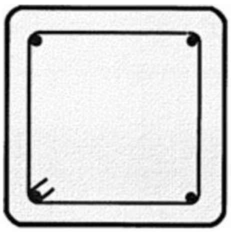

c) Concrete filled profiles

Figure 2.1 Main types of composite column (Eurocode, 1994)

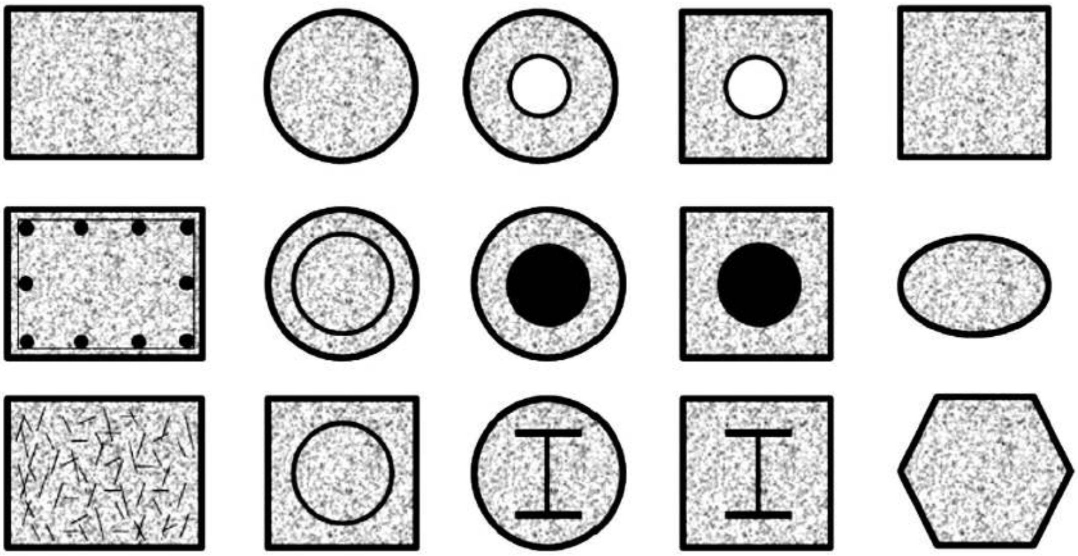

Figure 2.2 Available cross sections of CFST column (Eurocode, 1994)

a) CFST columns with additional steel bars profile

b) CFST columns with additional solid steel section

c) Constructed concrete filled double skin steel tubular pole

Figure 2.3 Advanced CFST columns (Eurocode 4, 2004)

2.3.1 CFST column design

There are a various design provisions for CFST composite columns given by the institutes of several countries, for example: American Institute of Steel Construction (AISC, 2005), Architectural Institute of Japan (AIJ, 1997), European Committee for

Standardization: British Standards Institution (Eurocode 4, 2004); and Chinese code (DL/T, 1999). Even though there are similar concepts to design CFST columns within these codes, significant differences can be noted at the same time. For instance, the AISC (2005) can be applied to CFST columns infilled with normal weight concretes having cylinder strength and steel yield strength up to 70 MPa and 525 MPa, resectivelly. In the provision of AIJ (1997), the high strength concrete has taken into account to design composite columns. That is concrete strength of 90 MPa can be utilized. Eurocode 4 (2004) says suitable for concrete with cylinder compressive strength of 20 to 50 MPa and steel grades from S235 to S460. Finally, DL/T (1999) only relates to CFST columns with concrete cylinder strength ranges from 25 MPa to 67 MPa and yield strength of steel from 235 MPa to 420 MPa.

Liew and Xiong (2015) proposed design guide for CFST columns by considering the same aspects of Eurocode 4 (2004). The significant considerations of their guide are allowed to fill the gap existed in previous design codes. The design guide can be applied for the CFST columns with concrete cylinder strength up to 90 MPa and steel yield strength up to 550 MPa. The CFST columns under compression only in this design guide should be checked for:

- local buckling resistance
- cross section resistance
- member resistance

The guide presented a recommendation regarded the maximum value of steel tube local buckling. The local buckling can be prevented by adopting two special methods. The first one aims to reduce the effective width of the steel plates by welding stiffener plates as shown in Figure 2.4. The second process involved the increase of plate thickness. On the other hand, the local buckling for a steel profile fully incased in concrete can be neglected.

The cross section resistance involves its resistance to compression; shear forces and combined compression and bending. Normally, the cross section design resistance to compression is computed by the summation of plastic resistances of CFST column components; concrete, steel tube, encased steel section and reinforcements. In order to calculate the plastic resistance to axial compression of circular cross section the confinement effect must be considered in the design formula.

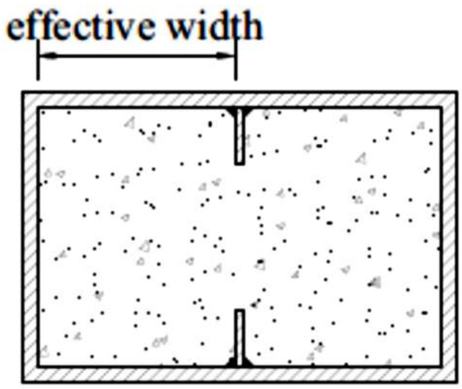

Figure 2.4 Longitudinally setting of stiffener plates to prevention local buckling of CFST columns (Liew and Xiong, 2015)

The resistance to the shear forces can be calculated for steel tube and inner steel section only. In some cases the shear force acting on steel tube and/or inner steel higher than the ultimate design value by about 50%. The design guide required to reduce design steel tube strength or encased steel section in the shear zones by (1-reduction factor) multiplied by yield strength of steel or by reducing web thickness of the shear zones as presented in Figure 2.5 below.

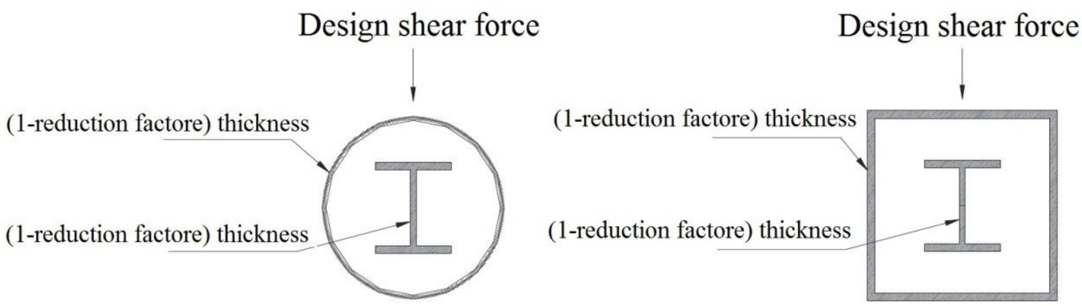

Figure 2.5 Modification of steel thickness of shear area (Liew and Xiong, 2015)

The cross-section resistance of CFST column for combined compression and moments may be calculated depends on interaction curve and the tensile strength of concrete can be omitted. Figure 2.6 presents the interaction curve that can be utilized to compute the resistance of cross-section of composite column to compression and moments actions.

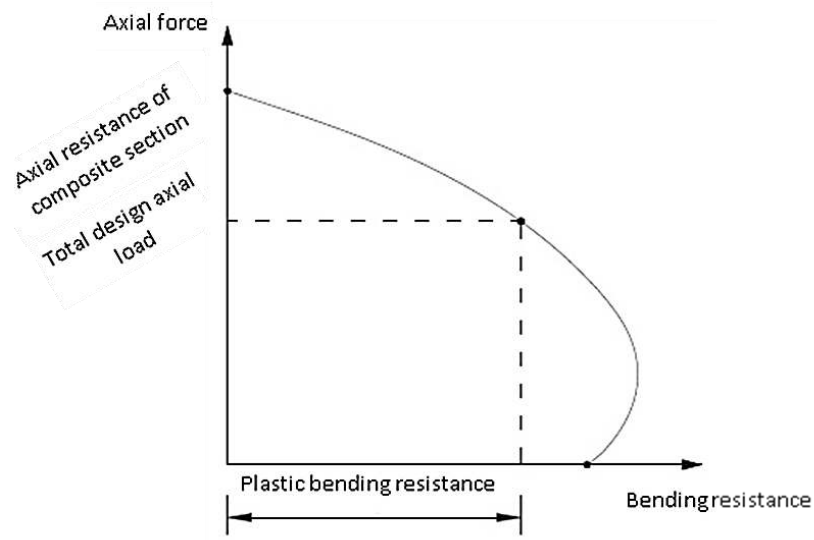

Figure 2.6 Interaction curve for combined compression and bending (Liew and Xiong, 2015)

The resistance to compression can be computed for a member subjected to axial compression only. Buckling curves must be used in this stage of design. The use of buckling curve is useful simplification because these curves allow for member initial imperfections. From the main parameters required to complete calculations are the effective flexural stiffness of a CFST column and the buckling length of a composite column for the relevant buckling mode. The buckling length values must be found for specified boundary conditions as demonstrated in Figure 2.7.

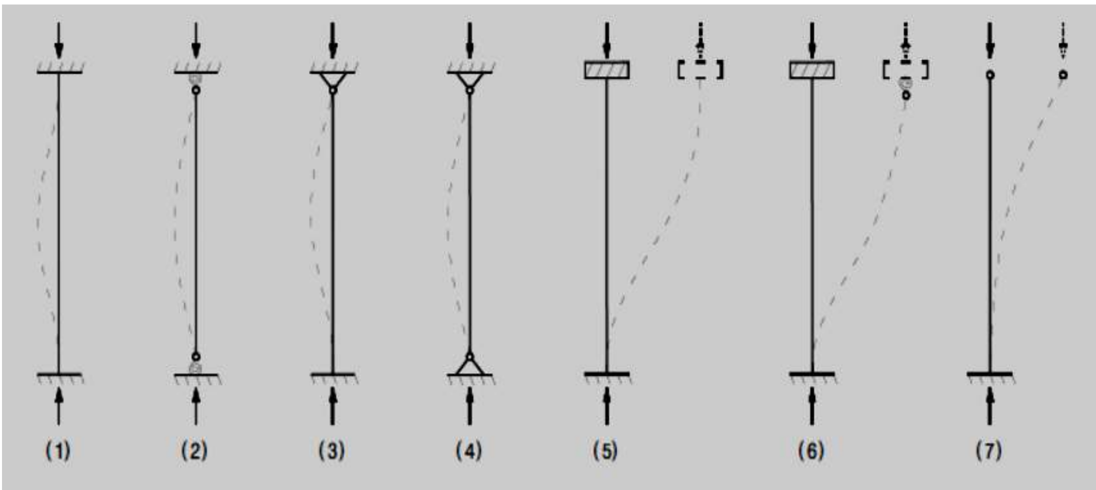

Figure 2.7 Buckling lengths for CFST columns (Liew and Xiong, 2015)

2.3.2 Construction of CFST columns

Based on the condition of site and contract, commonly there are two procedures can be applied to fill hollow tube with concrete; off-site or on-site. The off-site one has benefits in decreasing the number of site processes and speeding up the building process. However, the on-site is generally can be utilized for columns characterize by its long lengths. The filling steel tube and so as to save time may be done rapidly and in parallel with other site activities. In general, the design criteria of CFST column allow combining the advantages of steel frame and conventional composite column (Wang, 2014).

2.3.2.1 Specification of concrete

In general, concretes have two main states, the first one is called as the fluid state and the second is known as hardened state. In order to monitor concrete in both these two states, binders, water, aggregates and admixtures must be logically regulated. Considering composite structure aspects, concrete must be behaved properly within workability, cohesion, ease of pumping, strength and shrinkage. The desirable workability gains concrete to the possibility of filling steel tube through two ways; pumped up or poured in from the top of tube. On the other hand, high strength or ultra-high strength concrete is a favorable option as it decreases the occupied area by the constructed column (Wang, 2003).

On one hand, the use of cement as a single binder in concrete increases strength up to 80 MPa. On the other hand the utilization of cementitious materials have two fold advantages: saving cost and improve concrete properties. For example, incorporation of fly ash increases flowability, thus to achieve certain slump it is possible to reduce water content by adding such additive.

Concrete having adequate slump, desirable cohesive and easily pumping maybe considered as an ideal building material in CFST column construction. The workability and strength intensity of normal concrete are a function of its water content. On the other side, high strength concrete mix the amount of water has to be carefully designed and workability is then influenced by the quantity of admixtures, mainly the superplasticisers and/or water reducing agents used (Wang, 2003; Wang, 2014).

2.3.2.2 Reinforcement

Inserting reinforcement into the tube in the fabrication shop is preferable. Cages of pre-welded up to 15 m in length can be bought by the steel work fabricator and then fitted into the steel tubes with spacers and rollers on the longitudinal reinforcement. This needs direction between the fabricator and the reinforcement supplier. It is important to check the reinforcement for quality assurance control prior to welding of the cap plates. Casting of concrete can then performed on site, as with a normal steel frame and utilizing similar column splice lengths. Care should be occupied to confirm that the bars do not block the holes when bottom filling the tubes, Figure 2.8 (Wang, 2014).

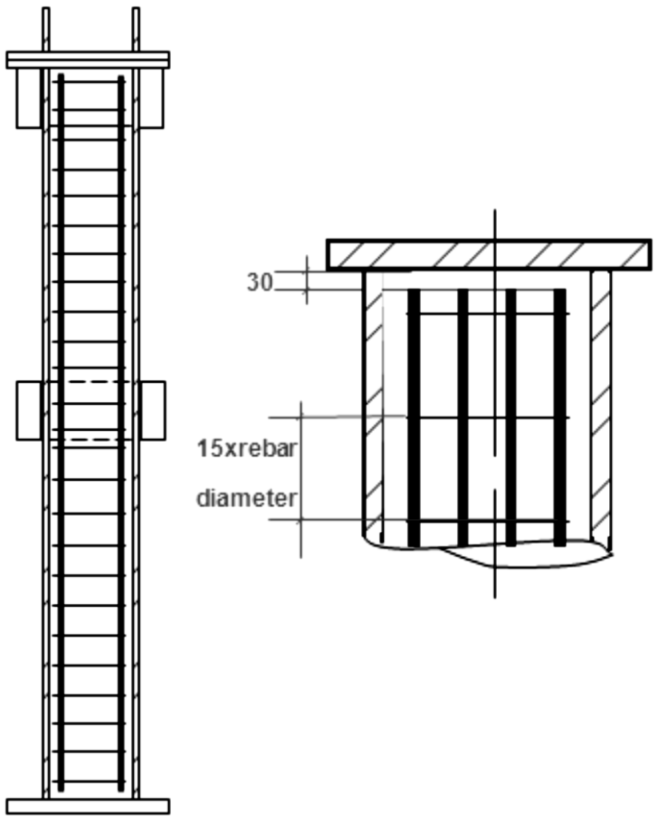

Figure 2.8 Placement of reinforcement cage (Wang, 2014)

2.3.3 Previous researches

In 1975, the first scientific research about the CFST columns was performed by Kloppel and Goder. As cited by Knowles and Park (1970) and Roik and Bergmann (1989), this research published in Germany. These authors used in their study two types of composite column; CFST and hollow columns. Moreover, tests were examined, with stresses and strains in both the concrete and steel organized for concentric load values. From their investigation, the initial design formulas for CFST columns were established.

Furlong (1967) investigated CFST columns having circular and rectangular cross section. In fact, it can be stated that this study is one of the earlier comprehensive research performed on the CFST columns. Explicitly, for the first time, Furlong studied the effect of interaction between concrete and steel on the structural behavior of CFST columns. He detected at strain values below 0.001, the steel and concrete perform independently of one another, as the Poisson's ratio of steel is higher that of concrete; in lateral expansion this difference yielded in a non-contact state between them at low strain values. On the other side, due to the laterally expansion of concrete, the Poisson’s ratio of steel and concrete began to approach a closed value as the strain passed 0.001. In this level, the steel tube behaves in such a way to confine the concrete. At the same time, the concrete core stabilizes the wall of steel tube, allowing the tube to attain its maximum yield strength capacity and avoiding local buckling. At the same line, the test data of Furlong study the structural behavior of CFST columns influenced by creep.

Schneider (1998) examined analytically and experimentally the performance of CFST columns concentrically loaded with different cross sections such that three circular, five square and six rectangular cross sections were experimented in order to study the influence of type of cross section and steel thickness on the structural behavior of CFST columns. Their study concluded that the CFST column with square or rectangular section had the lower stiffness, strength and ductility in compared to the column has circular cross section. The reason for the better performance of circular CFST column is related to the confinement stress provided by the circular cross section is higher and more uniform than rectangular and square sections.

The review of published literature in recent years shows that the SCC has been attracted the structural engineers for composite construction. As illustrated in earlier sections of this thesis, the SCC represents a revolution in the sector of concrete industry around the world whereby the fresh mixture can place under its self-weight and fill in the formwork in the process of casting. To this regard, the favorable characteristics of SCC gain such high performance concrete several advantages and innovative applications for structural purposes. From these unique applications, SCC has been used in composite columns having dense reinforcement and small cross sections (Han et al., 2005; Eramma and Niranjan, 2012).

In practice two processes can be used to cast fresh concrete (in-place) in CFST columns as can be seen in Figure 2.9 a and b. Figure 2.9a illustrates casting process by flowing fresh concrete at the top of a hollow section, whereas, Figure 2.9b depicts the procedure of using a cut opening near to the base to pump fresh concrete. Although the two approaches provides different advantages but the main purpose of these processes is to yield concrete having proper integrity. The first method (pumping concrete) requires steel tube maintenance after hardening of concrete. Placing concrete from the top may be yields segregation and voids in concrete being casted. The most attractive solution to such obstacles regarding the steel tube infilled with conventional concrete is to use SCC as it provides prevention of the segregation and does not require any vibration (Perea, 2010).

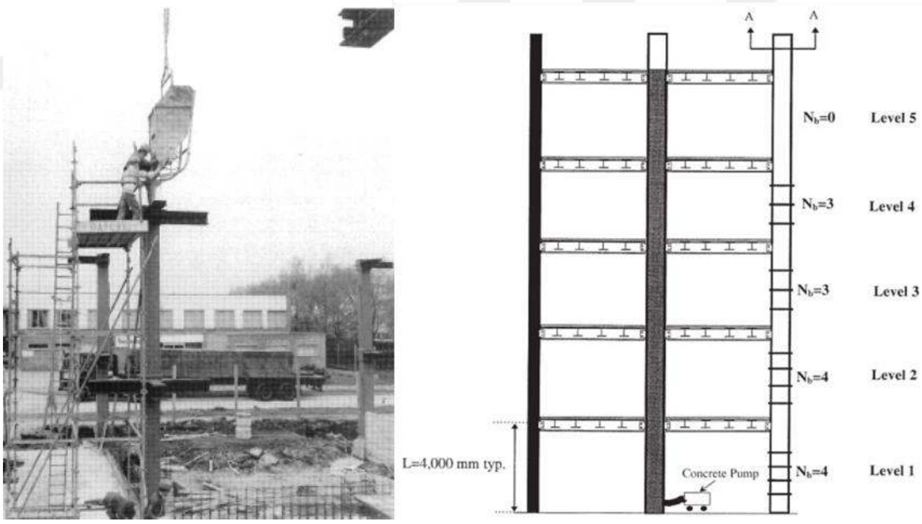

a) Pouring method b) Pumping

Figure 2.9 Procedure of filling concrete on site of CFST columns (Bergmann et al., 1995; Uy and Das, 1999)

From the broad literature survey performed in this thesis, it is indicated that the structural behavior of steel tube columns infilled with SCC incorporated fibers has not been studied comprehensively.

Muciaccia et al. (2011) experimentally investigated the SCC efficiency to infill of structural steel tube column, structural behavior with respect to the use of expansive SCC and the code prescription appropriateness when referring to SCC. To this aim they used in the test configuration different parameters such as geometry and length of steel tube, the length to diameter and diameter to thickness (D/t) ratios. The mix design involved three different kinds of concrete; conventional vibrated concrete, SCC and expansive SCC (produced by using expansive agent). They concluded that by the use of SCC in the construction of such columns, the elimination of vibration process contributes to lessen the cost of CFST columns as concrete vibration methods are commonly hard and costly to perform for the considered shape. The study also highlighted that the use of SCC in place of conventional concrete does not need another methodology in the design procedure of CFST columns. Moreover, the axial capacity of the column can be evaluated by employing the Eurocode 4 approach, with minor adjustments with respect to the confinement influences of the concrete core.

In the published research of Han et al. (2005), another experimented work conducted to study the structural performance of SCC filled steel tube columns subjected to an axial load can be found. A total of 50 hollow structural steel tube columns with different sectional types (rectangular and circular), various yielding steel strengths (from 282 to 404 MPa) and several D/t ratios (from 30 to 134). The study contained in its manuscript comparisons of the experimental values with predicted column strengths using the available international provisions such as ACI-1999 (American Concrete Institute), AISC-LRFD-1999 (American Institute of Steel Construction), AIJ-1997 (Architectural Institute of Japan), BS5400-1979 (British Standard Institute) and EC4-1994. The comparison revealed to the suitability of the use of existing design codes which are established for normal concrete to the SCC filled hollow steel tube columns. On the other hand, as given in existing design codes, they used their test results to examine the limiting diameter or width to thickness ratio for the columns. In this regard, the strength indexes calculated by using Eq.2.1 versus D/t ratio and versus width to thickness ratio are graphically presented, Figure 2.10 a and b, respectively. These figures also present the limiting values of the diameter (width)-to-thickness ratio for such sections as given in ACI, AIJ and EC4 provisions. Figure 2.10 a and b depicts that the strength index decreases with the increase in the ratio of D/t and (width)-to-thickness, regardless the section type due to the reduction of confining effect. They also noted that even though D/t and (width)-to-thickness ratio increased, there is no significant effect on the strength index. For this they said: such behavior refers that the D/t ratio effect in these columns does not clearly perform, since the core of concrete can prevent the local buckling.

$$\text{Strength index (SI)} = \frac{N_u}{N_{uo}} \tag{2.1}$$

Where N_u is the maximum load resulted from the experimental tests and N_{uo} is $N_{u,ACI}$ defined in the following equation:

$$N_{u,ACI} = 0.85\, f_c' A_c + f_y A_s \tag{2.1a}$$

Where f_c' is the compressive strength, A_c is the cross-sectional area of the concrete specimen core, f_y is the yield stress of steel, and A_s is the cross sectional area of steel.

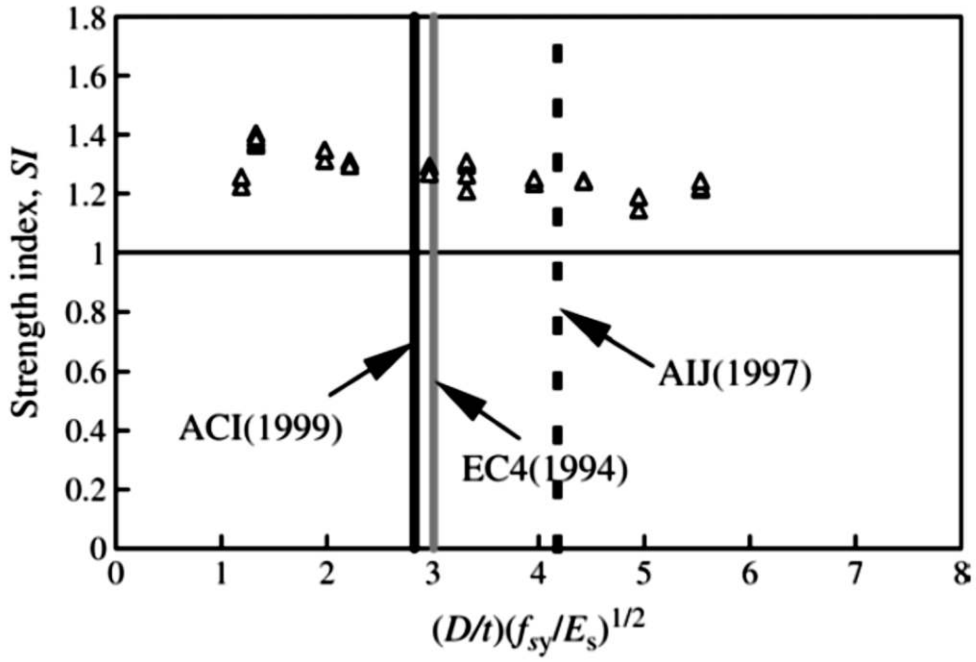

a)

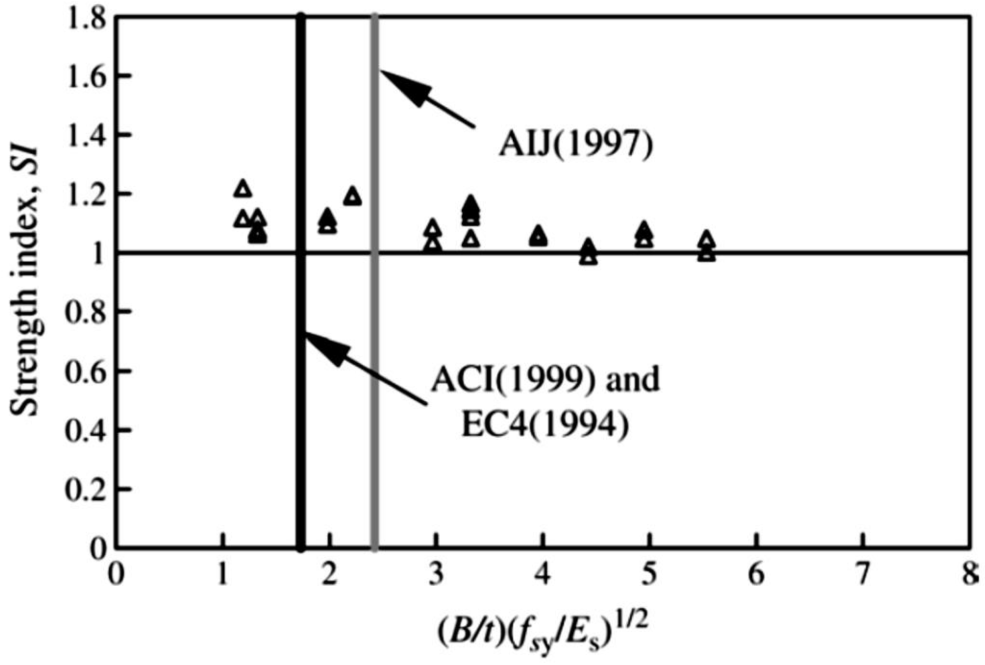

b)

Figure 2.10 Strength index versus $(D/t)(f_{sy}/E_s)^{1/2}$ and (width to thickness ratio)$(f_{sy}/E_s)^{1/2}$, a for circular section, b for rectangular section (Han et al., 2005)

Generally, the largest the cross sectional profile of the CFST columns the higher the hydration heat and shrinkage of the concrete filled steel tube. To investigate the hydration heat and shrinkage of concrete-filled steel tubular, an experimental study was conducted by Han et al. (2005). Towards this objective they used SCC in their study. It was reported that the rapid increase in shrinkage of SCC occurred at a first early days until it reached a relatively steady value after about 100 days. The characteristics of the plain concrete temperature during the hydration process of cement are similar to that of SCC. Due to the constraint of the outer tube, the results of concrete shrinkage showed that after 3 years the shrinkage value of the concrete core inside tubes is less than 40% of that of related to the exposed concrete.

Rui et al. (2012) believed that the SCC filled steel tubular stub columns can be used to produce CFST columns having good capacity of bearing axial compression and high resistance to deformation. Their research also showed that when the bearing capacity at elastic stage, the CFST columns made with SCC can reach above 75% of ultimate load.

Zhu et al. (2010) proposed a new design model for CFST columns having square profile filled with high strength SCC. The experimental study focused on the investigation of centrally loaded behavior of CFST columns as well as to advice a method to estimate the ultimate strength. Details of cross-sections of test specimens are presented in Figure 2.11. The properties of new composite columns in terms of strength and deformation are investigated. To this purpose, several influencing factors such as strength of concrete, length to width and width to thickness ratios and ratio of steel section were employed. SCCs have been used in this study because the authors believed that it will be used in composite columns in the future due to its high performance. The steel tube with square cross section was found to enhance strength and ductility; the employment of steel section significantly affects the response of post peak of concrete and its positive impact on the concrete strength can be abandoned. The findings agree well with the experimental results, Figure 2.12.

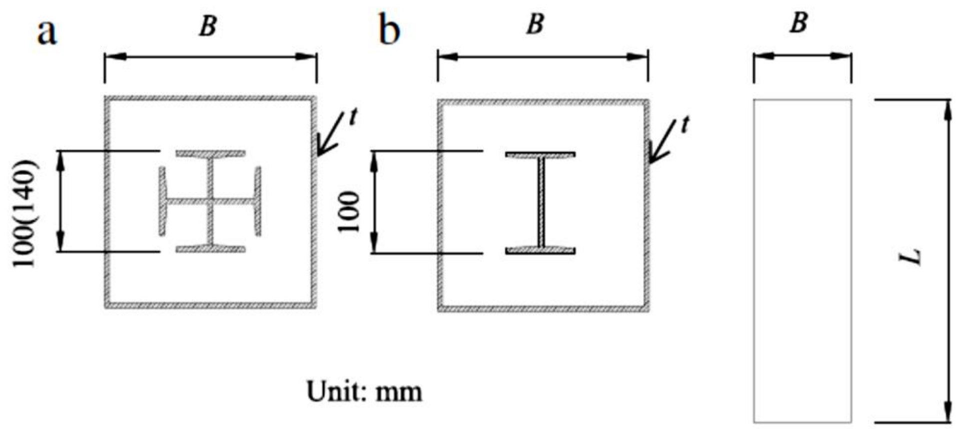

Figure 2.11 (a) Cross-section of test specimen with cruciform steel section; (b) Cross-section of specimen with I-shaped steel section (Zhu et al., 2010)

In spite of differences in fresh properties of normal vibrated concrete and SCC, it can be considered that there is no significant difference between the material properties of conventional vibrated concrete and SCC (ACI 2007). On the other side, Han et al. (2005) stated that at ambinet temperature there is no difference between the structural behaviour of steel tubular columns filled with SCC and those filled with conventional concrete. However, in the litreture there have been some controversial studies about the fire performance of normal concrete and SCC (Blontrock and Taerwe, 2002; Kodur and McGrath, 2003; Persson, 2004; Noumowe, et al., 2006;

Reinhardt and Stegmaier, 2006). It is commonly believed that the concrete in-filled steel tubular works as a heat sink in the composite sections. At the same time, the fire resistance of CFST columns can be increased by using special type of tubes such as the steel hollow sections which prevent spalling of concrete, Figure 2.13 (Lu et al., 2010). Lu et al. (2010) made an investigation into the fire performance of SCC infilled double skin tubular columns. They used three types from the presented profiles in Figure 2.13 to achieve the purposes of their study. The study reported important conclusions, i.e. SCC filled double skin tubular columns can have higher limiting temperatures on outer steel tubes than unfilled and CFST columns. This indicates columns have double skin profile can have better fire endurance than conventional reinforced concrete and CFST columns. However, it is noteworthy to said that under fire exposure the SCC tends to behave like high strength concrete, i.e. higher possibility of explosive spalling (Persson, 2004; Noumowe, et al., 2006; Reinhardt and Stegmaier, 2006).

The composite action between the concrete core and the inside steel tube wall significantly effects the structural performance of CFST columns. As explained earlier, the presence of core concrete prevents inward local buckling of the tube while the steel tube offers lateral confinement to the concrete (Lu et al., 2015). The use of concretes having high brittleness to infill steel tube columns must be avoided as much as possible due to the side effects to load transfer and concrete confinement.In another meaning, one can say that the brittle concretes yield CFST columns with uncomplimentary structure performance i.e., unfavorable axil load capacity (Tao et al., 2008). Fujimoto et al. (2004) and Zeghiche and Chaoui (2005) reported that the load capacity and ductility of the CFST columns increased with decreasing slenderness ratio which is certain to increase the construction cost.

The other way of eliminating inherent brittleness of concrete is to introduce fiber reinforced concrete (Güneyisi et al., 2015a). In this regard, the improvement of composite columns by using fiber reinforced concrete has been investigated for several decades especially so as to discuss the feasibility of enhancing fire resistance of CFST columns (Kodur and Lie, 1996; Kodur 1998, 1999). Recently, the structural behavior of fiber reinforced CFST columns at non elevated temperature has been extensively investigated. The steel tubular columns filled with low and normal strength fiber reinforced concrete have been examined by Tao et al., (2009) and

Ellobody (2013). In such researches, the CFST columns were of slender columns or/and examined with eccentrically load, and the use of fiber were selected to increase strain intensity accompanying with flexure strength increment as fiber reinforced concrete possesses favorable flexural and tensile strengths. As a result, several beneficial effects of composite behavior in terms of strengths are achieved. In addition, the ductility and the energy absorption capability of CFST columns made with fiber reinforced concrete are significantly enhanced because the use of fiber contributes to stiffness which delays the growing of lateral deflection.

Based on the above survey, it appears that using fiber reinforced CFST column is an effective alternative to enhance structural behavior of composite columns. In fact, the studies conducted on steel tube columns filled with glass fiber reinforced SCC free or not of nS are particularly missing.

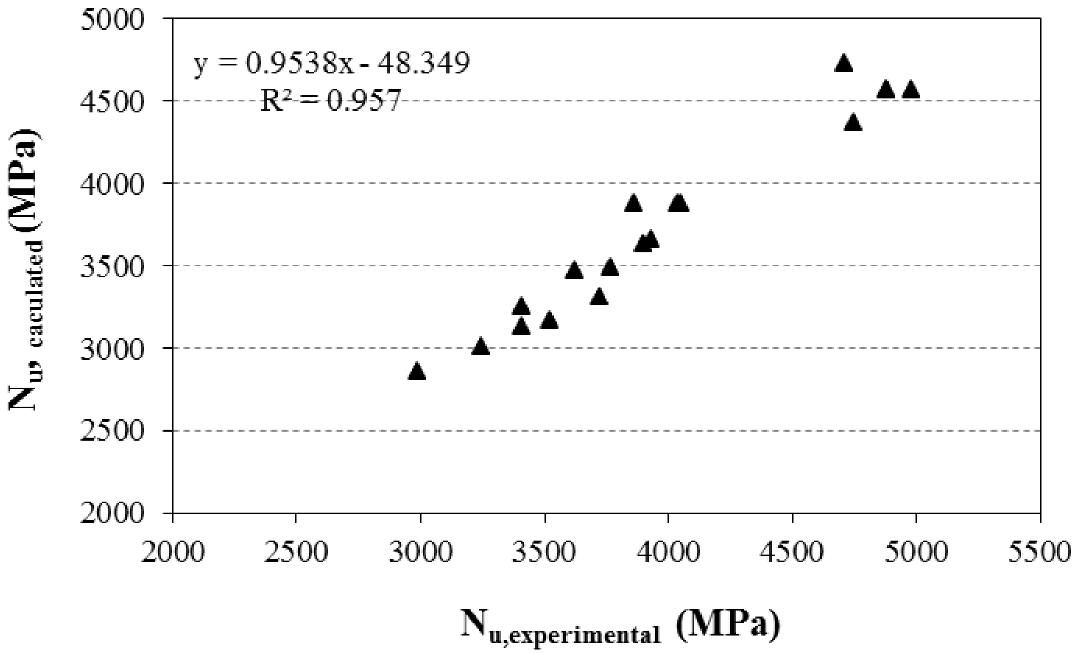

Figure 2.12 Experimental ultimate strength versus calculated ultimate strength (Zhu et al., 2010)

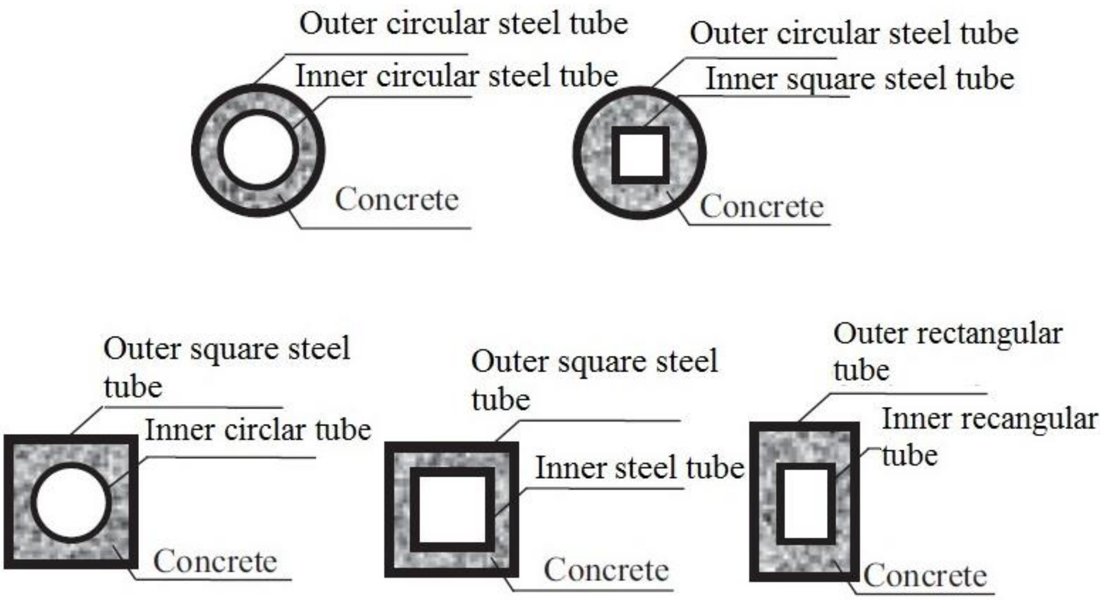

Figure 2.13 Various typical profiles of concrete filled double skin tubes sections (Lu et al., 2010)

CHAPTER 3

METHODOLOGY

In this study, an experimental investigation was firstly performed to study the fresh and hardened properties of glass fiber (GF) reinforced self-compacting concrete (GFRSCC) incorporating nano-silica (nS). To this aim, five volume fractions of GF and three different nS contents were used at w/b of 0.35 to cast 15 GFRSCC mixtures. The samples were cured for 28 and 90 days. Fresh and hardened properties were examined and analysed with respect to nS content and presence of GF. After that, a detailed numerical analysis was conducted to understand the structural response of the steel tubular columns filled with GFRSCC under the action of uniaxial compression. For this, the capacity of such composite columns were evaluated by using four international design codes, namely, Eurocode 4, ACI, AIJ and DL/T. The main experimental and numerical parameters of the study were nS and GF content, strength level of core concrete, diameter to thickness (D/t) ratio, yield strength of the steel tube used. The details of the study are given below.

3.1 Experimental study

3.1.1 Materials

The mixtures produced in this study were prepared with CEM-I 42.5R Portland cement (PC), silicon dioxide nanoparticles, and fly ash (FA). The utilized cement has a Blaine fineness of 326 m^2/kg and a specific gravity of 3.15. Commercial hydrophilic fumed silica manufactured in Belgium imported by Evonik industries in Istanbul was utilized in this investigation. The specific surface area of nano particles was 150 m^2/g. Local FA was supplied by the Thermal Power Plant in Çatalağzı - Turkey. In all mixture proportions the cement content was replaced with FA by one level of 25% by the weight. Table 3.1 provides an account on the chemical compositions as well as the physical traits of PC, nS, and FA. Photographic view of nS powder is given in Figure 3.1.

Table 3.1 Chemical and physical properties of PC, nS and FA

Analysis report	PC	FA	nS
CaO (%)	62.12	4.24	-
SiO_2 (%)	20.25	56.2	$\geq$ 99.8
Al_2O_3 (%)	5.31	20.17	-
Fe_2O_3 (%)	4.04	6.69	-
MgO (%)	2.82	1.92	-
SO_3 (%)	2.73	0.49	-
K_2O (%)	0.92	1.89	-
Na_2O (%)	0.22	0.58	-
Loss of ignition (%)	3.02	1.78	$\leq$ 1.0
Specific gravity	3.15	2.25	2.2
Blaine fineness (m^2/kg)	326	379	-
Surface-volume ratio (m^2/g)	-	-	150±15
Average primary particle size (nm)	-	-	14

Figure 3.1 Silicon dioxide nano particles

The GF came with a glass content of 95%, tensile strength of 3400 MPa and specific gravity of 2.60. The other specifications of GF are tabulated in Table 3.2. Moreover, the photographic view of the GF used in this study shows in Figure 3.2.

Table 3.2 Properties of GF

Modulus of elasticity	77 GPa
Application temperature limits	-60°C - +650°C
Melting temperature	1120°C
Specific weight	2.60
Fiber length	12 mm

Figure 3.2 Glass fiber used in this study

In all self-compacting concrete (SCC) mixtures, the coarse aggregate was crushed limestone produced by mixing two different maximum sizes. Besides river sand was used as a fine aggregate. The coarse, medium and fine aggregate had specific gravity of 2.72, 2.70 and 2.66, respectively. The particle size categorization was achieved through sieve analysis. Figure 3.3 portrays the gradation curves of the each type of aggregate as well as the aggregate mix curve.

High range water reducing admixture (HRWRA), based on polycarboxylic-ether formulation with a specific gravity of 1.07, was used in all mixes to attain the required slump flow for SCC. The properties of HRWRA are tabulated in Table 3.3.

Table 3.3 Properties of HRWRA

Properties	HRWRA
Name	Glenium 51
Specific gravity	1.07
State	Liquid
Color tone	Dark Brown
Chemical explanation	Polycarboxylic polymer
Optional dosage	1-2% by binder content

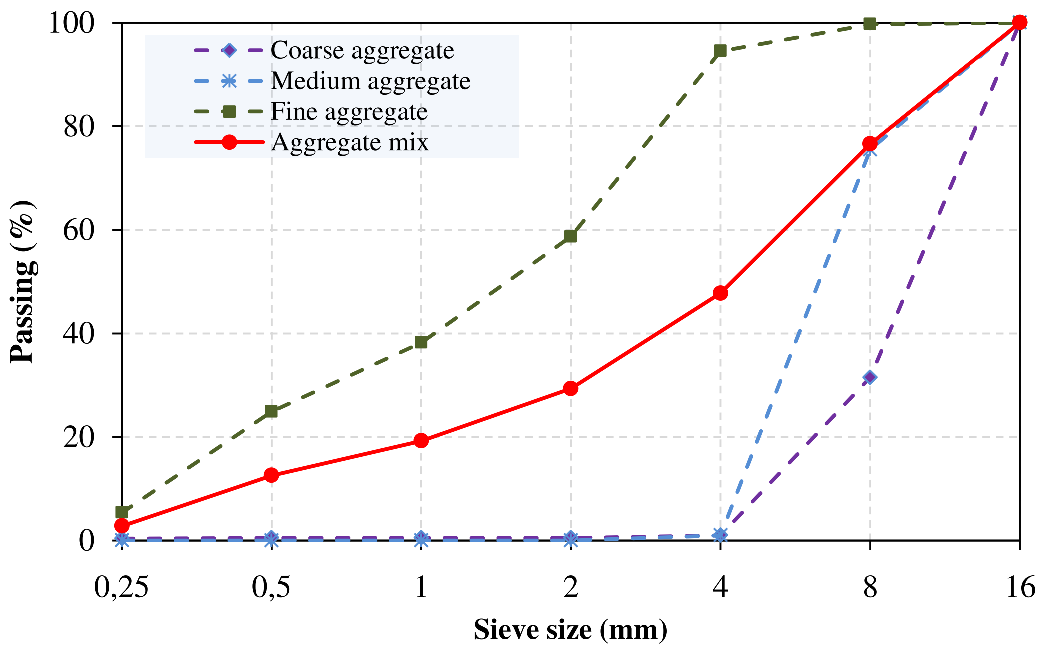

Figure 3.3 Aggregate gradation curve

3.1.2 Mixture proportioning and casting

Fifteen mixtures were prepared to encompass an array of distinct mixtures with a constant w/b ratio of 0.35 and a total binder content of 550 kg/m^3. Various substitution levels of nS as 0%, 2%, and 4 % by the weight of cement were utilized. On the other hand, GF volume fractions of 0%, 0.35%, 0.70%, 1.0%, and 1.5% by the total volume of concrete were incorporated. For all the mixtures, a constant substitution extent of 25% by total weight of the binder content was contemplated for FA. The total volume of aggregate in all mixtures was produced by mixing 25% crushed limestone coarse aggregate, 25% crushed limestone medium aggregate and 50% river sand. The SCC mixtures at each level of nano particles content were implemented with the five volume fractions of GF.

Information on the proportioning of the GFRSCC mixture is provided in Table 3.4. Regarding mix ID, the glass fiber as GF and nano-silica as nS. As an example, nS0GF0 represents plain concrete (free of nS and glass fiber), whereas nS2GF35 signifies that the SCC mixture comprises 2% nano-silica content and 0.35% glass fiber content.

To achieve the same homogeneity and uniformity in all mixtures, a special batching and mixing procedure were followed since mixing sequence and duration are very vital in the production. Regarding to this procedure, the both fine and coarse natural aggregate were mixed for about one minute in a power-driven revolving pan mixer. The addition of mixing water was added into two steps. About quarter of the total water quantity was added in the second minute of mixing stage. Then, at the third minute constitutes was allowed to absorb water. Afterwards, the powder materials (PC+FA and/or nS) were added to the wetted aggregate mixture for mixing extra 2 min. For the mixtures without fiber, the remained mixing water, including HRWRA was added into the mix to be mixed for 3 min. After that the mixture was left to rest for about 2 min. Finally, the concrete was mixed for additional 2 min. For the mixture incorporating GF, the fiber was added before adding the rest of mixing water with HRWRA. The SCC mixtures containing fiber were mixed for 5 min. and then left to rest for 2 min. Thus, the SCC mixtures without fiber were mixed for a total time of 9 min., while those including GF were mixed for a total time of 11 min. excluding the resting time. At the end of mixing stage, the fresh mixtures were poured into the moulds to complete casting process. After casting, all moulded specimens (150 mm cubes, Ø100x200 mm cylinders, Ø150x300 mm cylinders, and 100x100x500 mm prisms) were covered with plastic sheet to eliminate water evaporation, and left in the casting room for 24 h at 20±2 °C and then they were de-moulded and 28 and 90 days water curing period was applied. Figure 3.4 presents wetted mixture with GF.

Table 3.4 Details of mix proportions in kg/m^3

Mixture ID	w\b	Cement	FA	nS	Water	Gravel		Natural sand	HRWRA	GF
						Coarse	Medium			
nS0GF0	0.35	412.5	137.5	0	192.5	384.3	384.3	768.5	5.5	0
nS0GF35	0.35	412.5	137.5	0	192.5	384.3	384.3	768.5	6.05	9.1
nS0GF70	0.35	412.5	137.5	0	192.5	384.3	384.3	768.5	7.15	18.2
nS0GF100	0.35	412.5	137.5	0	192.5	384.3	384.3	768.5	7.69	26
nS0GF150	0.35	412.5	137.5	0	192.5	384.3	384.3	768.5	8.79	39
nS2GF0	0.35	401.5	137.5	11	192.5	383.3	383.3	766.6	7.14	0
nS2GF35	0.35	401.5	137.5	11	192.5	383.3	383.3	766.6	12.08	9.1
nS2GF70	0.35	401.5	137.5	11	192.5	383.3	383.3	766.6	13.18	18.2
nS2GF100	0.35	401.5	137.5	11	192.5	383.3	383.3	766.6	14.28	26
nS2GF150	0.35	401.5	137.5	11	192.5	383.3	383.3	766.6	15.93	39
nS4GF0	0.35	390.5	137.5	22	192.5	382.4	382.4	764.7	20.88	0
nS4GF35	0.35	390.5	137.5	22	192.5	382.4	382.4	764.7	21.99	9.1
nS4GF70	0.35	390.5	137.5	22	192.5	382.4	382.4	764.7	23.62	18.2
nS4GF100	0.35	390.5	137.5	22	192.5	382.4	382.4	764.7	24.72	26
nS4GF150	0.35	390.5	137.5	22	192.5	382.4	382.4	764.7	26.37	39

Figure 3.4 GF with other SCC mixture components

3.1.3 Evaluation of fresh properties

The recommendations forwarded by the EFNARC (2005) (European Federation for Specialist Construction Chemicals and Concrete Systems) were complied with during the execution of the slump flow diameter, $T_{500\ mm}$ slump flow time, V-funnel flow time, L-box height ratio, and L-box T_{200} and T_{400} flow time tests. A rough draft of the testing equipment is provided in Figure 3.5. Utilized for describing the flowability of newly prepared concrete in unrestricted circumstances, slump flow value testing involves a rather delicate procedure. This procedure represents the initial inspection to ensure that the consistence of the fresh concrete satisfies the specification. Under normal circumstances, the slump flow value test is applicable for all SCC mixtures. Concrete segregation resistance and uniformity can be achieved by way of testing and gauging the $T_{500\ mm}$ time. The calculated time takes for concrete flow to arrive at a diameter of 500 mm (EFNARC, 2005). EFNARC categorizes the standard slump flow for an array of applications into three classes. Table 3.5 exhibits the upper and lower limits for these classes as well as the standard application areas.

The V-funnel flow time test value describes the filling ability (fluidity) as well as flow-rate of fresh concrete. The V-shaped funnel used in this research had a volume of approximately 0.0105 m^3. The computation for the V-funnel flow time is achieved with the employment of a V-shaped funnel. This funnel is topped-up with fresh cement which is then allowed to flow out. The length of time it takes for the funnel to be emptied of cement is deemed the V-funnel flow time.

The viscosity of the SCC can be ascertained through a computation of the $T_{500\ mm}$ slump flow time and V-funnel flow time. Although viscosity cannot be straight forwardly determined this way, the outcomes from the above mentioned computations can verify the flow rate linked to viscosity. Viscosity classifications according to EFNARC (2005) in terms of the calculated V-funnel and T_{50} slump flow times are displayed in Table 3.5.

The L-box test can be employed to assess the capacity of a fresh concrete mix to flow through cramped spaces and tight gaps (including areas with congested reinforcement) without segregation and loss of uniformity. This test entails the horizontal movement of a known volume of fresh concrete through openings between smooth, vertical reinforcing rods. The height of concrete, clear of the reinforcing rods is then calculated for a result. The passing capacity classes in related to the L-box height ratio values can be viewed in Table 3.5.

Table 3.5 EFNARC recommendation (EFNARC, 2005)

Class		**Slump flow diameter (mm)**
Slump flow classes		
SF1		550-650
SF2		660-750
SF3		760-850
Class	T 50 (s)	V-funnel time (s)
Viscosity classes		
VS1/VF1	≤2	≤8
VS2/VF2	>2	9-25
Passing ability classes		
PA1	≥0.8 with two rebar	
PA2	≥0.8 with three rebar	

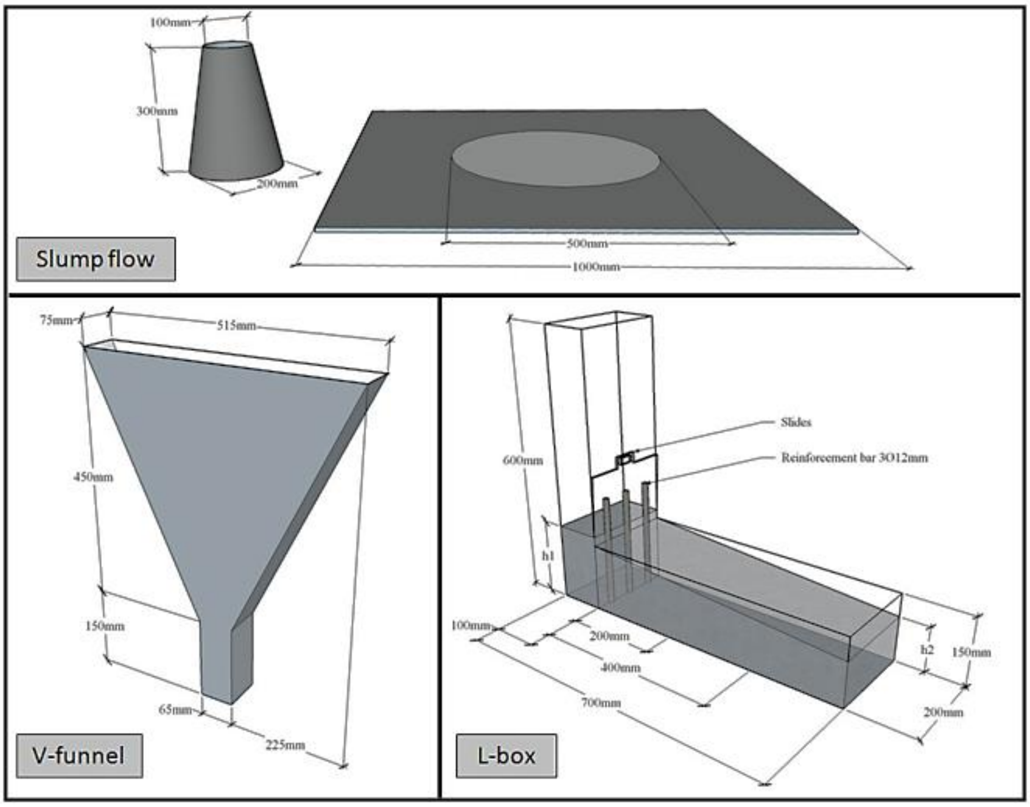

Figure 3.5 Sketch of test apparatus used for measuring the fresh state of SCC (Güneyisi et al., 2015b)

The rheology of the mixture is computed with the employment of an ICAR rheometer (Figure 3.6a). A fresh concrete mixture is introduced into a vessel measuring 305 mm in diameter up to a height of 305 mm. The radius of the inner cylinder (R_i) is 63.5 mm, while that of the outer cylinder (R_o) is 152.5 mm. The outer cylinders are ribbed to avert slipping that may occur between the steel surfaces and the concrete (Saak et al., 2001a). A four-bladed vane with a diameter and height of 127 mm is positioned in the centre of the fresh concrete mixture-filled vessel. As exhibited in Figure 3.6b, there is an 89 mm space above and below the vane. Subsequent to recording the breakdown rate and time, number of points, time for each point, initial speed, and final speed as an input, the flow curves for each fresh concrete mixture was computed. The initial vane rotation speed was 0.5 rps for a 20 second breakdown period. Torque measurements were then noted for seven speeds stretching in a downward arrangement from 0.5 rps to 0.05 rps. In order to distinguish the rheological parameters of the characteristics of fresh concrete, Equation 3.1 was harnessed to plot the flow curves in relative units following computation for the best fit in line with regards to all mixtures.

$$T=G+HN \quad (3.1)$$

Where T, G, H, and N denote the torque (Nm), the incline of this line (Nm.s) is associated to plastic viscosity, while the intercept of this line with the T-axis (Nm) is related to the rotational speed (rev/s) (Koehler and Fowler, 2004).

The formula proposed by Ferguson and Kembłowski (1991) provides the opening for converting 'N' and 'T' into basic rheological parameters. The rotational velocity and torque acquired through the rheometer needs to be taken into consideration during computations to depict non-linear rheological characteristics. Equations 3.2 and 3.3 below were modified by Nehdi and Rahman (2004) to realize specific objectives.

$$\tau = \frac{(R_i^2+R_o^2)}{4\pi h R_i^2 R_o^2} T \quad (3.2)$$

$$\dot{\gamma} = \frac{(\mathrm{R_i^2+R_o^2})}{(\mathrm{R_o^2-R_i^2})} \mathrm{N} \quad (3.3)$$

Formulas 3.2 and 3.3 can be applied for any kind of material separately from the actual rheological characteristics. The velocity distribution in the gap needs to be in a linear fashion and this is only achievable if the opening is less than ($R_i/R_o > 0.99$) (Feys et al., 2007). A minor error in the test outcome is to be expected in the event this requirement is not met (Nehdi and Rahman, 2004; Macosko, 1994).

In a similar vein, 'G' and 'H' were utilized in the equation 3.4 and 3.5 of Reiner-Riwlin to ascertain plastic viscosity, μ, and yield stress, τ_o separately from the dispersion of velocity in the gap between the outer and inner cylinders (Wallevick, 2003; Hu et al., 1995).

$$\tau_0 = \frac{G}{4\pi h}\left(\frac{1}{R_i^2} - \frac{1}{R_o^2}\right)\frac{1}{\ln\left({R_o}/{R_i}\right)} \quad (3.4)$$

$$\mu = \frac{H}{8\pi^2}\left(\frac{1}{R_i^2} - \frac{1}{R_o^2}\right) \quad (3.5)$$

The modified Bingham model, as portrayed in Equation 3.6, is also suitable for describing the rheological behaviour of SCC. This model is not only considered an expansion of the Bingham model with a second order term, but also a second order Taylor development of the Herschel-Bulkley equation (Feys et al., 2007).

$$\tau = \tau_0 + \mu\dot{\gamma} + c\dot{\gamma}^2 \quad (3.6)$$

In the modified Bingham model, the taking of the ratio of the second order term to the linear term can pave the way towards describing non-linear behaviour, indicating shear thinning, shear thickening, and the Bingham model when $c/\mu < 0$, $c/\mu > 0$, and $c/\mu = 0$ respectively.

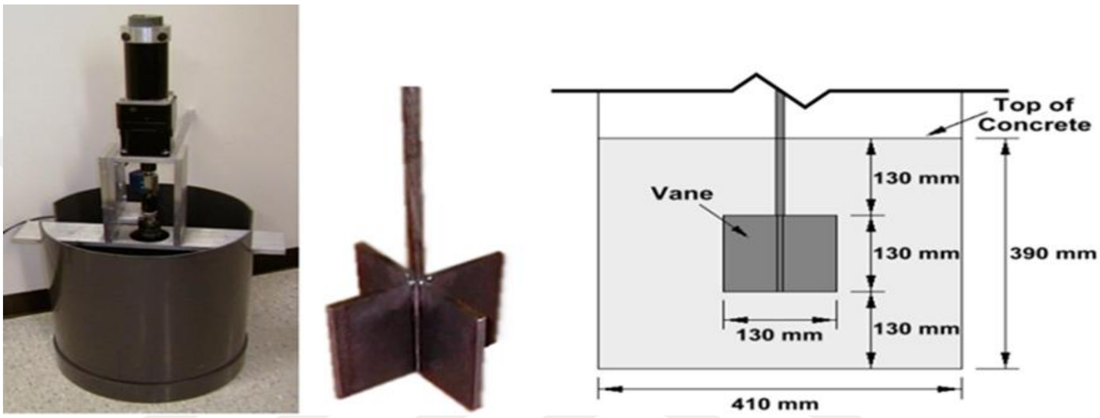

a) b)

Figure 3.6 Views of a) rheometer and b) detailed schematic representation

3.1.4 Evaluation of mechanical properties

Compressive testing was computed according to ASTM C39 (2012). The testing was likewise performed on three cubic forms measuring 150x150x150 mm by the 2000 kN capacity-testing device at 28 and 90 days. Static modulus of elasticity was determined on cylinder specimens, which is 150×300 mm as per ASTM C469 (2014). The modulus of elasticity is found by measuring the slope of the straight line portion of the stress strain curve. According to ASTM C496 (2011), splitting tensile strength was examined at 28 and 90 days. For this, three cylinder samples for each mixed examination, which dimension is Ø100x200 mm, though, It has been identified the splitting tensile strength (f_{st}) in MPa by Equation 3.7.

$$f_{st} = 2P/\pi dL \quad (3.7)$$

Where P, d, L is the maximum load in N, diameter in mm, and length of the cylinder mould correspondingly.

Many ways have been suggested by international standards to determine the fracture parameters. A simplest methods to calculate the fracture energy, as the greatest important fracture parameter of concrete, fracture energy was calculated by using work of fracture method introduced by the technical committee RILEM 50-FMC (1985). Prismatic specimens having 100x100x500 mm dimensions have been used. In this test, exhausting three-point bending test on notched prisms and determining the work wanted to generate a crack with unit surface area planned in a plane parallel to the crack direction, as the beam is broken in two parts, the specific fracture energy is calculated according to Equation 3.8 (Beygi et al., 2014).

$$G_f = \frac{W_f}{b(d - \alpha_0)} \tag{3.8}$$

Where W_f, b, d, α_0 are total amounts of fracture works, width of the beam, height of the beam, and notch depth, respectively. A closed-loop testing machine with a capacity of 250 kN was utilized to offer the load, Figure 3.7. Moreover, as shown in Figure 3.7, the ratio of notch to depth (a/D) of the beam was 0.4, and the notch was created by sawing in order to accommodate large aggregates in more abundance decreased the effective cross section to 60x100 mm. The span between two supports was 400 mm, and the mid span deflection was calculated by a linear variable displacement transducer (LVDT). Also, net flexural strength (f_{flex}) providing from the notch beam, moreover, it was calculated as providing in Equation 3.9.

$$f_{flex} = \frac{3P_{max}\,S}{2B(W-a)^2} \tag{3.9}$$

Where P_{max} is fracture load, S is the span of beam, B is width of beam, W is depth of beam and a is notch depth of beam. As well, it can be seen in Figure 3.8, the test is usually stopped at B, before the specimen is fully broken. Considering that the area under the ideal curve is intended and the effect of must be eliminated (Beygi et al., 2014) proposed the following expression to calculate the area under the ideal load-displacement curve as calculated according to Equation 3.10.

$$W_f = W_m + 2\,(\frac{A}{u_B - u_A}) \qquad (3.10)$$

Where W_m is the area under the load–displacement curve which is corresponding to the surface area AMBA and A is a coefficient introduced.

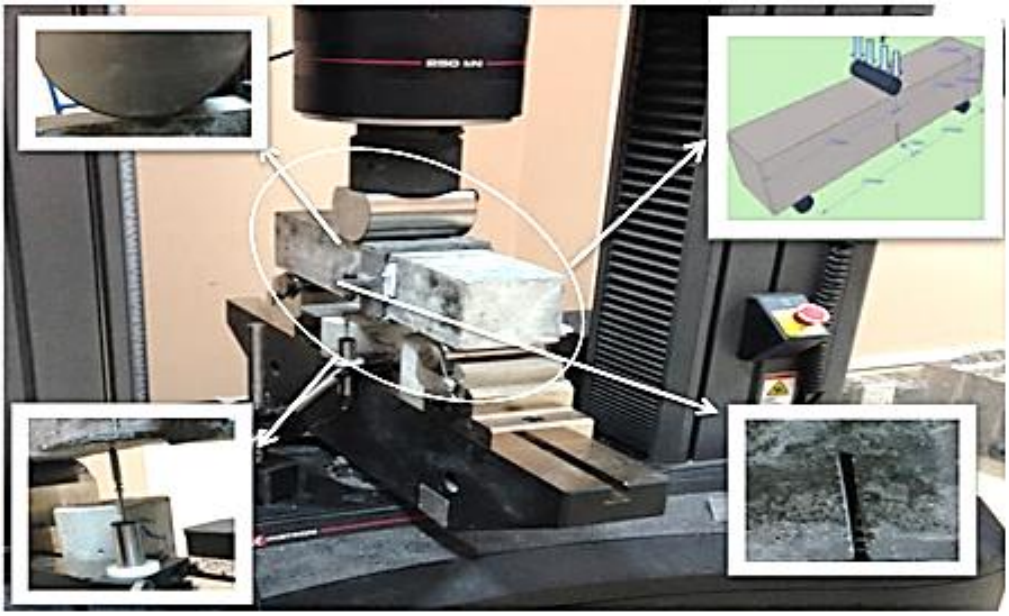

Figure 3.7 Fracture test set up for the beam specimen

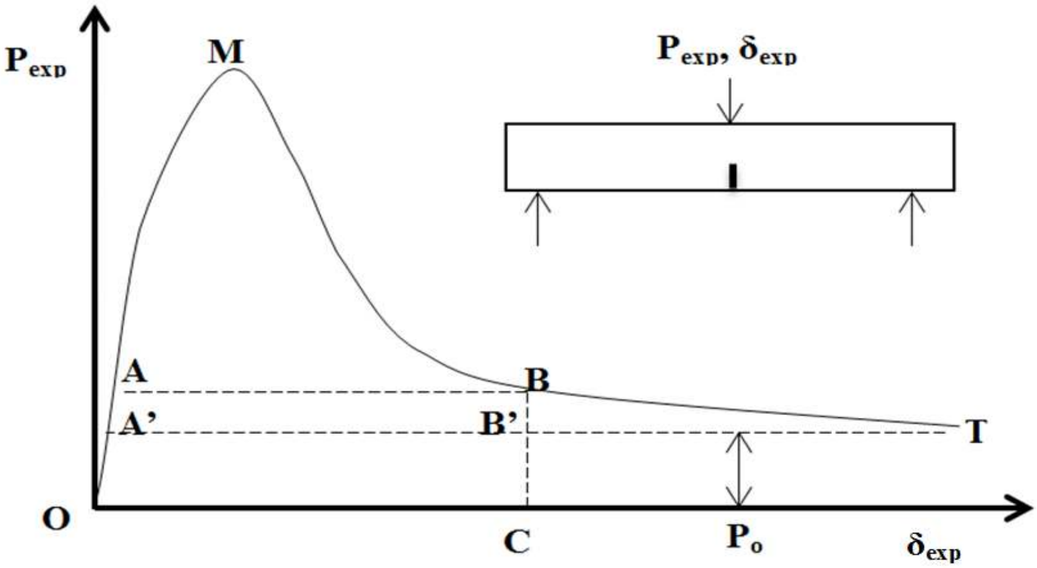

Figure 3.8 Fracture energy relationship (Beygi et al., 2014)

3.2 Numerical study

3.2.1 Introduction to CFST column

The application of concrete-filled steel tubular (CFST) columns as composite members in construction sectors have been extensively increasing day by day. Nowadays, industrial plants, subways, multi-storey construction and arch bridges construct with these composite members. The CFST columns characterized by several advantages in terms of structural performance such as superior strength and stiffness, proper ductility, low brittleness and good strain energy absorption abilities. CFST columns construction has established to be cost-effective in building resources materials as well as satisfying for rapid construction and therefore its application has been developed in construction building industries worldwide (Yuan and Yang, 2013).

The performances of concrete and steel with the presence of new innovative materials have significantly enhanced and the cross section with these materials becomes lighter, hence, the load carrying capability of the column is significantly influenced (Güneyisi et al., 2016a). The main benefits of CFST columns can be illustrated as follows (Chang et al., 2013):

- The confinement effect of surrounding steel as well as contribution in load carrying capacity of CFST columns represent the main structural advantages resulting from the use of such columns.
- Inhibition or delay of local buckling of the steel tube infilled with concrete.
- The construction period is also diminished by excluding the permanent formwork usually used for conventional concrete steel column.

From the above, the use of concrete-filled steel tubes in various areas of constructions is becoming an attractive solution. Moreover, as a result of the increase in the load carrying capacity, stiffness, and ductility as well as economy and rapid construction, use of CFST columns has become prevalent (Chang et al., 2013; Güneyisi et al., 2016a). In order to dependably predict the strength and ductility of circular CFST columns, correct constitutive models must be developed for confined concrete. However, it has been found that there are inconsistencies in empirical models projected by investigators for confined concrete (Liang and Fragomeni, 2009). On the other hand, there are also inconsistencies in the capacity prediction of axially loaded CFST column given in current design codes such as Eurocode 4 (2004) and ACI 318 (2005).

3.2.2 Details of study

The main objective of the analytical study is to evaluate the behavior of structural steel tube infilled with GF reinforced self-compacting concrete (GFRSCC) subjected to compressive load. Towards this aim, the first part started with applying four available codified formulations, namely, Eurocode 4 (2004), ACI 318 (2005), Japanese (AIJ) (2001), and Chinese (DL/T) (1999) so as to compute the axial load carrying capacity of circular CFST short columns. The calculation involved the use of set of data comprising the experimented compressive strength (results of 15 concrete mixtures tested experimentally at 28 and 90 days), three different column outer diameters and three steel yield strengths. Moreover, to study the structural responses of CFST column under compression forces, different aspects have been employed. The interaction between both of diameter to thickness (D/t) ratio and core concrete strength and the variance of axial capacity have been graphically presented. Despites, the same parameters included in the experimental research- nano silica (nS) and GF and curing period – have been also discussed with respect to their actions on the performance of CFST column. The test configuration taken into account is uniaxial compression test which is schematically described in Figure 3.9.

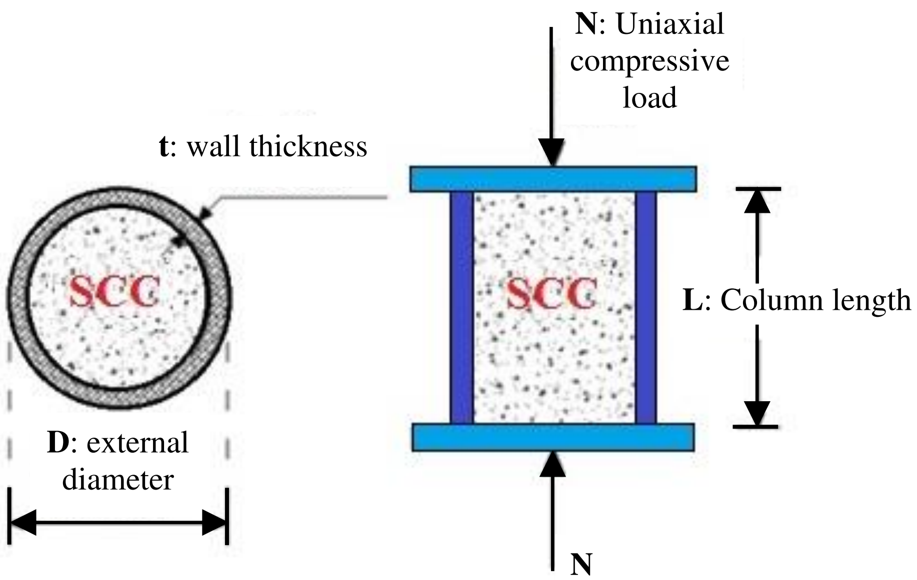

Figure 3.9 Presentation of load applied to the section of circular CFST column

3.2.3 Design code formulas

3.2.3.1 Eurocode 4

One the most reasonable treatment to date is that which is modeled by the Eurocode 4 (2004) (EC4). In this relation, the contributions of the concrete core and the steel tube as well as the confinement effect of the steel tube are considered. In this regard, the confinement coefficients for the steel (η_a) and core of concrete (η_c) are involved. Therefore, both of the steel and concrete strengths are influenced in such a way that the triaxial state of stress condition leads to increase strength of concrete core by η_c, whereas the hoop stresses yield a decrement in the steel yield strength by η_a.

The equations recommended by EC4 for computing axial capacity of a circular CFST column ($N_{u,\,EC4}$) are proposed as:

$$N_{u,EC4} = \left(1 + \eta_c \frac{t}{D} \frac{f_y}{f'_{cyl,150}}\right) f'_c A_c + \eta_a f_y A_s \tag{3.11}$$

Where

$$\eta_a = 0.25(3 + 2\bar{\lambda}) \qquad (\eta_a \leq 1.0) \tag{3.12}$$

$$\eta_c = 4.9 - 18.52\bar{\lambda} + 17\bar{\lambda}^2 \quad (\eta_c \geq 0) \tag{3.13}$$

in which the relative slenderness ($\bar{\lambda}$) of CFST column can be calculated from following equation:

$$\bar{\lambda} = \sqrt{\frac{N_{pIR}}{N_{cr}}} \tag{3.14a}$$

Where:

N_{pIR} is the cross-section plastic resistance of the CFST column, given as:

$$N_{pIR} = f_y A_s + f'_{cyl,150} A_c \tag{3.14b}$$

N_{cr} is the Euler buckling load of the pin-ended CFST column, represented by:

$$N_{cr} = \frac{\pi^2 (EI)_{eff^2}}{I^2} \tag{3.14c}$$

Where:

$(EI)_{eff^2}$ is the effective flexural stiffness of CFST and can be computed as:

$$(EI)_{eff^2} = E_s I_s + K_e E_{c2} I_c \tag{3.14d}$$

Where:

E_s and E_{c2} is the elastic modulus of steel and concrete, respectively. The elastic modulus of concrete $= 22000\left[\left(f'_{cyl,150} + 8\right)\right]^{0.3}$

Typically, when $\bar{\lambda} = 0$, the sectional capacity (the zero length strength), $P_{0;EC4}$ can be simplified as

$$P_{0,EC4} = \left(1 + 4.9\frac{t}{D}\frac{f_y}{f'_{cyl,150}}\right) f'_{cyl,150} A_c + 0.75 f_y A_s \tag{3.15}$$

3.2.3.2 ACI 318R code

The American Concrete Institute (ACI-318R, 2005) for calculating the ultimate axial capacity of the circular CFST column was designated as $N_{u,\,ACI}$ in calculations. This relation does not contain the interaction between the steel tube and concrete core and the effectiveness of the concrete confinement. The steel tube limiting thickness to prevent buckling is based on realizing yield stress in a hollow tube under the action of monotonic axial loading which is not a significantly requirement for CFST columns. The equation for axial capacity of a circular CFST column, N_u is expressed by following formulae:

$$N_{u,ACI} = 0.85\, f'_{cyl,150} A_c + f_y A_s \tag{3.16}$$

Where $f'_{cyl,150}$ is the concrete cylinder compressive strength (150×300 mm), A_c is the concrete specimen core cross-sectional area, f_y is the yield stress of steel, and A_s is the cross sectional area of steel.

3.2.3.3 AIJ

AIJ (1997) (Architectural Institute of Japan. Recommendations for design and construction of concrete filled steel tubular structures, 1997) is another international code used for determining the capacity of the composite columns. In particular, AIJ conservatively evaluate the effects of confinement, which provide significant underestimations on the sectional capacity of CFST columns. Thus, when using different CFST design provisions to forecast the sectional ability of CFST columns, the estimates by AIJ compared with the test results are expected to be more conservative (Wang et al., 2015). The equation for axial capacity of a circular CFST column, $N_{u,\,AIJ}$ is expressed by following equation:

$$N_{u,AIJ} = 0.85\, f_{cyl,100}\, A_c + (1.0 + \eta) f_y A_s \quad \left(\frac{l_k}{D} \leq 4\right) \tag{3.17}$$

where l_k is the effective length of a CFST column; and η is the confinement factor which is equal to 0.27. According to this formula, the composite action represented by the confinement factor improves the load carrying capacity which is independent of the material strength and the cross section geometry of the column (Lu and Zhao, 2010).

3.2.3.4 Chinese code DL/T

The formulae proposed by Chinese code DL/T (1999) considered CFST column has one material not as a composite with a total area of A_{sc} with a nominal yielding strength of f_{scy}. Moreover, Chinese code DL/T (1999) introduces a factor of ξ for the confinement effect to describe the action between the concrete and steel tube. The equations for axial capacity of a circular CFST column ($N_{DL/T}$) are given as:

$$N_{u,DL/T} = f_{scy} A_{sc} = f_{scy}(A_s + A_c) \tag{3.18}$$

In which:

$$f_{scy} = (1.212 + B\xi + \xi^2 x^2) f_{ck} \tag{3.19a}$$

$$B = 0.1759 \frac{f_y}{235} + 0.974 \tag{3.19b}$$

$$C = -0.1038 \frac{f_{ck}}{20} + 0.0309 \tag{3.19c}$$

$$\xi = \frac{A_s f_y}{A_c f_{ck}} \tag{3.19d}$$

$$f_{ck} = 0.67 f_{cu} \tag{3.19e}$$

Where: ξ the confinement factor; A_{sc} and f_{scy} the area of composite section and the nominal yielding strength of the composite section respectively, f_{cu} the compressive strength of 150 mm cube, and f_{ck} the characteristic concrete strength.

3.2.4 Details of main computation steps

The computation of ultimate axial capacities of the circular self-compacting concrete-filled steel tubular by using the four design codes (EC4, ACI 318, AIJ and DL/T) which have been illustrated earlier in section 3.2.3 conducted as follows:

- The experimental results of compressive strength at 28 and 90 days have been employed.
- So as to comprise different specification regarded steel material characteristics, yield strength of the steel tube fy selected as 185, 275 and 450 MPa.
- Three different diameter-to-thickness (D/t) ratios of the CFST column cross section of 30, 60 and 90 were utilized in all computations.
- The length to diameter ratio of short composite columns was 2 to ensure that they would be with a small slenderness effect and would not fail in overall buckling. At the same time wall thickness of the steel tube was 3.5 mm.

It should be mentioned that the conversion of compressive strength of standard concrete cylinders 150*300 mm (f_c') to compressive strength of 150 mm cubes (f_{cu}) calculated by using Table 3.6 (Eurocode 2, 2004).

Table 3.6 Conversions between f_c' and f_{cu} (Eurocode 2, 2004)

Compressive strength of concrete cylinder (150*300 mm) (MPa)	**Compressive strength of 150 mm cube (MPa)**
12	15
16	20
20	25
25	30
30	37
35	45
40	50
45	55
50	60
55	67
60	75
70	85
80	95
90	105

CHAPTER 4

RESULTS AND DISCUSSION OF EXPERIMENTAL STUDY

4.1 Fresh properties

The capacity to fill and the stability of GFRSCC with and without nS can be determined by four decisive factors; flowability, passing capacity, viscosity and segregation defiance. The mixture in the fresh state requires a favourable standing with regard to at least one of the aforementioned decisive factors. In order to determine the level of aforementioned factors of fabricated GFRSCCs, slump flow diameter, T_{50} slump flow time, V-funnel flow time, L-box height ratio and L-box T_{20} and T_{40} flow times were gauged and graphically represented.

The mixtures generated during this endeavour come with a slump flow diameter that varies between 615 and 745 mm. Figure 4.1 portrays the disparities in the slump flow diameter in relation to the GF volume fraction. A preliminary analysis of the slump flow diameter results (Figure 4.1) shows that folwability of fresh concrete is influenced by the use of nano material additions in SCC production and by their replacement level. This can be seen in the values of SCC+4% nS, which are considerably lower than those of free of nS. These results confirm the one mentioned, for example, by Senff et al. (2009) and Güneyisi et al. (2016b). A comparison between all mixtures results shows that the use of nS may yield in greater resistance to folwability when compared to those produced with cement only. Güneyisi et al. (2016b) state that the observed increased resistance to fluidity due to the replacement of cement by nS may result from the ultra-surface area of such particles and the occurrence of unsaturated bonds, making them oversensitive and attraction of water molecules with the surface of these particles and lead to form a typical chemical bond between water and nano particles. So, the fluidity of concrete is affected as the free water available will be decreased, and yielding in a higher viscosity of fresh mixtures. The slump flow diameter was methodically reduced with the introduction of GFs methodically reduced with the introduction of GFs. This is attributed to the fact that GFs, requisite additional quantities of water to moisturize GF and for growing internal cohesive resistance between constituents of concrete mixture (Hughes and Fattuhi, 1975; Ahmed et al., 2017). The FA25GF1.5nS4 mixture recorded the lowest slump flow diameter of 615 mm, while the FA25GF0nS0 mixture recorded the highest slump flow diameter of 745 mm. Although a reduction in the slump flow diameter was occurred with a rise in the GF volume fraction from 0% to 1.5% lead to decrease in slump flow by 8%, 10% and 12% with respect to 0%, 2% and 4% nS, respectively. Moreover, the acquired results fell within the EFNARC limitations. For example, while the inclusion of GF in excess of 0.7% led to an alteration of the slump flow category from SF2 to SF1 with nS at 4%, the introduction of more than 1% of glass fiber also altered the slump flow category from SF2 to SF1 with incorporation of 2% nS.

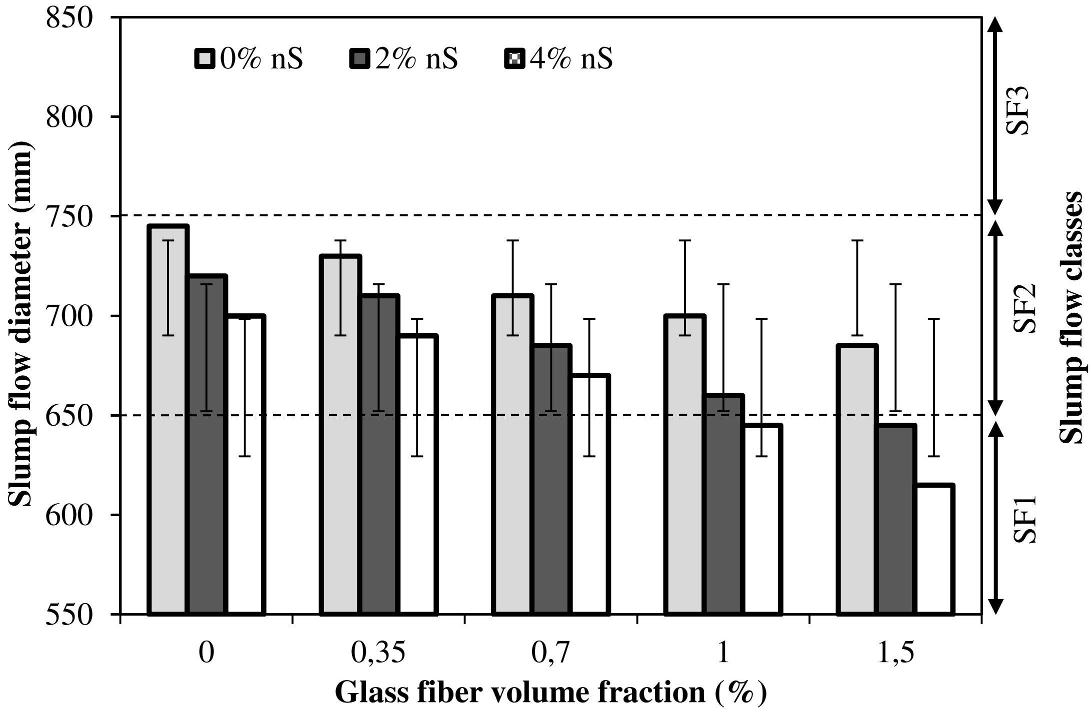

Figure 4.1 Variation of slump flow diameter and for different GF reinforced SCCs

Figure 4.2 showed that to achieve the desired workability in terms of slump flow diameter, the demand for HRWRA increased as more GF and nS incorporated into mixtures. For example, it can be seen the maximum dosage of HRWRA were achieved in nS0GF150, nS2GF150 and nS4GF150 mixes when compared to those free of GF. The HRWRA dosage for aforementioned mixes increased by about 60%, 123% and 26% due to the use of 0%nS+1.5% GF, 2% nS+1.5% GF and 4% nS+1.5% GF in producing SCC, respectively. The results demonstrated in Figure 4.2 depicted that the incorporation of 4% nS remarkably increased the required amount of HRWRA regardless GF content. The same attitude with previous studies which had presented that the incorporation of nano material contributes to the increase of HRWRA required to attain desired SCC flowability (Beigi et al., 2013; Jalal et al., 2012; Güneyisi et al., 2015b; Güneyisi et al., 2016b).

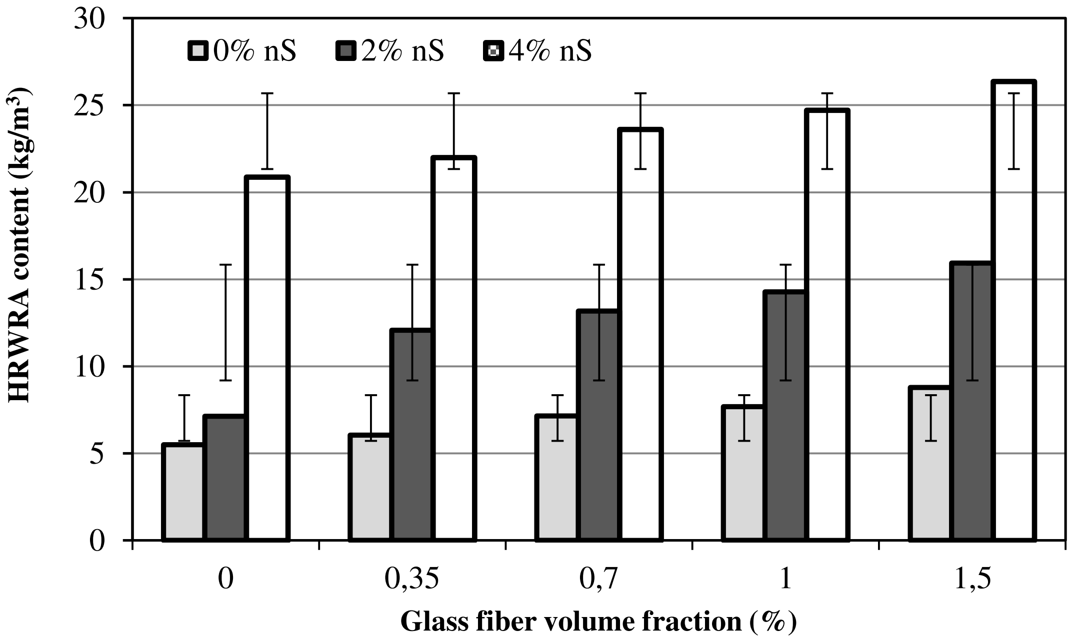

Figure 4.2 Variation of HRWRA content

The time required to reach 500 mm slump-flow of different GFRSCC mixtures were represented as columns in Figure 4.3 with respect to percent of volume fraction of GF. First of all, by comparing Figure 4.3 with Figure 4.1 it can be concluded that the recorded slump flow time, which indicate the flow ability and viscosity (by inference) of a GF reinforced SCC mixture, generally reduced with increasing slump flow diameter. It was observed from Figure 4.3 that $T_{500\ mm}$ slump flow time of SCC mixtures free of nS were 3.7, 4.2, 4.5, 5.4 and 6.5 s by considering the systemically increasing of GF content from 0 to 1.5%. Furthermore, $T_{500\ mm}$ increased by 43%, 38% and 35% with 0%, 2% and 4% nS for concretes made with various volume fraction of GF. In spite of several advantages yield by using fiber in concrete (improving durability and mechanical properties), there is strong undesirable effect on the fluidity of concrete with incorporation of fibers to it (Ding et al., 2008). For example to this behavior, Tassew and Lubell (2014) reported that the addition of GF to ceramic concrete reduces its flowability. However, in this study the presence of 25% FA in all mixture reduces the side effects of nS and GF on the workability of SCC. In the light of the fact about the role of some conventional cementitious mineral admixtures, such as FA, it can be said that the ball bearing effect yields by the spherical particles of conventional mineral admixtures can lead to reduce slump flow time (improving of concrete workability) (Uysal and Yilmaz 2011; Boukendakdji et al., 2012). Moreover, regarded the results of slump flow time, it is worth mentioning here that the range of $T_{500\ mm}$ between 2-5 s maybe preferred because the viscosity is sufficient to avoid segregation as reported by Barfield and Ghafoori (2012).

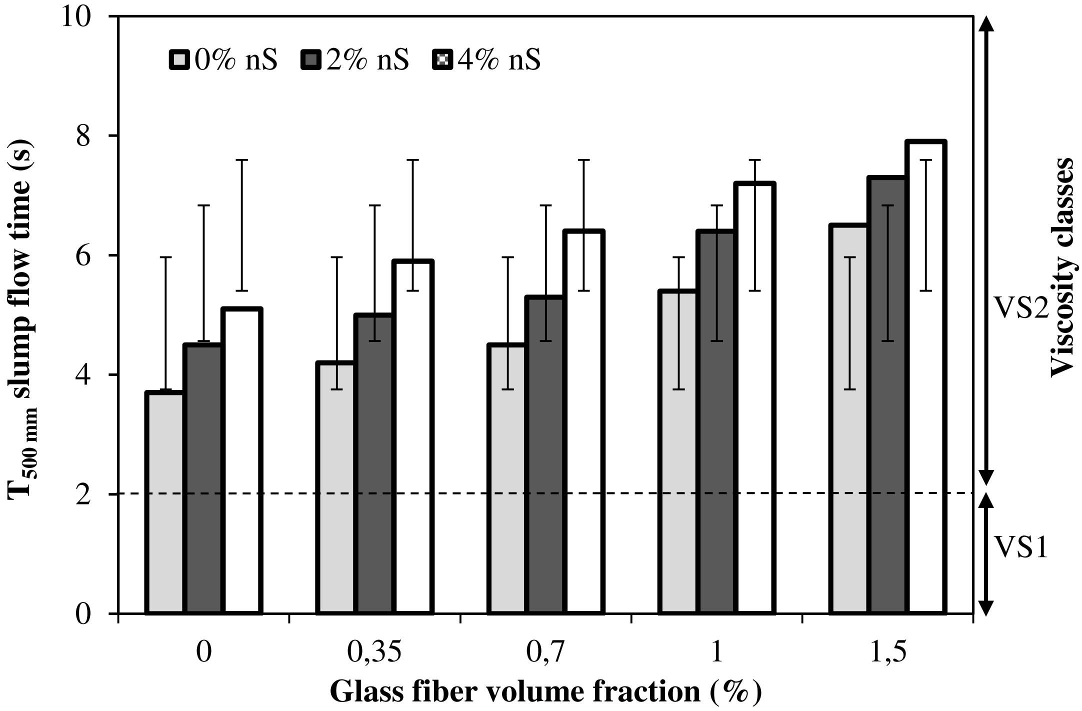

Figure 4.3 Variation of slump flow time

Figures 4.4 depicts the V-funnel flow time for the 15 different SCC mixtures produced in the experimental work study. Also in the same figure the V-funnel flow time for all SCC mixtures is presented in relation to the viscosity classes in line with the EFNARC (2005) limitation. The outcomes as can be seen, revealed the V-funnel flow times were affected by the GF and nS content. An increment in the use of GF from 0% to 1.5% resulted in a rise in V-funnel flow time from 11.5 to 16.7 s in the case of unused nS, while inclusion of 4% nS led to rise V-funnel flow time from

15.2 to 22.8 s, respectively. In fact of these obtained results one can observe that the V-funnel flow time of the mixtures exhibited an almost similar behaviour to that of the $T_{500\ mm}$ slump flow time. GF contents of 0% to 1.5% lead to increase V-funnel flow time by about 45% regardless nS contents. The results also revealed that an increase in the nS content increased the V-funnel flow time. Güneyisi et al. (2012) believed that incorporating mineral admixtures having high surface area in the binary system of SCC increases concrete viscosity and water demand of concrete will increase. In the present thesis, the mixes FA25GF1.5nS0, FA25GF1.5nS2 and FA25GF1.5nS4 recorded the highest V-funnel value alterations of 16.7, 19.3 and 22.8, respectively, while the mixtures FA25GF0nS0, FA25GF0nS2 and FA25GF0nS4 forwarded the lowest value alterations of 11.5, 13.3 and 15.2, respectively. These results disclose that an elevation in the amount of glass fibers from 0% to 1.5% together with a dissimilar quantity of nS did not lead to any alteration of the viscosity classes which was maintained as VF2. However, this raise in the usage of GF obstructed the flow of concrete through the funnel and hence raised its viscosity level.

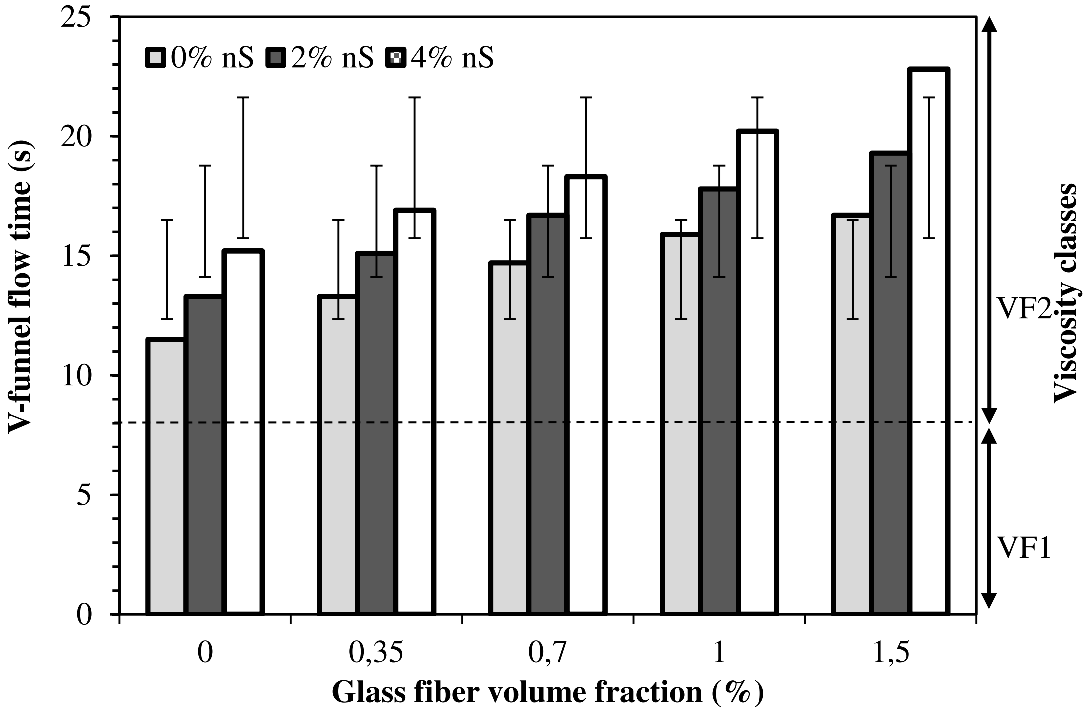

Figure 4.4 Variation of V-funnel flow time

The relation between $T_{500\ mm}$ slump flow and V-funnel flow times is presented in Figure 4.5. In accordance with EFNARC (2005) limitation, this relation can be used to evaluate concrete viscosity. It can be clearly seen, all types of SCC mixtures produced in the experimental work were classified as VS2/VF2. On the other hand, the observation of the all SCC results which are presented in Figure 4.5 revealed that there are increments in concrete viscosity due to the incorporation of nS and GF. The higher viscosity index yielded for SCC made with 4% nS and 1.5% GF, whereas the lower was observed for plain concrete, Figure 4.5. This conclusion agrees with research stating that incorporating nanoparticles generally made the concretes more viscous (Ding et al., 2008; Senff et al. 2009; Hosseini et al., 2010; Güneyisi et al., 2015b; Güneyisi et al., 2016b). Furthermore, as seen from Figure 4.5, good correlation coefficient was observed for $T_{500\ mm}$ flow time and V-funnel flow time (R^2= 0.94). Considering viscosity class of VS2/VF2, these concretes are feasible for ramps and walls, columns with respect to EFNARC recommendations (EFNARC, 2005).

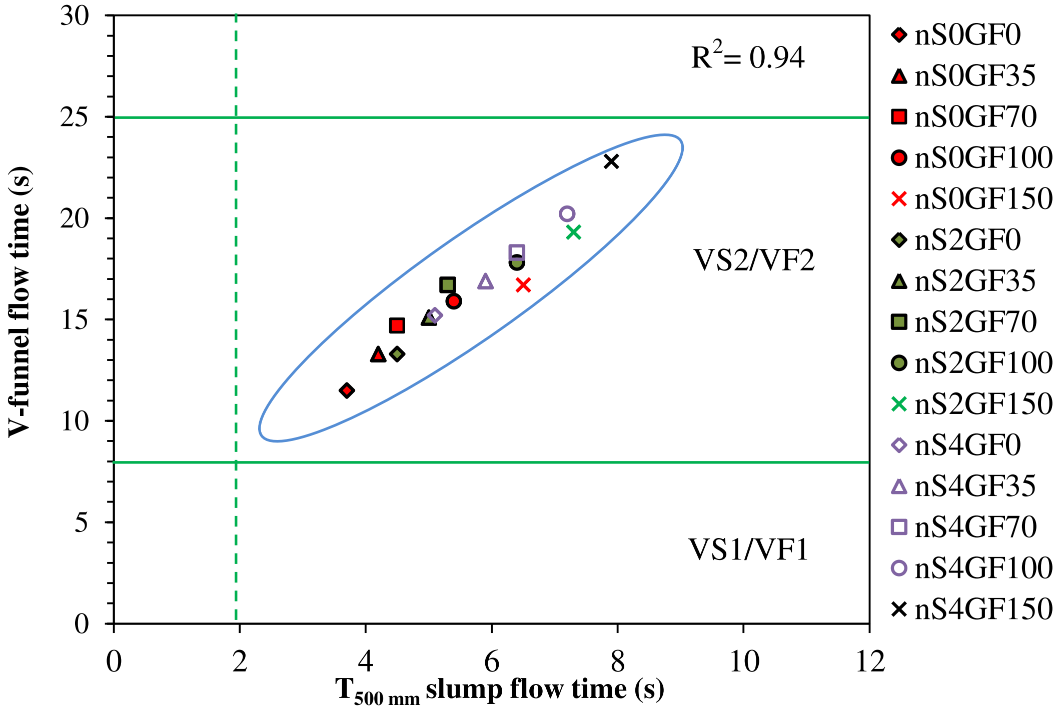

Figure 4.5 $T_{500\ mm}$ slump flow time vs. V-funnel flow time

Figure 4.6 illustrates the passing capacity of the mixtures in expressions of L-box height ratio (H2/H1). The passing capacity of the mixtures is evaluated through the three bars L-box test. According to the EFNARC (2005), the three bar L-box test involves a simulation of more congested reinforcement section and the ratio acquired through this test needs to be equivalent or higher than 0.8 to verify the acquired passing ability of the SCC for passing. In a circumstance where the L-box height ratio is observed to be 1.0, then the SCC is deemed to possess a faultless fluid conduct. In view of the above mentioned details regarding the passing capacity of SCC, it can be deemed that all the SCC mixes generated through this endeavour fall within the limitations of the EFNARC recommendations. As exhibited in Figure 4.6, the L-box height ratios for all the mixtures ranged between 0.83 and 0.94 depending mainly on the volume fraction of GF and nS incorporation level used in the concrete production. An elevation in the cohesiveness and viscosity of the SCC mixtures due to the introduction of glass fibers led to a lowering of the L-box height ratio. A further decrease in the L-box height ratio occurred when the nS content was raised. Therefore, the L-box height ratio of SCC decreases with the increasing volume fraction of GF and nS contentment due to their bearing effect on internal fraction. Also the results revealed that the use of GF caused to reduce H_2/H_1 ratio by 9.5%, 6.5% and 6.7% for concrete incorporated 0%, 2% and 4% nS, respectively. The effect of nS on passing capacity resulted herein unlike that reported by Jalal et al. (2012). In their study they observed that the addition of nS enhances the ratio of H2/H1 of the SCC. However, in this study the behavior of SCC in terms of evaluated passing ability is conformed to the performance of $T_{500\ mm}$ slump flow and V-funnel flow times.

The times needed to arrive at the 200 and 400 mm marks along the horizontal section of the L-box beginning from its sliding door are denoted by T_{200} and T_{400}. These observations can be used to give an indication about the easy flow of the fresh concrete mixtures. The results attained through this investigation regarding the T_{200} and T_{400} flow times are displayed in Figure 4.7. According to the results, an increase in the T_{200} and T_{400} flow times was detected with a rise in nS content as well as an elevation in the GF volume fraction. On the other hand, utilization of GF remarkably decreased flow times as much as 40% regardless the use of nS. The use of nS in mixtures lead to decrease of L-box height ratio as well as increased in T_{200} and T_{400} L-box flow times (Güneyisi et al., 2015b).

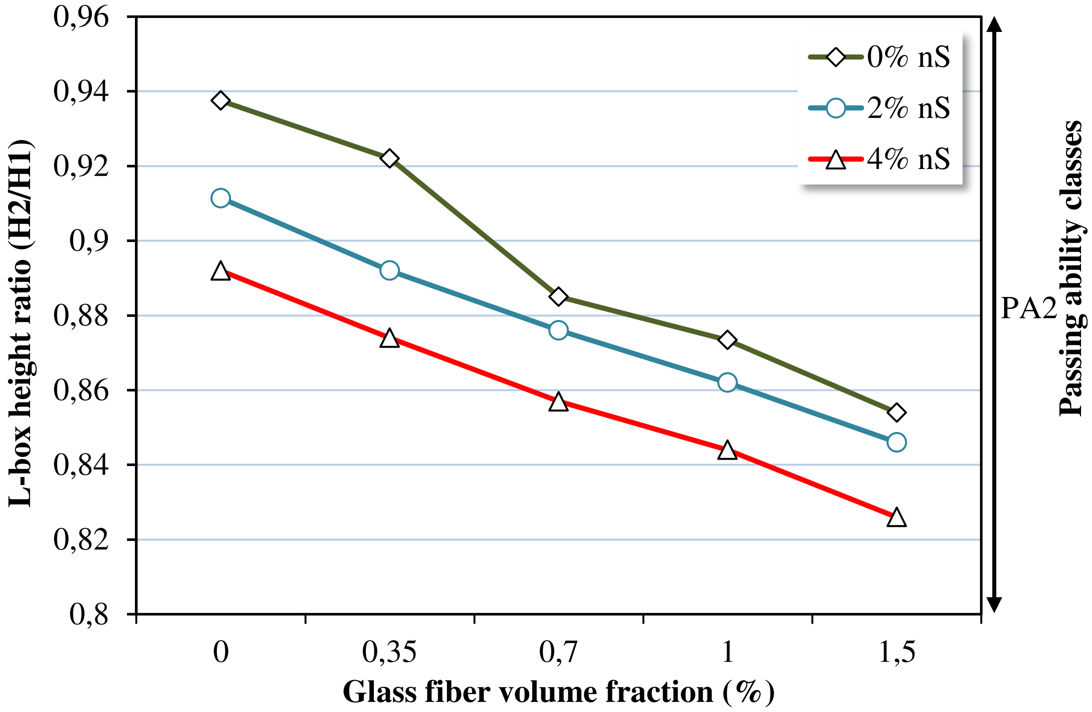

Figure 4.6 L-box height ratio and passing ability classes

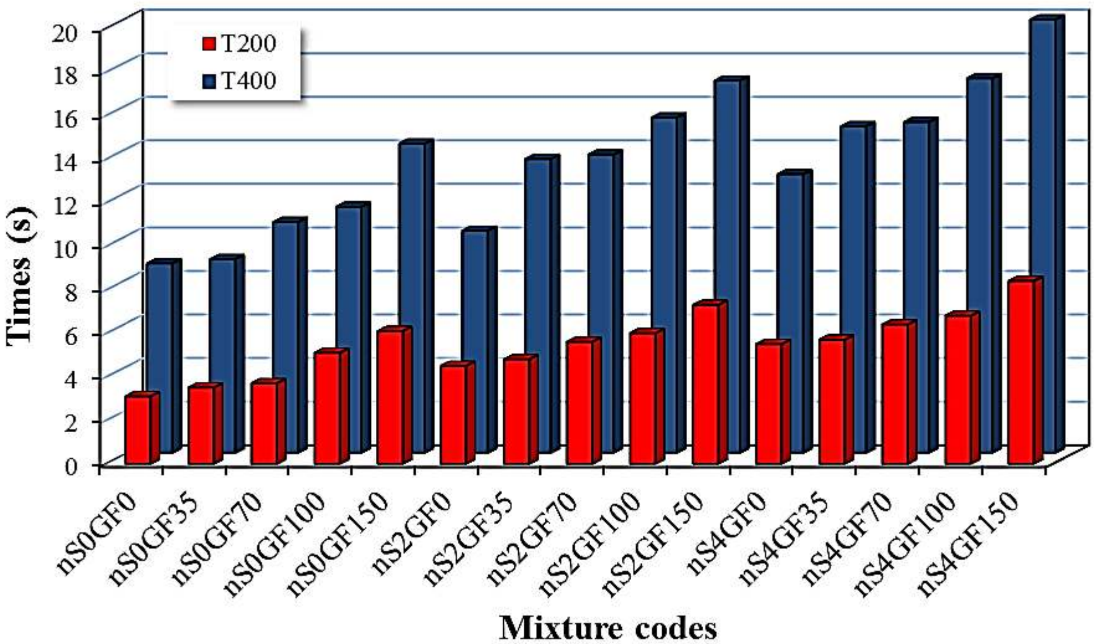

Figure 4.7 Variation of T_{200} and T_{400} L-box flow time

It is well known that the constituent properties of concrete such as cement, aggregate, fines and ultra-fines, admixture and fiber significantly influence the properties of concrete in its fresh state. However, the conventional tests of fresh properties of new high performance concrete, like SCC, maybe not adequate to gain engineers the clear sights about the actual freshly concrete. Koehler and Fowler (2004) believed that for estimating fresh characteristics of SCC incorporated special ingredients, it is necessary to use concrete reheometer.

In fact there are two important rheological parameters for fresh concrete; viscosity and yield stress. If yield stress stands for the pressure needed to make fresh mixture initiate to flow, viscosity expresses how fast the concrete flows, once yield stress has been surpassed (Öz, 2014). Saak et al. (2001b) reported the proper design of SCC involves the use of minimum yield stress and viscosity so as to prevent segregation risk since the concrete will have low workability if the viscosity or yield stress is too high. However, a low viscosity concrete will exhibit a rapid initial flow and then break while it may stay to creep forward over an additional period for a high viscosity (EFNARC, 2005).

The recorded torque (in Nm) and rotational velocity (in rps) realized through the utilization of a rheometer can be observed in Figures 4.8 a, b and c. The results of SCC mixtures of 0% nS with 0%, 0.35%, 0.7%, 1% and 1.5% GF are depicted in Figure 4.8a, while 2% and 4% nS with 0%, 0.35%, 0.7%, 1.0% and 1.5% GF are portrayed in Figure 4.8b and c. Upon the application of the Bingham model on the data above, a negative yield stress was detected in several of the mixtures. As such, the Bingham model was not employed for a description of the rheological characteristics of the SCC. Instead, modified Bingham models was engaged for this purpose. A rise in the content of nS leads to a methodical increase in torque. The highest possible boost in torque occurred in SCC mixtures generated with an elevated content of GF. As revealed through the results, the values of torque rise progressively in tandem with increases in the nS content and the GF volume fraction. The greatest torque value was traced to the mixture nS4GF150, while the nS0GF0 mixture recorded the lowest torque value. For the mixture nS0GF0, the torque value variation was between 0.07 and 0.824 Nm, for nS0GF35 it was between 0.095 and 1.023 Nm, for nS0GF70 it was between 0.193 and 1.678 Nm, for nS0GF100 it was between 0.243 and 2.208 Nm, and for nS0GF150 it was between 0.276 and 2.347 Nm (Figure 4.8a). As for the mixtures nS2GF0, nS2GF35, nS2GF70, nS2GF100, and nS2GF150, the torque values varied between 0.87 and 0.97, 0.76 and 1.164, 0.191 and 1.846, 0.258 and 2.379, as well as 0.397 and 3.126 Nm, respectively (Figure 4.8b). To round up, the torque values for the mixtures nS4GF0, nS4GF35, nS4GF70, nS4GF100, and nS4GF150 varied between 0.11 and 1.027, 0.14 and 1.398, 0.251 and 2.148, 0.337 and 2.594, as well as 0.447 and 3.43 Nm respectively.

The modified Bingham model was utilized to realize the shear rates and shear stresses for the SCC mixtures generated with nS contents of 0%, 2%, and 4% and GF volume fractions of 0%, 0.35%, 0.7%, 1%, and 1.5% (Figures 4.9 a, b and c). The results indicated that the increase in GF and nS content caused to increase in the torque values up to 70%. Furthermore, the results showed that the increase in GF content from 0% to 1.5% lead to increase in the shear stress, besides, the incorporation of 0%, 2% and 4% caused to increase shear stress systematically. As a result, the incorporation of nS and/or GF increases concrete viscosity significantly.

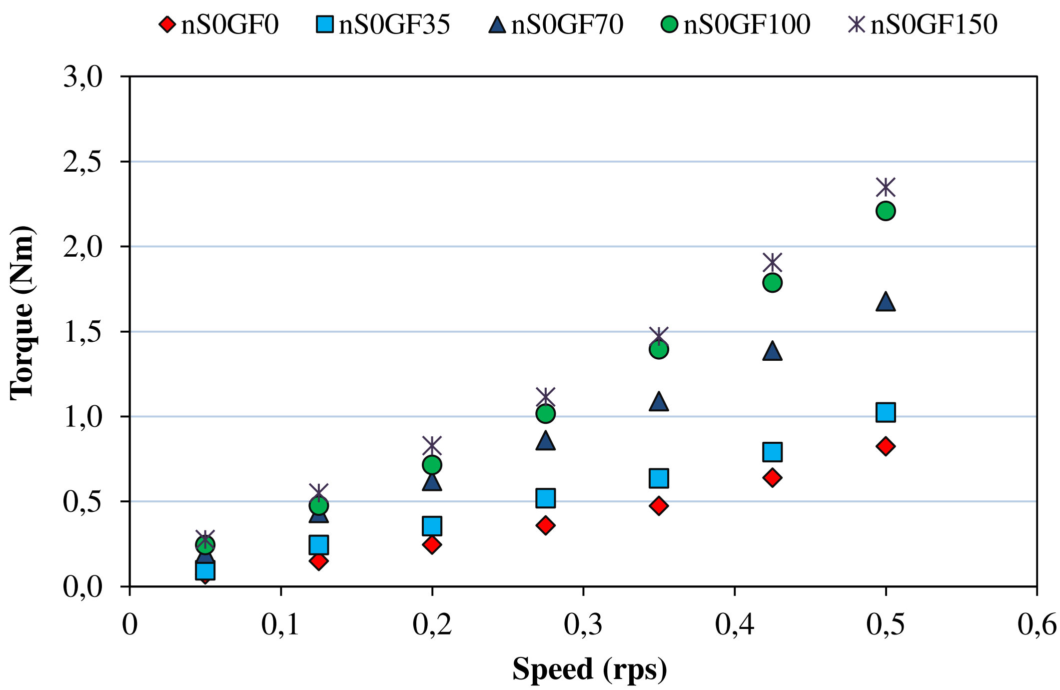

a)

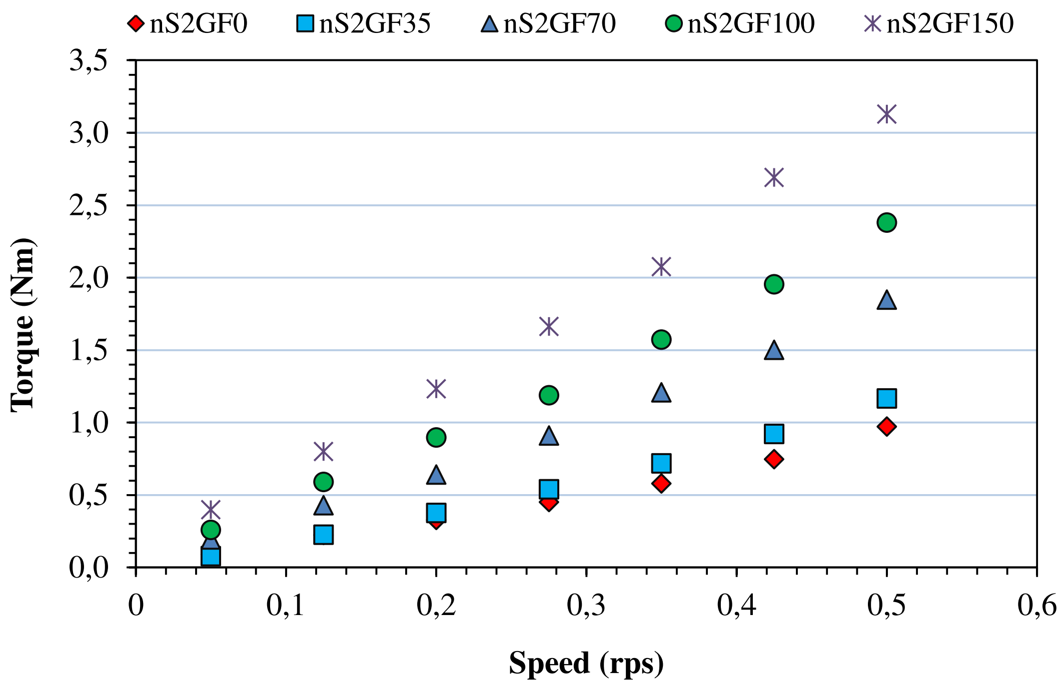

b)

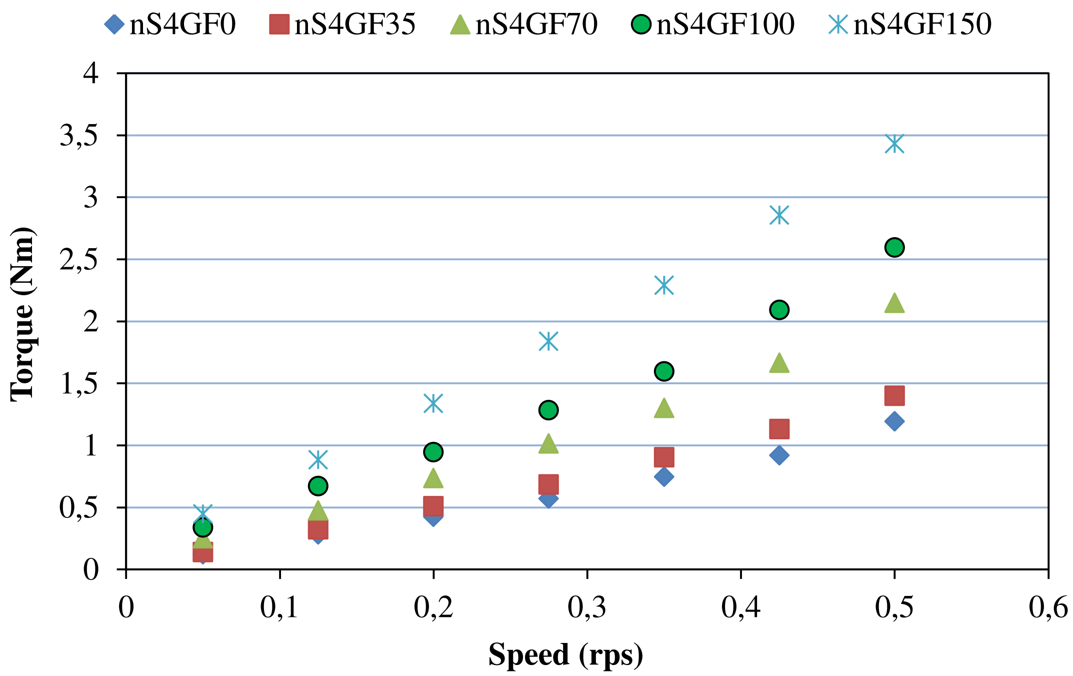

c)

Figure 4.8 Torque vs. rotational speed for GF reinforced SCC with: a) 0%, b) 2%, and c) 4% nS contents

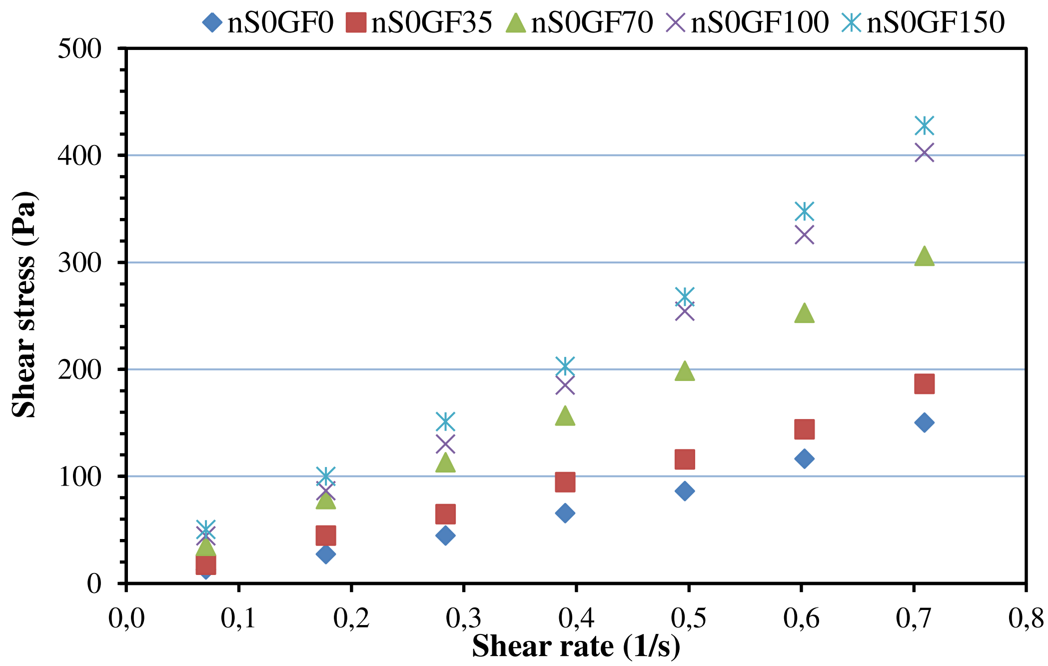

nS0GF0
nS0GF35
nS0GF70
nS0GF100
nS0GF150
500
400
300
200
100
0
Shear stress (Pa)
0,0
0,1
0,2
0,3
0,4
0,5
0,6
0,7
0,8
Shear rate (1/s)

a)

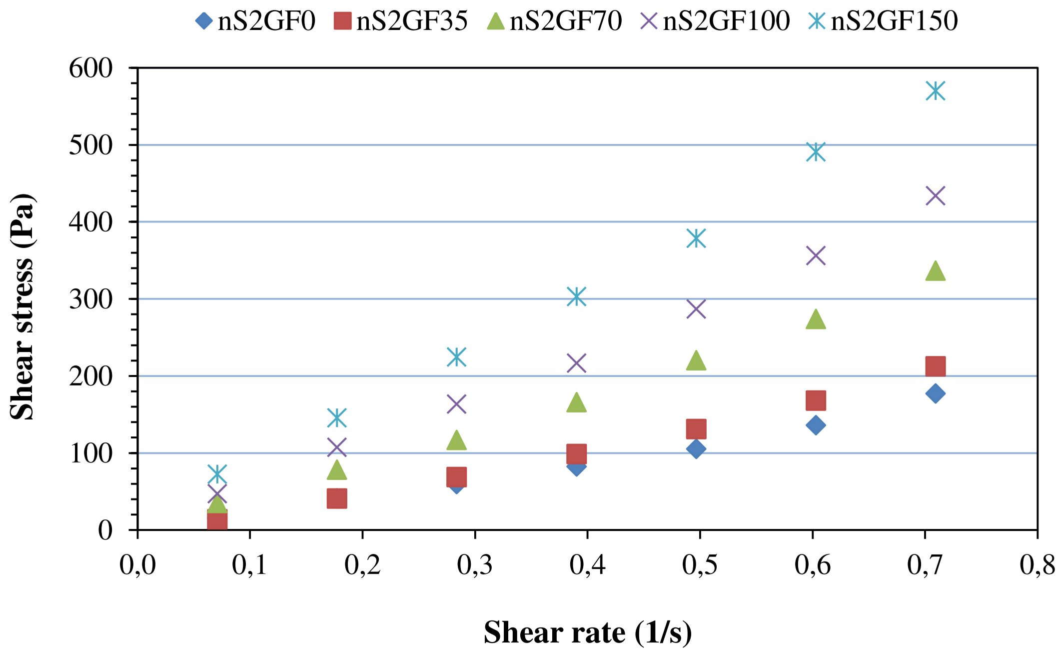

nS2GF0
nS2GF35
nS2GF70
nS2GF100
nS2GF150
600
500
400
300
200
100
0
Shear stress (Pa)
0,0
0,1
0,2
0,3
0,4
0,5
0,6
0,7
0,8
Shear rate (1/s)

b)

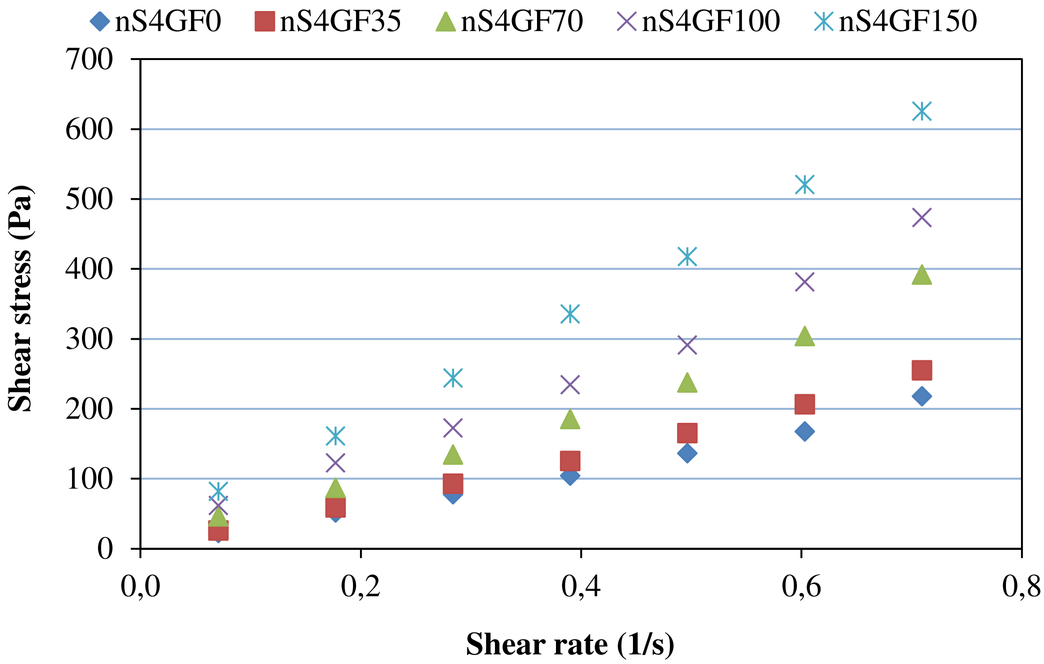

c)

Figure 4.9 Application of the modified Bingham model on the rheological data for GF reinforced SCC with: a) 0%, b) 2%, and c) 4% nS contents

4.2 Mechanical properties

In this study, the strength properties were covered by 3 different tests, namely compressive and splitting tensile strengths and static modulus of elasticity conducted at 28 and 90 days. Compressive strengths are among the most vital mechanistic properties of concretes, which at times mirror the total performances of hardened concrete in terms of the service lives of structures. The result for each SCC composite with nS present or absent at a different GF volumetric fraction is shown in Figures 4.10a and 4.10b. Compressive strength in the range of 70.5 to 84.1 MPa and 77.1 to 94.1 MPa were attained in 28 day and 90 day. The results of present test indicated that the use of 0.35% and 0.7% GF results in a very slight decrement in compressive strengths. Similar results for SCC made with 0.3% and 0.7% GF have been observed by Qureshi and Ahmed (2013) and Fard (2016). While increases in GF up to a 1.5% volumetric fraction result in increases in compressive strengths for SCC composites comprising 0% nS. Embedded fibers afford concretes a way of halting growths in cracks and upgrading their load-carrying capacities. Moreover, increasing the amount of GF may be result in decreasing incidences of cracks in SCC, meanwhile producing increase in compressive strength.

Additionally to those SCC composites containing 2% and 4% nS, increases in GF at 0% to 1.5% volumetric fractions resulted in increases in compressive strengths. Likewise, SCC compressive strength at age 28 day increased by 3.83% and 8.24% with increases in nS content from 2% to 4% without GF, respectively, and between 4.87% and 12.8% with 1.5% GF. Furthermore, the increase in 90 day compressive strength getting between 6.01% and 9.35% with increase in nS content from 0% to 2%, 4% without GF respectively, and between 7.94% and 13.44% with 1.5% GF. This is due to filling and pozzolanic activity of nS in reinforcing fiber zone and cement matrix. In other related studies with different nS replacement levels compressive strengths are also exhibited similar trend in contribution to the compressive strength of the concretes. Li (2004), Qing et al. (2007), Hou et al. (2013), Nazari and Riahi (2011a), and Nik and Orman (2013) found that the replacement of cement with 5.0% nS can significantly improve compressive strength. At the same time, other previous works stated dissimilar behavior regarding this replacement level (Nazari and Riahi, 2011b; Najigivi et al., 2013). These contradictions witnesses rather than compressive strength test must be considered to verify the optimal level of nS.

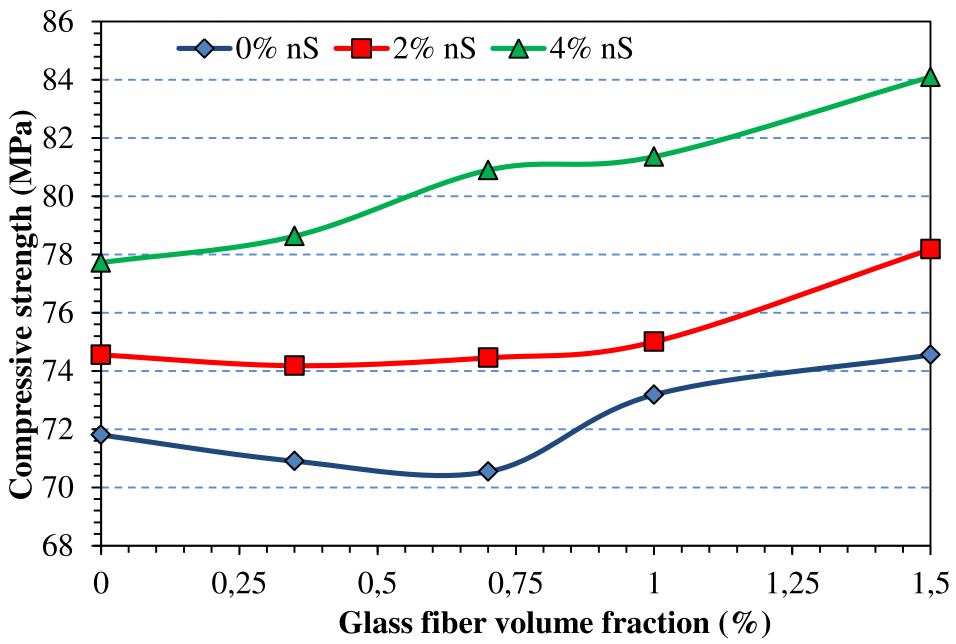

a)

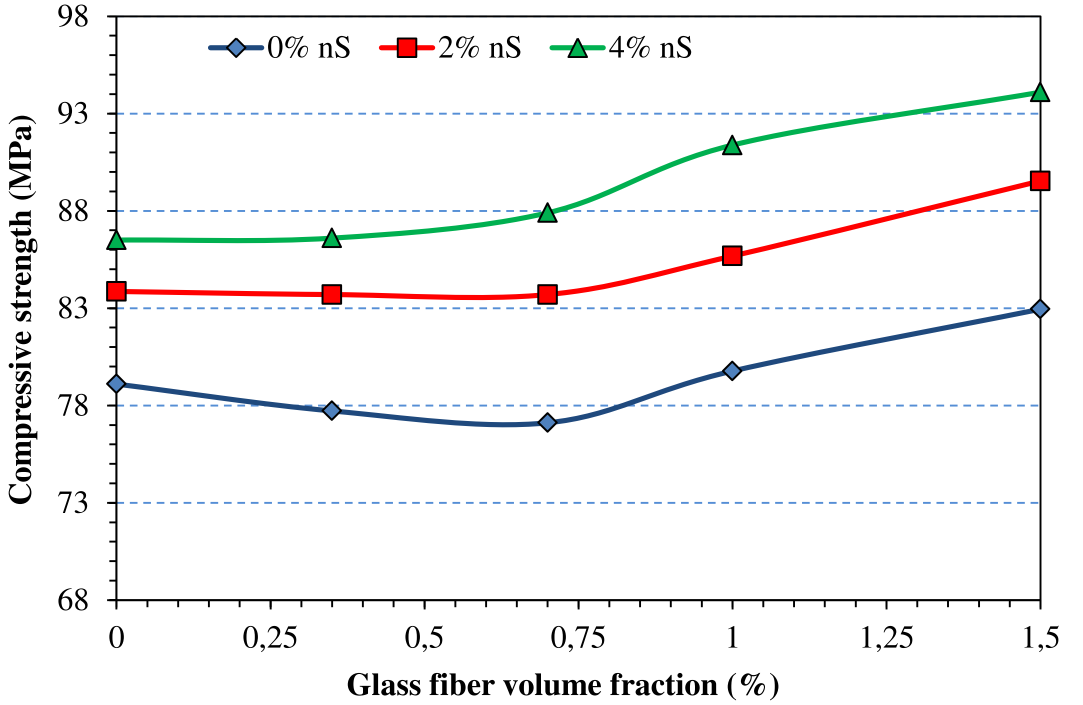

b)

Figure 4.10 Compressive strength of GFRSCCs at a) 28 days and b) 90 days

The splitting tensile strength of SCC is much lesser than its compressive strength since it can be developed more rapidly with propagation of cracks. Splitting tensile test method conducted herein covers the purpose of the tensile strength of cylindrical concrete specimens according to ASTM C496 (2011), are graphically presented with respect to the five different volume fractions of GF (0%, 0.35%, 0.70%, 1.0% and 1.5%) in Figure 4.11a and 4.11b for the 28 and 90 day curing period, respectively. It was clearly spotted from the figures that increasing of GF volume fraction lead to increase in the splitting tensile strength of SCC. On the other hand, the result also indicated that the SCC produced with glass fiber gave the highest splitting tensile strength with deferent contents of nano-silica. For example, from the Figure 4.10a the splitting tensile strength with 0% nS increased by 5%, 9%, 18% and 26% for SCC produced with 0.35%, 0.7%, 1%, 1.5% GF, respectively, in comparison to that of plain SCC. Similarly, the splitting tensile strength with 2% NS increased by 8%, 14%, 18% and 25%, either using 4% nS, the splitting tensile strength increased by 3%, 10%, 16% and 23% at age of 28 day.

Furthermore, the result shows that the splitting tensile strength increases with increasing the nS content. In this regard, the maximum improvement in splitting tensile strength at 28 day due to the use of 2% and 4% nS is calculated as 9% and 16%, respectively, for SCC made with 0.7% GF. At the same line for those tested at 90 day, the maximum percent is computed as 14% and 24% for nS2GF70 and nS4GF35, respectively. Quercia et al., (2012) introduced an experimental investigation to study the mechanical and durability properties of self-compacting concrete containing precipitated silica in colloidal suspension or fumed powder nS were studied. The percentage of nS was 3.8% by weight of cement. They reported that the splitting tensile strength after 28 days of curing was enhanced by about 21.51% and 9.91% for powder and colloidal nS, respectively. The development of denser and harder C-S-H gel due to the addition of nS improves the interfacial transition zone cause to improve tensile strength of concrete (Mukharjee and Barai 2014).

Depend on the results, the splitting tensile strength of GFRSCC increases with increasing the GF volume fraction up to 1.5% and nS up to 4%.

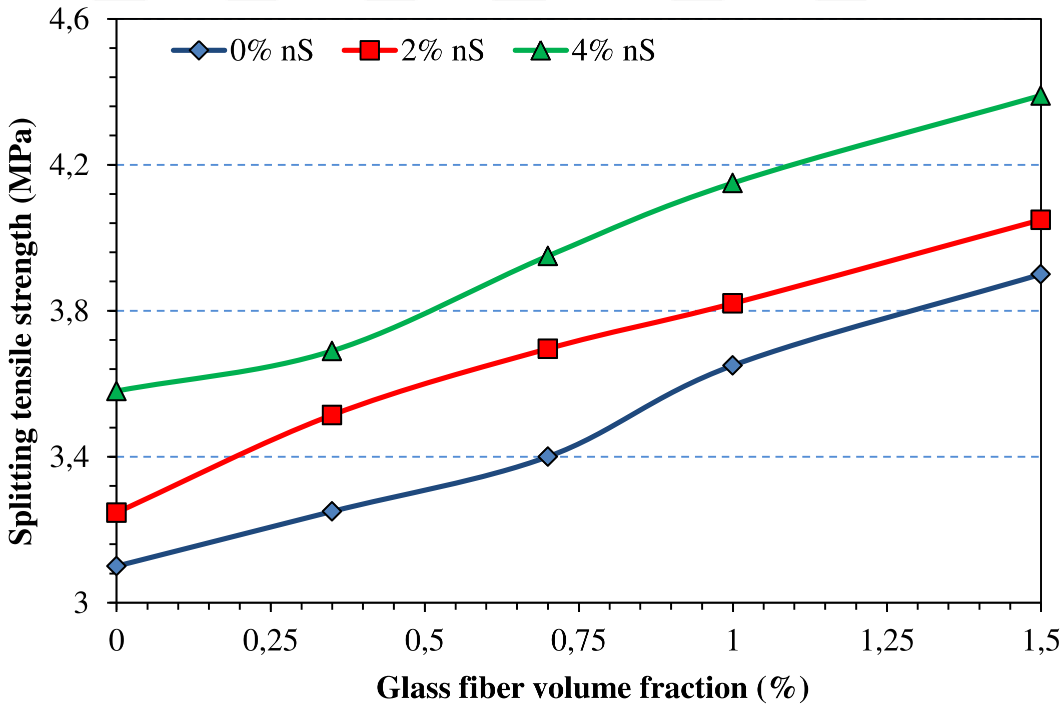

a)

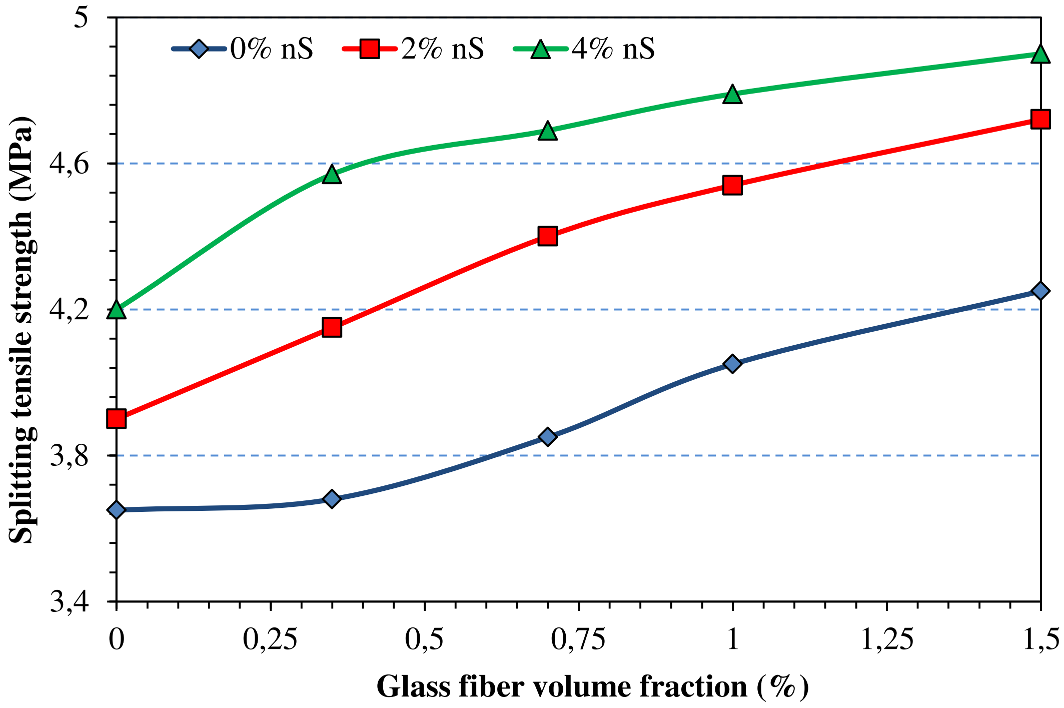

b)

Figure 4.11 Splitting tensile strengths of GFRSCCs at a) 28 days and b) 90 days

The variations in 90 day modulus of elasticity values of the SCC are plotted within the Figure 4.12 taking into consideration GF volume fractions. The modulus of elasticity values varied between 43.2-45.9 GPa, 46-49.3 and 47.8 and 50 GPa for concrete containing 0%, 2% and 4% nS, respectively. A comparison of the modulus of elasticity variation with that of compressive and splitting tensile strengths clearly shows similar trend. The result of present test shows that, the SCC produced with 4% nS had a higher modulus of elasticity by 8%, 11%, 13%, 10% and 9% with 0, 0.35, 0.7, 1, and 1.5% GF, respectively, than those produced with 0% nS. On the other hand, modulus of elasticity of SCC was increased with increasing GF volume fraction from 0 to 1.5% with different ratios of nS. Corinaldesi and Moriconi (2009) also observed the addition of nS in concrete mixes improves modulus of elasticity slightly due to increase in bonding between the aggregates and mortar. However, this enhancement is not so significant when compared with compressive strength as they reported. In the study of Reddy et al. (2013) also reported similar performance regarding the use of GF. They concluded that the addition of fiber in general increased the value of modulus of elasticity of self-compacting concrete.

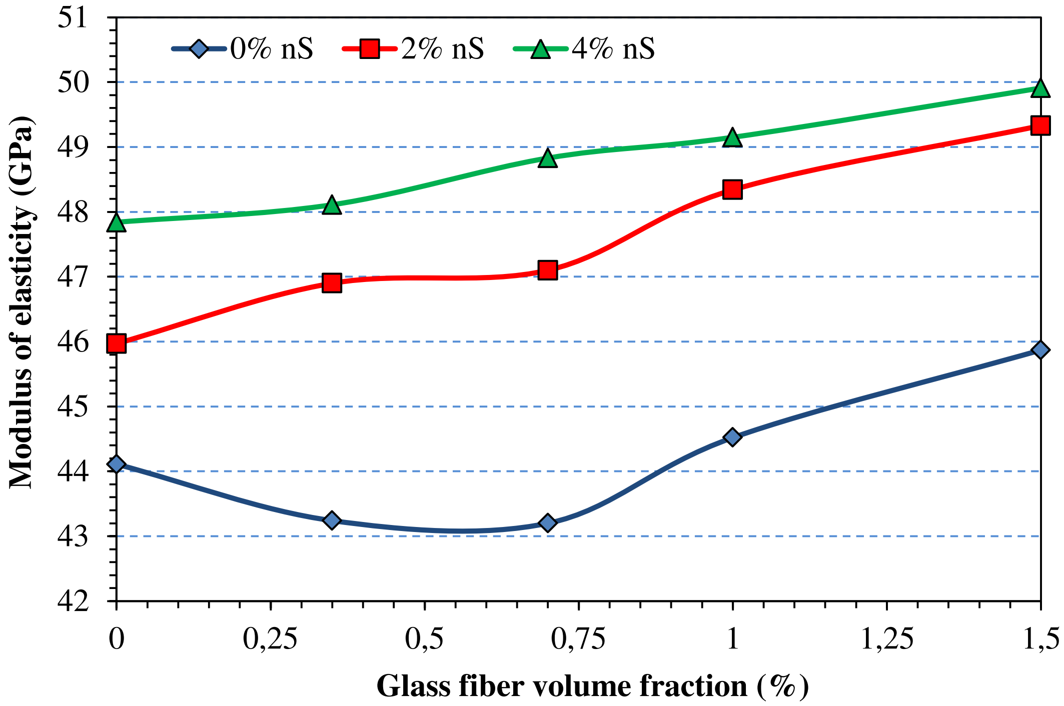

Figure 4.12 Modulus of elasticity of GFRSCCs at 90 days

Net flexural strength found from three-point bending test on the notched specimen with respect to volume fraction of GF are shown in Figure 4.13. The GFRSCC with and without nS mixes had net flexural strength varying from 5.76 to 7.15 MPa. The highest value of the net flexural strength was observed in SCC mixture made with 4% nS and 1.5% GF as 7.15 MPa. The net flexural strengths of SCC without fiber were 5.76, 5.83 and 5.87 MPa at 0%, 2% and 4% nS contents, respectively. The enhancement in flexural strength due to the incorporation of GF and nS were found to be in the range of 6% to 14% and 19% to 22%, respectively. Kayali et al. (2003) reported that the main and major contribution of the fibre was due to the increase of tensile strain capacity of the concrete. Gao et al. (1997) believed that the reason for increasing net flexural strength with employment of fibre is that, after cracking of the matrix, the fibres will resist the load until the loss of the interfacial bond between the fibres and the matrix.

The fracture energy defined as the total energy dissipated over a unit area of the cracked ligament, representing the amount of work for the complete failure of a tested specimen (Yu et al., 2016). The area under the curve of the load versus displacement is denoted the energy necessary to break the material. Fracture energy was verifying versus GF volume fraction percentages at each of 0, 2 and 4% nS. The variation in fracture energy of SCC composites with and without nS at various GF volume fractions are graphically shown in Figure 4.14. The result shows that the fracture energy increases with increasing GF volume fraction in all series. Moreover, the increase in the nS content lead to improve fracture energy of SCC. The figure obviously shows that the addition of GF had the significant effect on the fracture energy. In this study the fracture energy for SCC mixtures ranging between 98 N/m to 168 N/m. Furthermore, the fracture energy with 0% nS increased by 1%, 12%, 27% and 37% with respect to SCC produced with 0.35%, 0.7%, 1%, 1.5% GF. While, the fracture energy with 2% nS increased by 10%, 24%, 32% and 43%, either using 4% nS, the fracture energy by 15%, 22%, 27% and 34% at age of 90 day. On the other hand, the increase in content of nS without GF from 0% to 2% and 4% leads to an increase in fracture energy by 12% and 28%, respectively, while, the increase in fracture energy with 1.5% volume fraction of GF was 18% and 25%, respectively. Depend on the results, the fracture energy of SCC increase with increase in GF and nS. In the study of Tavakoli et al. (2014), fracture parameters of SCC incorporating nS up to 6% were analyzed. They founded that the fracture energy magnitude increases with the increase of nS replacement level from 1% to 3% and then to decrease with the increase of nS content from 3% to 6%, thus in terms of fracture energy they concluded that the optimum nS percentage is 3%. So, it can be said that the small amount of nS can be used to improve fracture energy and this should be related to the efficiency of nS. Typical loads versus displacement curves for SCC at 0%, 2% and 4% nS contents are given in Figures 4.15a, 4.15b and 4.15c, respectively. These figures exhibited that addition of GF to SCC caused to increase both the ultimate load and area under the load-displacement curve.

The characteristic length is often considered to be a concrete property, and it gives a degree of the ductility/brittleness of the concrete. According to Mehta and Monteiro (2006), normal vibrated concrete has characteristic length between 200 and 400 mm and compared to high strength concretes and light-weight aggregate concrete this range can be considered higher. The variation in the characteristic length for SCC made with various GF volume fraction and nS content is presented in Figure 4.16. The results showed that addition of GF to SCC lead to increase in the characteristic length. Thus, it can be indicated that the incorporation of such fiber made concrete more ductile. The results also revealed that nS incorporating yielded higher characteristic length values. Thus, SCC composites made with nS are more ductile than the composite free of nS. The characteristic length of SCC with 4% nS was found to be higher than those of SCC with 0% and 2% nS content by 2% and 1%, respectively. The use of GF in SCC made it more ductile, this revealed from the increase in characteristic length for SCC made with GF. Furthermore, the characteristic length with 0% nS increased by 0.1%, 2%, 5% and 5% respectively for SCC produced with 0.35%, 0.7%, 1%, 1.5% GF. While, the fracture energy with 2% nS increased by 0.1%, 2 %, 5% and 6%, either using 4% nS, the fracture energy by 0.3%, 3%, 4% and 5% at age of 90 day. This mean that the brittleness of SCC decreases with the use GF and nS.

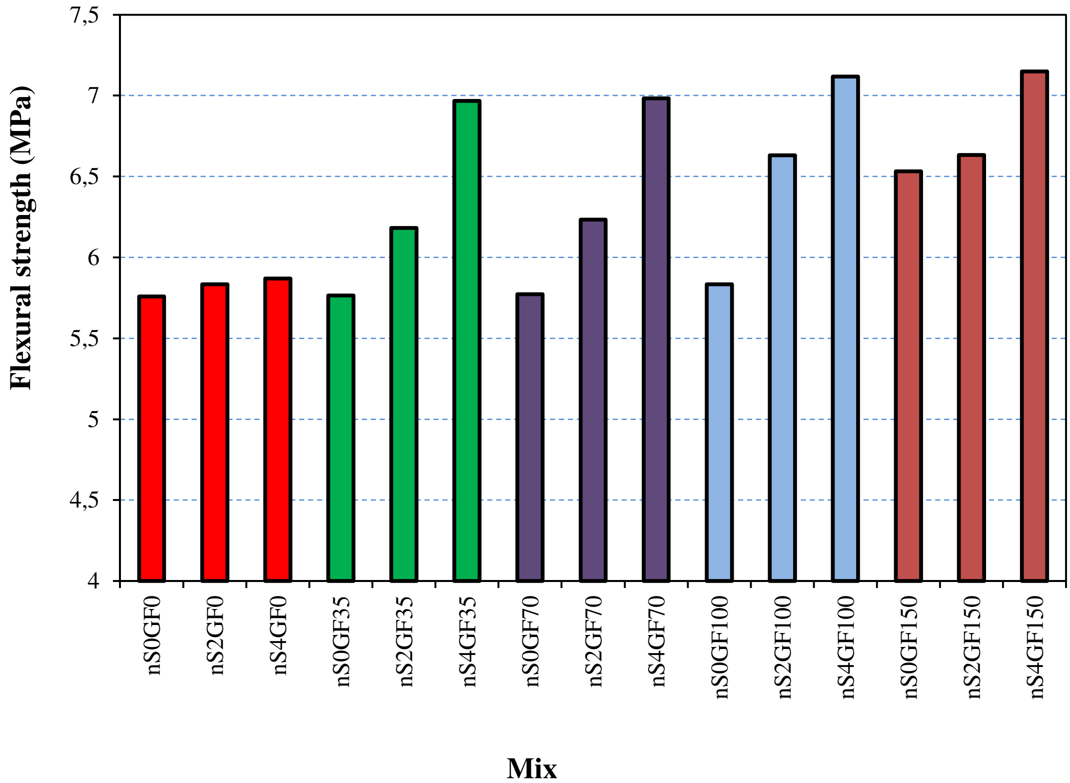

Figure 4.13 Flexural strength of GFRSCCs

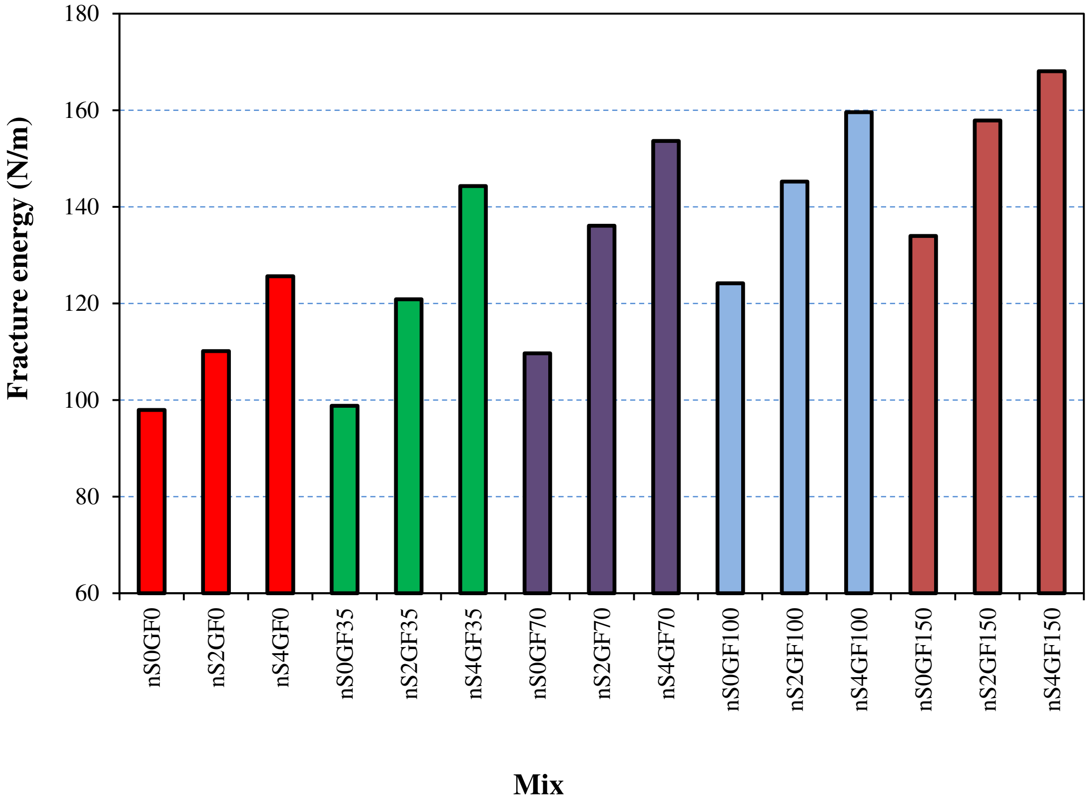

Figure 4.14 Fracture energy of GFRSCCs

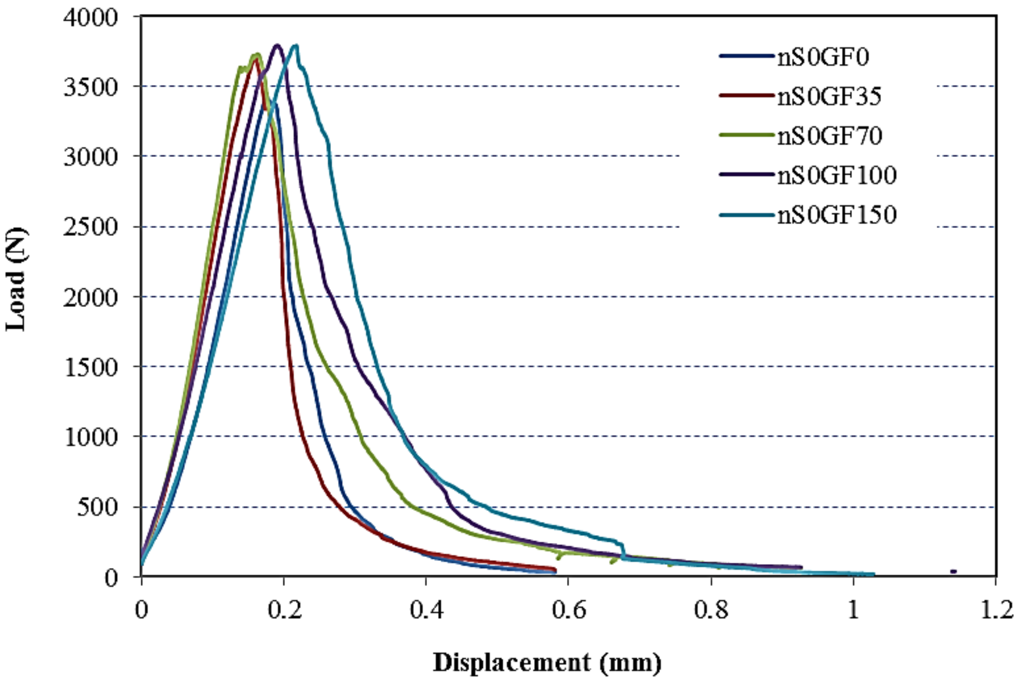

a)

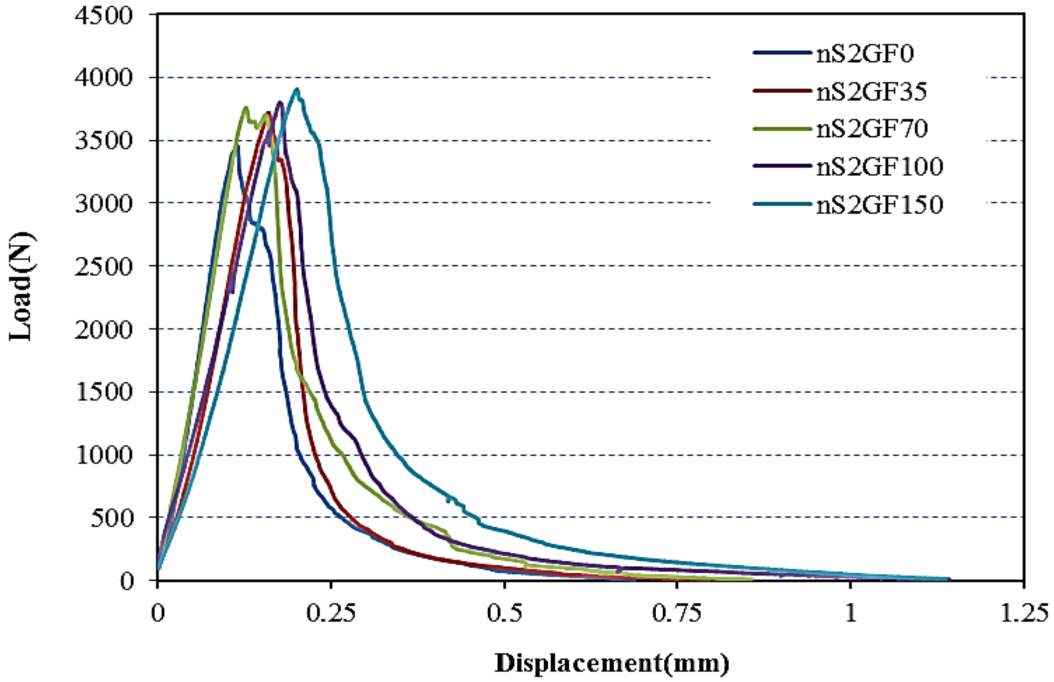

b)

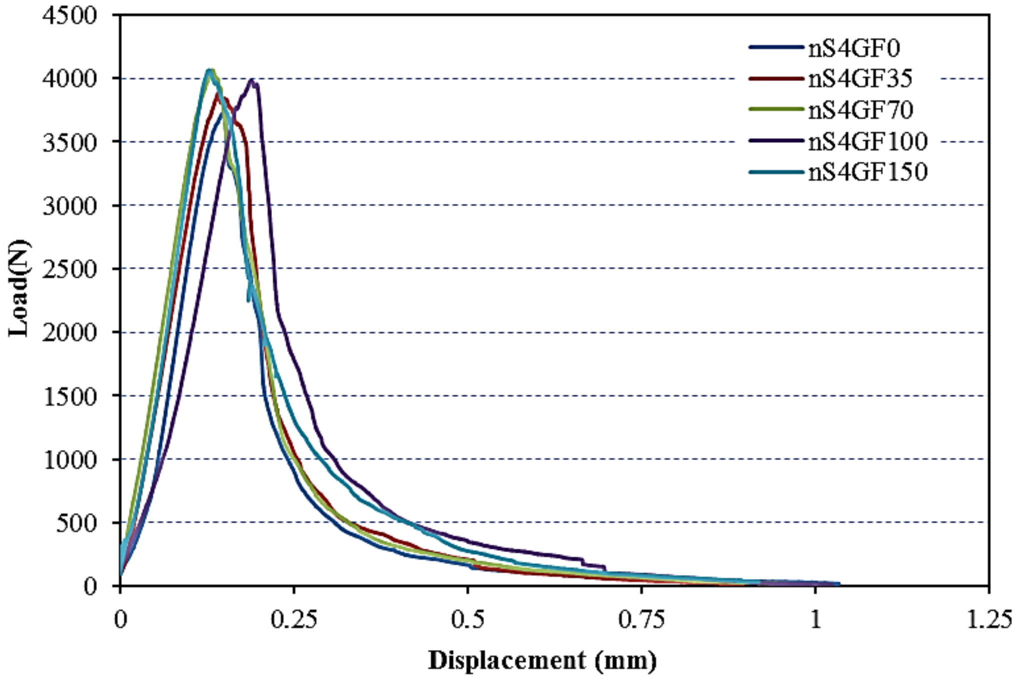

c)

Figure 4.15 Typical load vs. displacement curves according to nS incorporation level: a) 0% nS, b) 2% nS and c) 4% nS

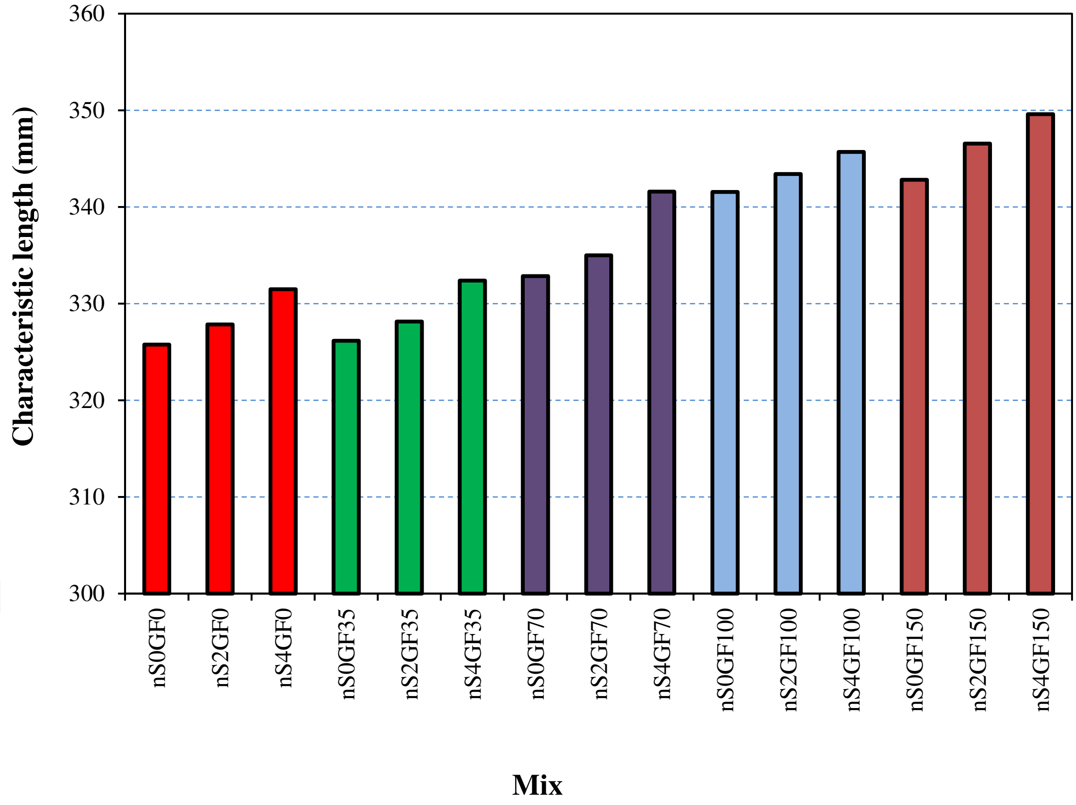

Figure 4.16 Characteristic length of GFRSCCs

CHAPTER 5

RESULTS AND DISCUSSION OF NUMERICAL STUDY

5.1 Ultimate axial capacities of CFST short columns

Table 5.1 demonstrates that the range of ultimate of axial capacity of (N_u) CFST short columns infilled with GFRSCCs with and without nS significantly affects over the existing design codes used in this study. As can be seen from the table, the minimum predicted value of N_u varies from 573 to 756 kN and from 604 to 792 kN irrespective of the design code at the age of 28 and 90 days, respectively. On the other side, the maximum computed value of N_u ranges from 5914 to 7494 kN and from 6547 to 8215 kN regardless the design method at the of 28 and 90 days, respectively.

The predicted data of axial capacity at 28 and 90 days calculated via Eurocode 4 (2004), ACI 318R (2005), AIJ (2001) and DL/T (1999) are graphically presented in accordance with glass fiber content (GF) in Figures 5.1 and 5.2, 5.3 and 5.4, 5.5 and 5.6 and 5.7 and 5.8, respectively. These figures are organized in such a way that each group includes three sub figures (a, b and c) to cover the use of three different diameter to thickness (D/t) ratios of CFST column; 30, 60 and 90. At the same line, each sub figure are divided into three groups with respect to yield steel strength value; 185, 275 and 450 MPa. The results reveal that the predicted N_u values tend to increase with increase in GF content regardless the nS contents and D/t ratios. For example to this trend, in Figure 5.1b the N_u value of CFST column has f_y of 275 MPa and SCC made with 4.0% nS varies as 3001, 3029, 3101, 3115 and 3201 kN with respect to 0.0, 0.35, 0.7, 1.0 and 1.5% of GF, respectively. However, this behavior as can be shown from these figures does not occur for all CFST columns, especially for steel tube infilled with concrete made with 0% nS. For instance, Figure 5.6c presents the predicted N_u of CFST columns having D/t ratio of 90 and calculated via AIJ, (2001). It can be clearly seen that the addition of 0.35% and 0.7% GF to concrete free of nS caused to decrease Nu values, whilst the use of same concrete but with GF content of 1% and 1.5% induced higher axial capacities in comparison to other percent of GF (0, 0.35 and 0.7%).

It is reported by Ellobody et al. (2006) that D/t ratio of circular steel tube has a significant effect on the composite action of CFST column. They believed that the small D/t ratio can remarkably enhance the confinement effect for the core of concrete. On the other hand, the high ratio of D/t ratio provides insufficient confinement for the concrete core and such behavior relates to the premature failure due to the local buckling of steel tube. In this study, the thickness of tube was kept constant as 3.5 mm and the change in the ratio of D/t was resulted from the proposed of different tube diameters so as to vary D/t ratio between 30 and 90. The results presented in Figure 5.1 to 5.8 depicte that when the same parameters of CFST column implemented (f_y, diameter to effective length (D/L) ratio, type of concrete and age) the higher D/t ratio the higher N_u due to the enhancement of composite action resulted from using of further concrete core. For example, the axial capacity calculated by using Chines provision which are presented in Figure 5.7 a-c show that the N_u value of CFST column with respect to D/t ratio of 30, 60 and 90 are 730-824, 2456-2837 and 5173-6030 kN, respectively, for 28 days curing period and f_y of 185 MPa.

The axial capacities of CFST columns were also analytically examined by employing various steel grade of the steel tube. Three different steel grades (S185, S275 and S450) were considered. It reported that the increases in steel yield strength lead to increase axial compression capacity of CFST columns (Patel et al., 2014; Liang and Fragomeni, 2009). In the current analytical study similar behavior has been reported. All the predicted ultimate axial capacities resulted via Eurocode 4 (2004), ACI 318R (2005), AIJ (2001) and DL/T (1999) revealed same behavior with respect to the relationship between the steel yield strength and axial capacity. For example, it can be seen from Figure 5.3c that the structural column infilled with SCC made with 4% nS and having steel grade of S185, S275 and S450 showed a variation in N_u value of 4603-5007, 4911-5315 and 5511-5914 kN, respectively.

Table 5.1 Range of predicted ultimate axial capacity

Approaches	**Age (days)**	**Range of predicted N_u (kN)**
Eurocode 4 (2004)	28	756 – 7494
	90	792 – 8215
ACI 318R (2005)	28	573 – 5914
	90	604 – 6547
AIJ (2001)	28	644 – 6513
	90	677 – 7172
DL/T (1999)	28	730 – 7277
	90	776 – 7907

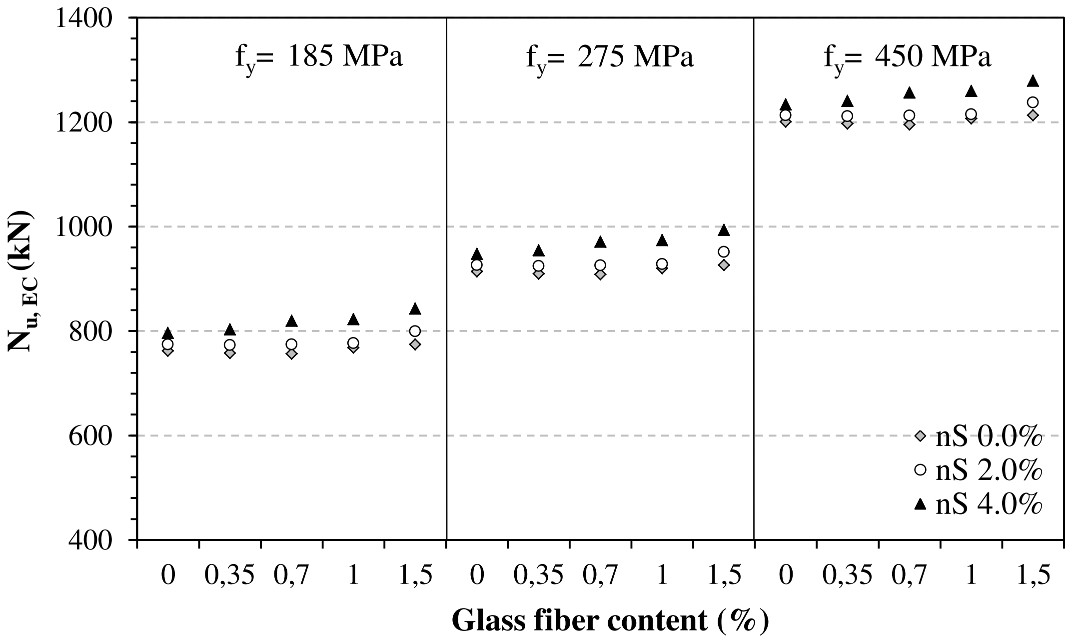

a)

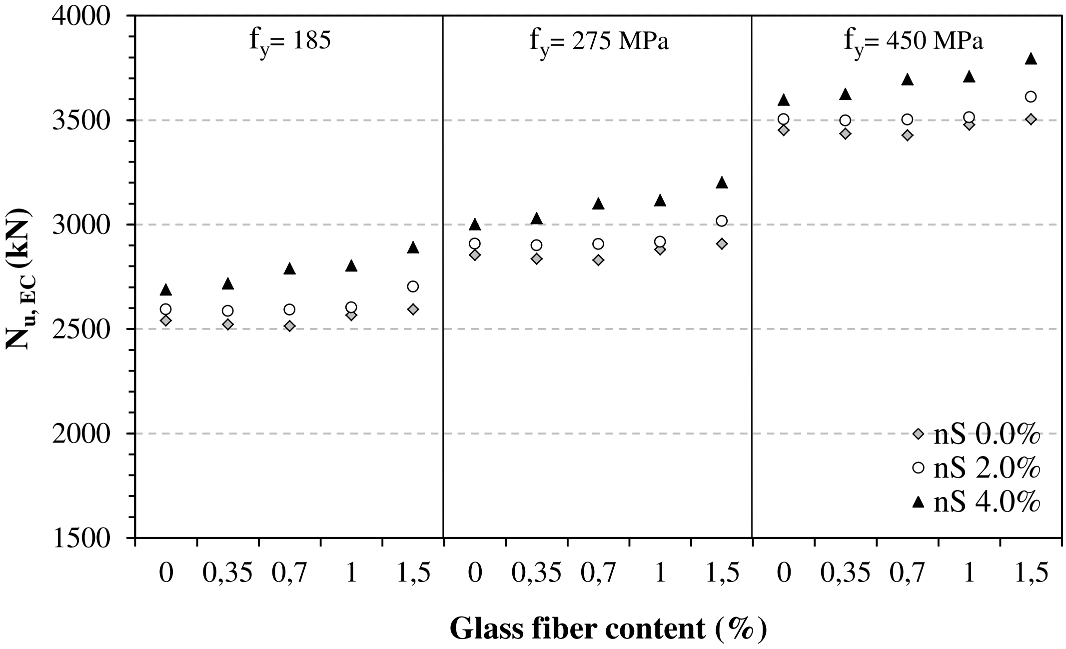

b)

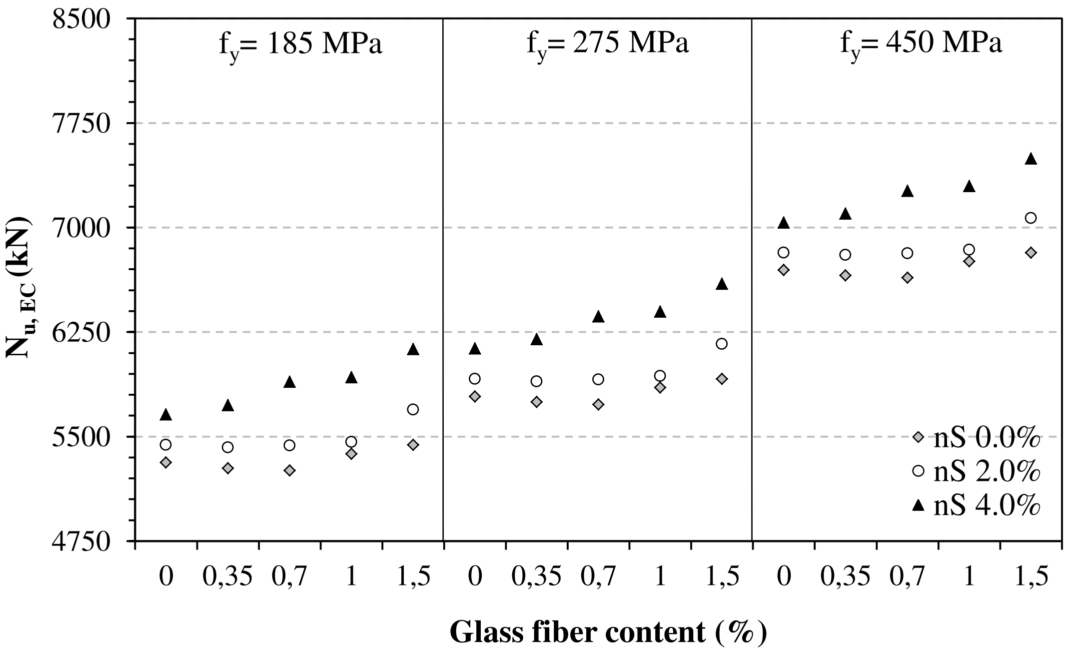

c)

Figure 5.1 Eurocode based axial capacity of the CFST columns having SCCs at 28 days in accordance with GF content for the steel tube D/t ratio of a) 30, b) 60 and c) 90

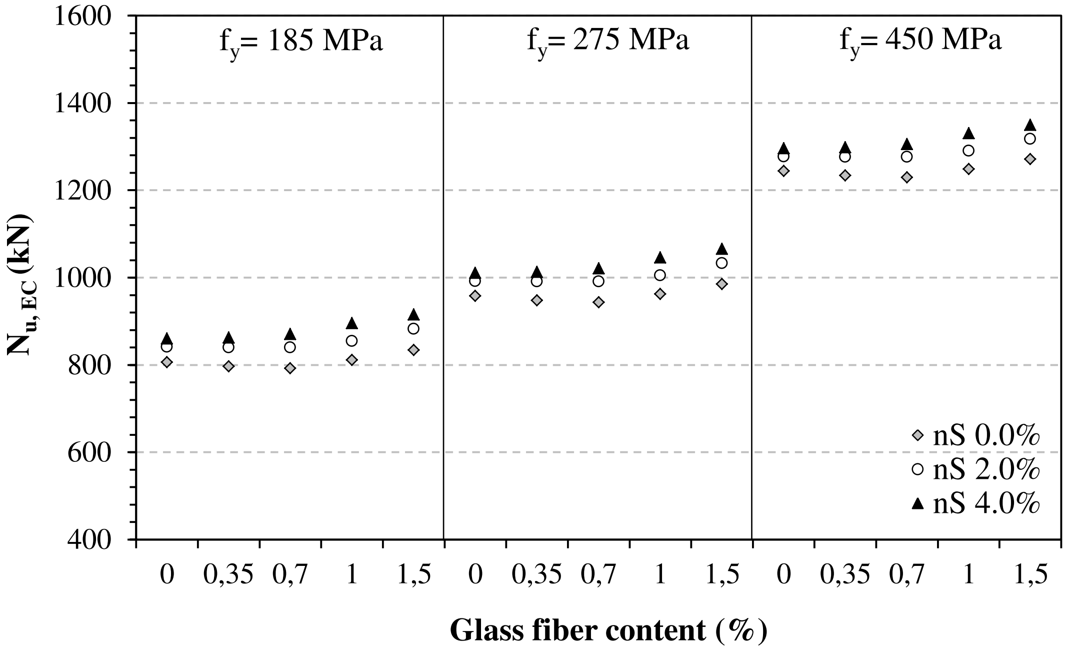

fy= 185 MPa
fy= 275 MPa
fy= 450 MPa
1600
1400
1200
1000
800
600
400
Nu, EC (kN)
nS 0.0%
nS 2.0%
nS 4.0%
0
0,35
0,7
1
1,5
Glass fiber content (%)

a)

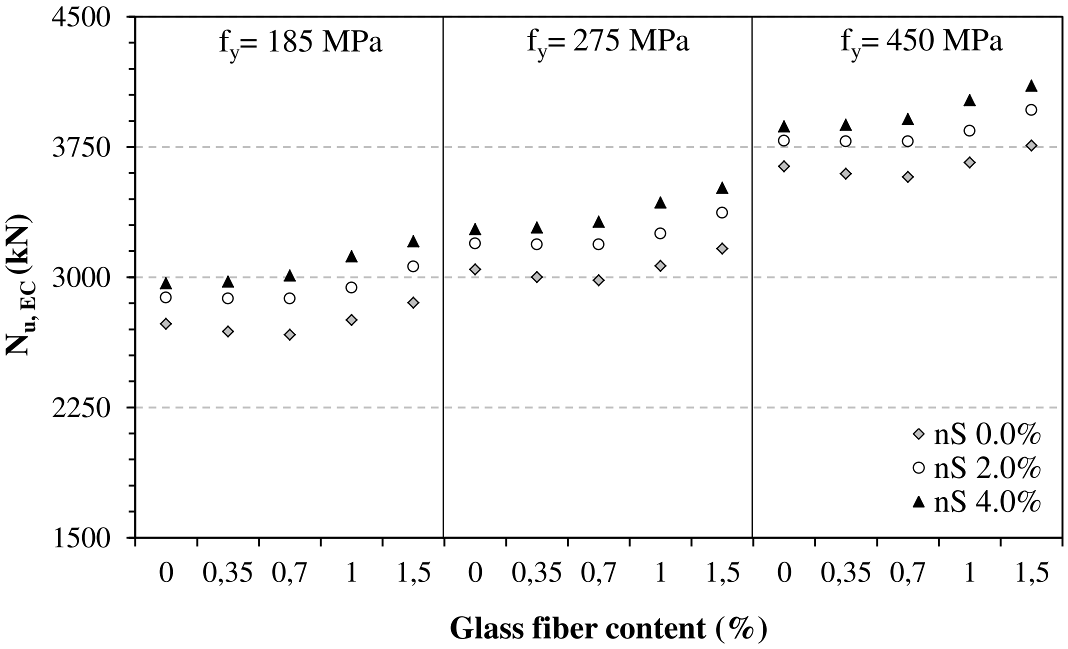

fy= 185 MPa
fy= 275 MPa
fy= 450 MPa
4500
3750
3000
2250
1500
Nu, EC (kN)
nS 0.0%
nS 2.0%
nS 4.0%
0
0,35
0,7
1
1,5
Glass fiber content (%)

b)

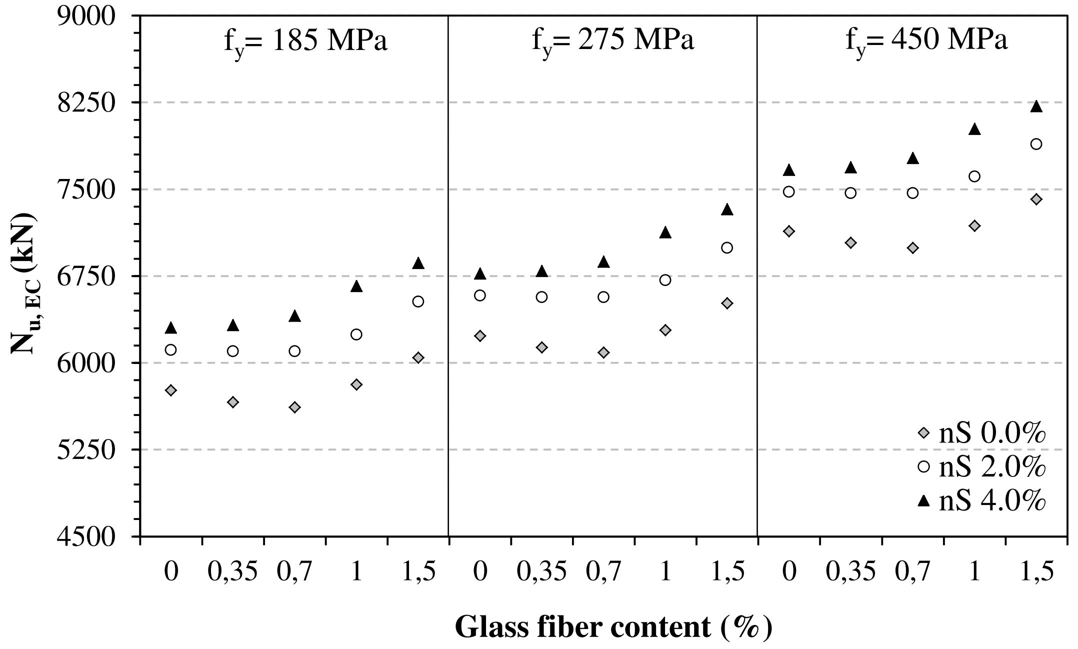

c)

Figure 5.2 Eurocode based axial capacity of the CFST columns having SCCs at 90 days in accordance with GF content for the steel tube D/t ratio of a) 30, b) 60 and c) 90

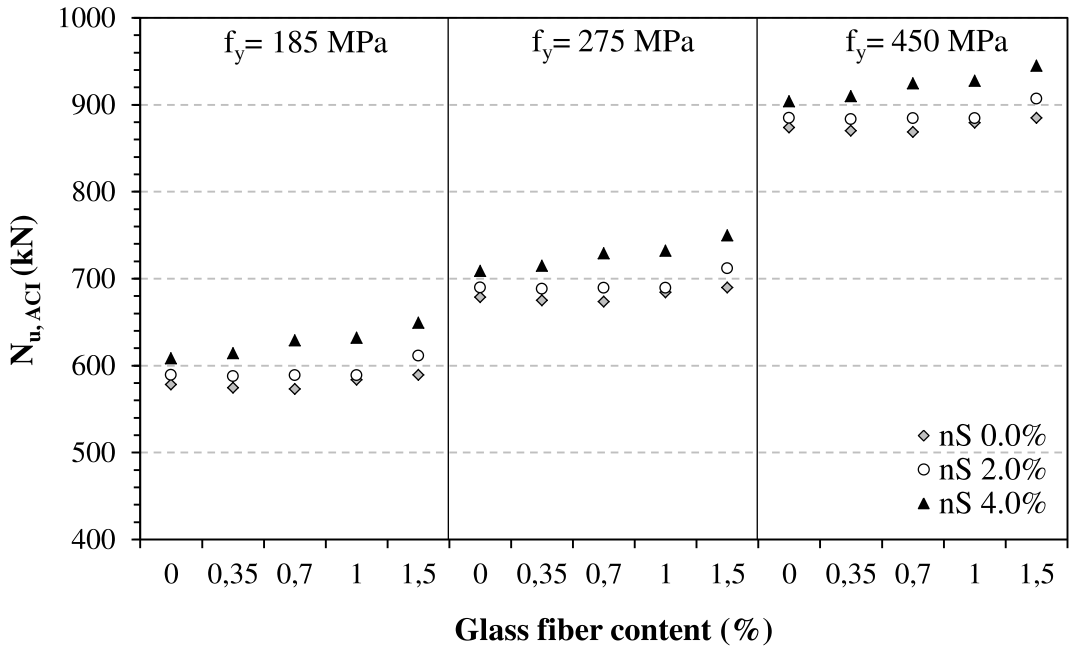

a)

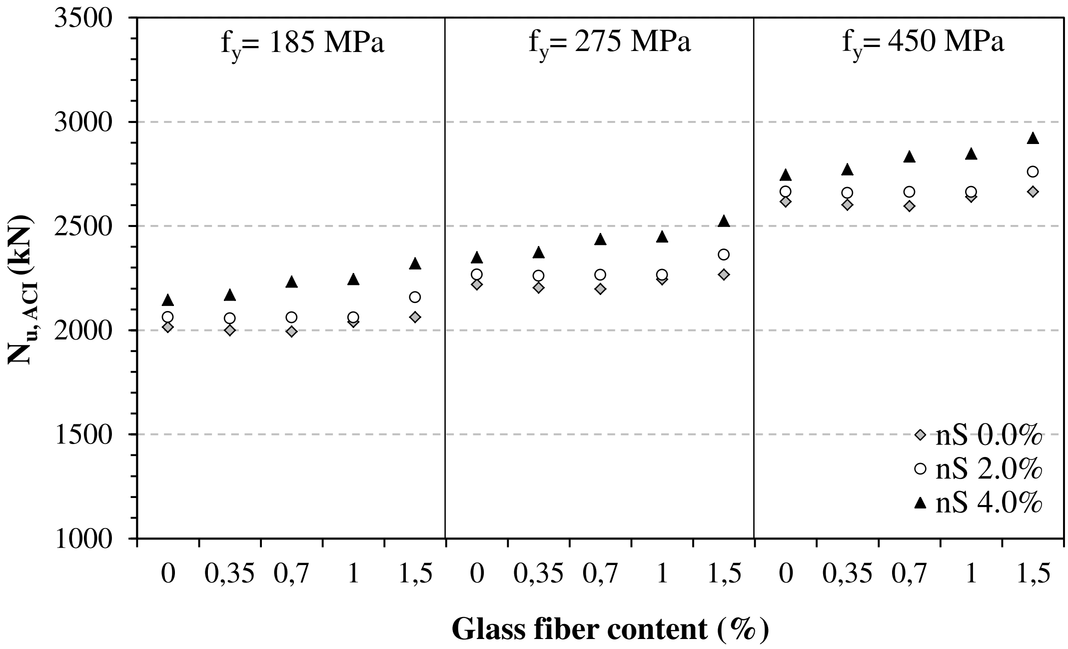

b)

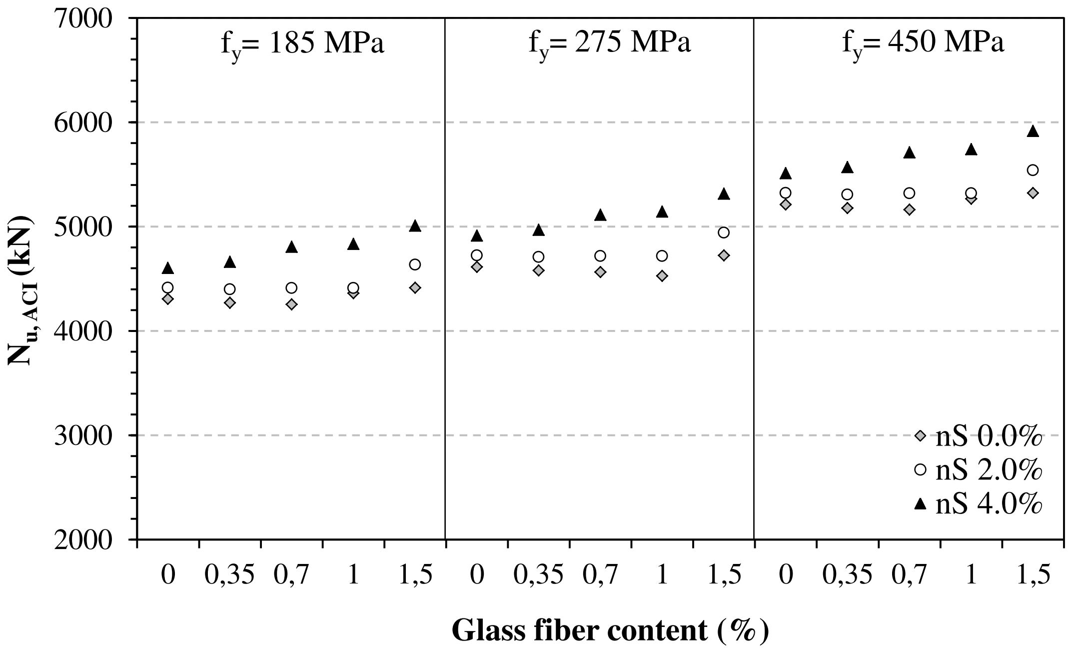

c)

Figure 5.3 ACI based axial capacity of the CFST columns having SCCs at 28 days in accordance with GF content for the steel tube D/t ratio of a) 30, b) 60 and c) 90

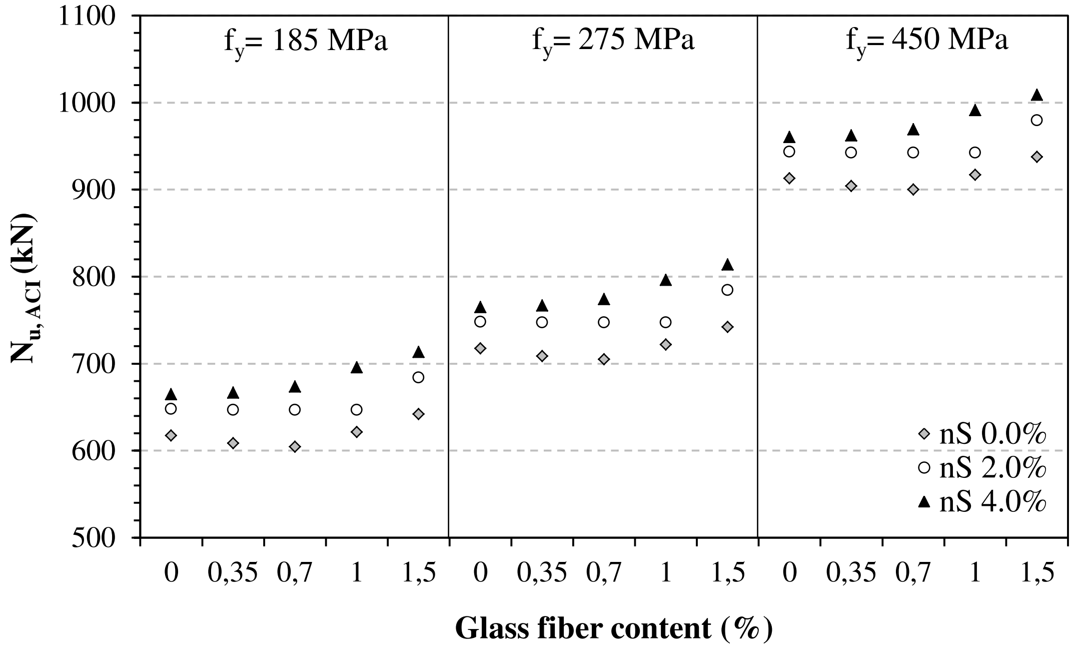

1100
1000
900
800
700
600
500
$N_{u,ACI}$ (kN)
f_y= 185 MPa
f_y= 275 MPa
f_y= 450 MPa
nS 0.0%
nS 2.0%
nS 4.0%
0
0,35
0,7
1
1,5
Glass fiber content (%)

a)

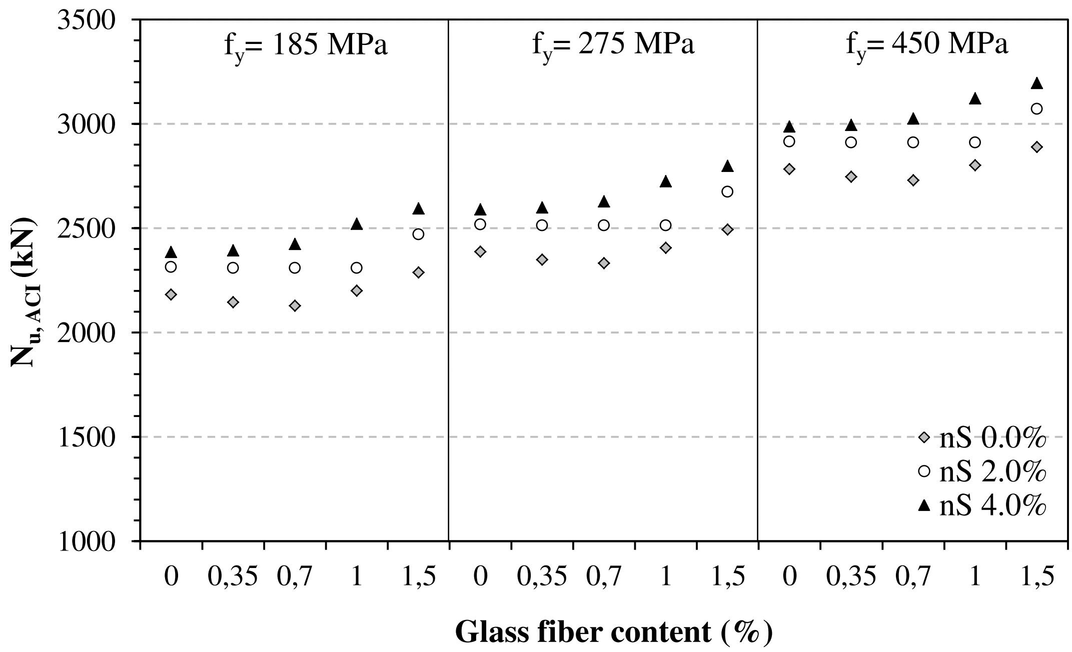

3500
3000
2500
2000
1500
1000
$N_{u,ACI}$ (kN)
f_y= 185 MPa
f_y= 275 MPa
f_y= 450 MPa
nS 0.0%
nS 2.0%
nS 4.0%
0
0,35
0,7
1
1,5
Glass fiber content (%)

b)

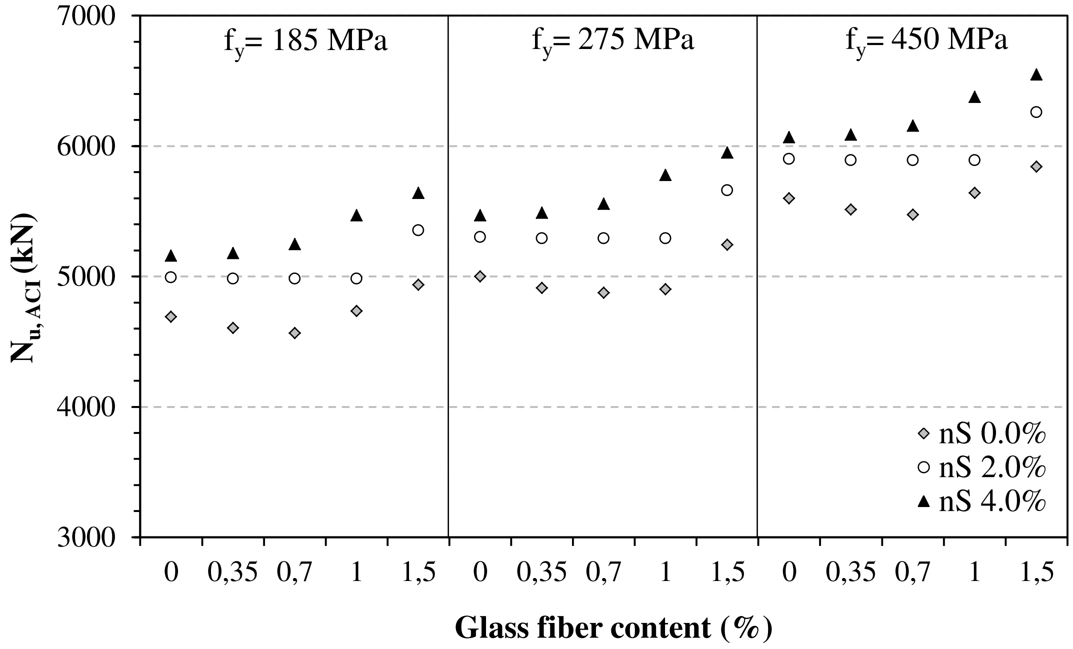

c)

Figure 5.4 ACI based axial capacity of the CFST columns having SCCs at 90 days in accordance with GF content for the steel tube D/t ratio of a) 30, b) 60 and c) 90

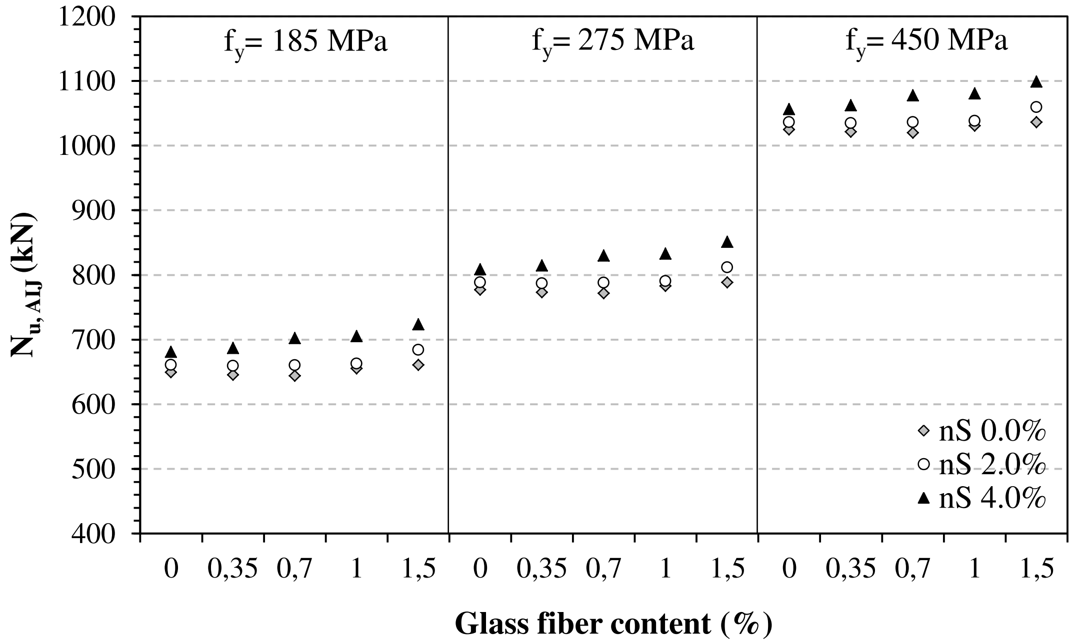

a)

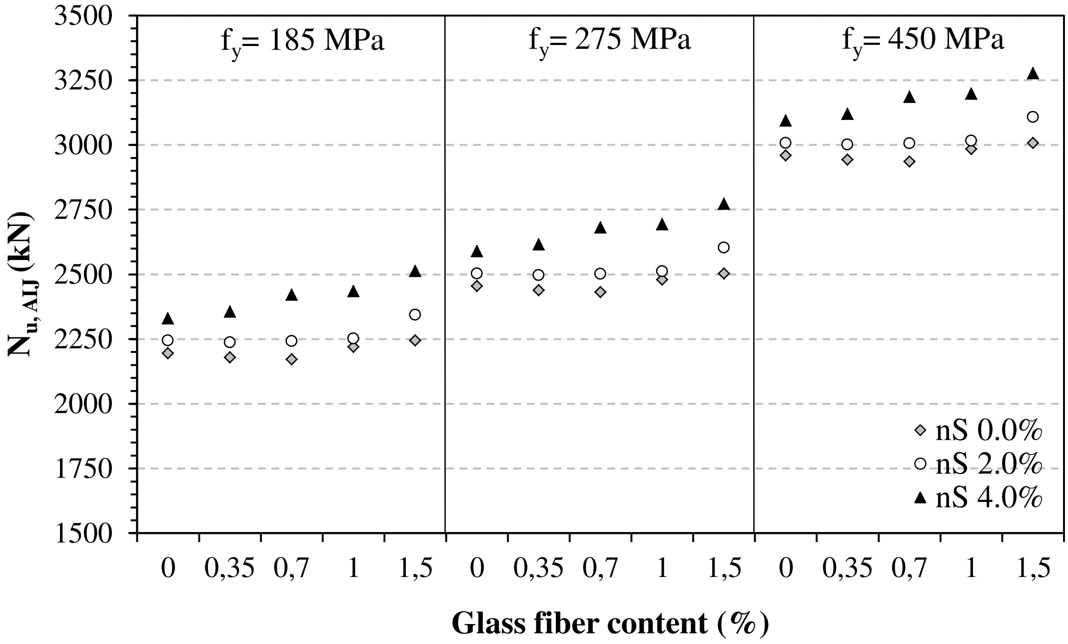

b)

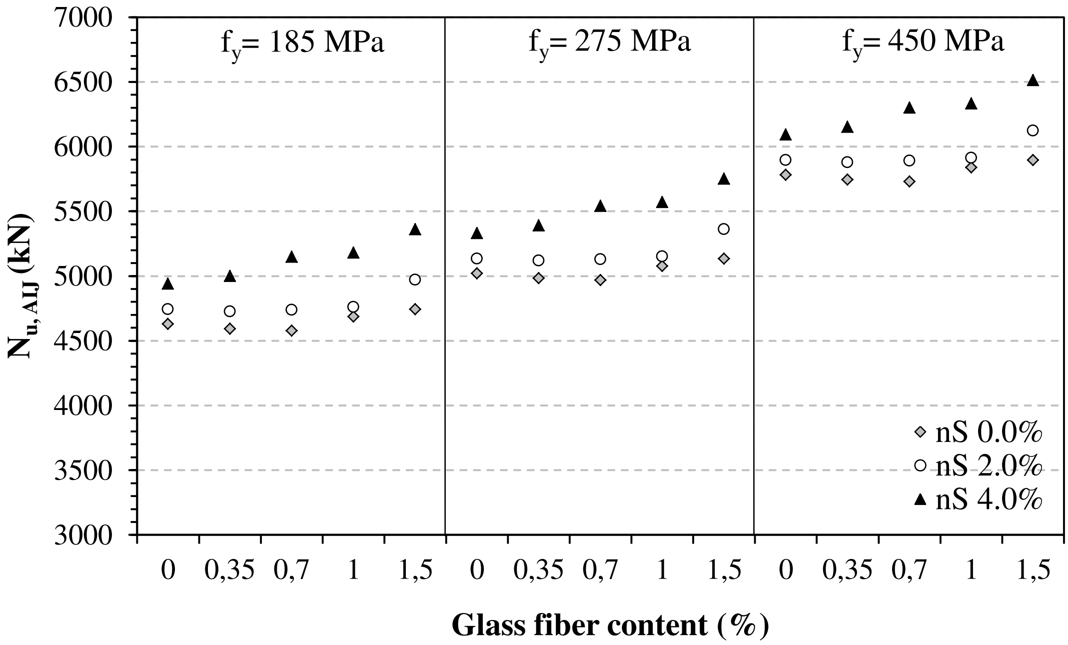

c)

Figure 5.5 AIJ based axial capacity of the CFST columns having SCCs at 28 days in accordance with GF content for the steel tube D/t ratio of a) 30, b) 60 and c) 90

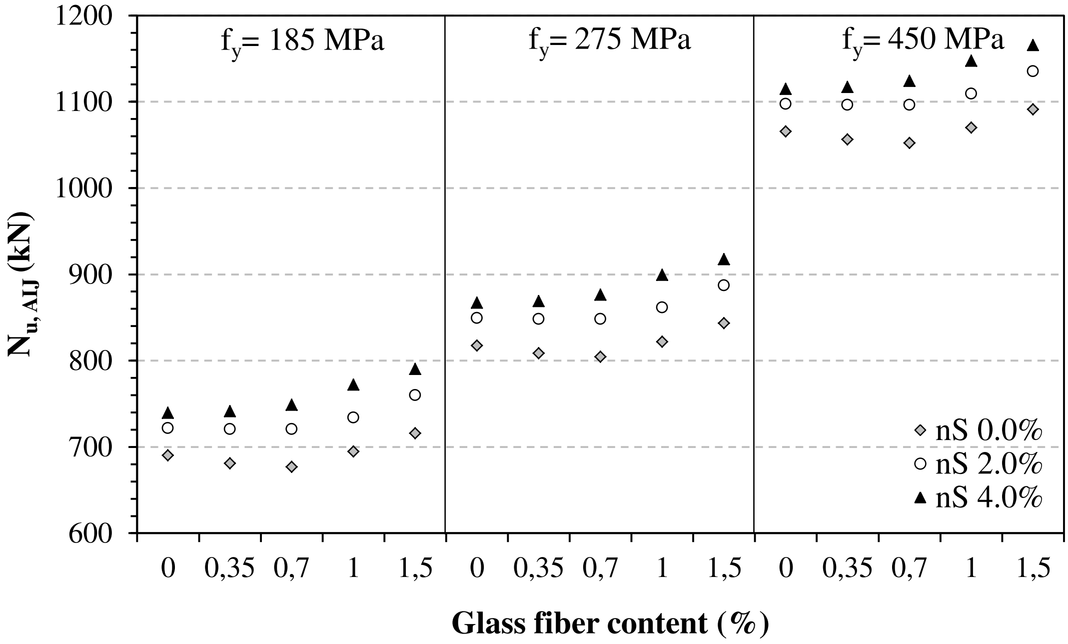

fy= 185 MPa
fy= 275 MPa
fy= 450 MPa
Nu,AIJ (kN)
Glass fiber content (%)
nS 0.0%
nS 2.0%
nS 4.0%

a)

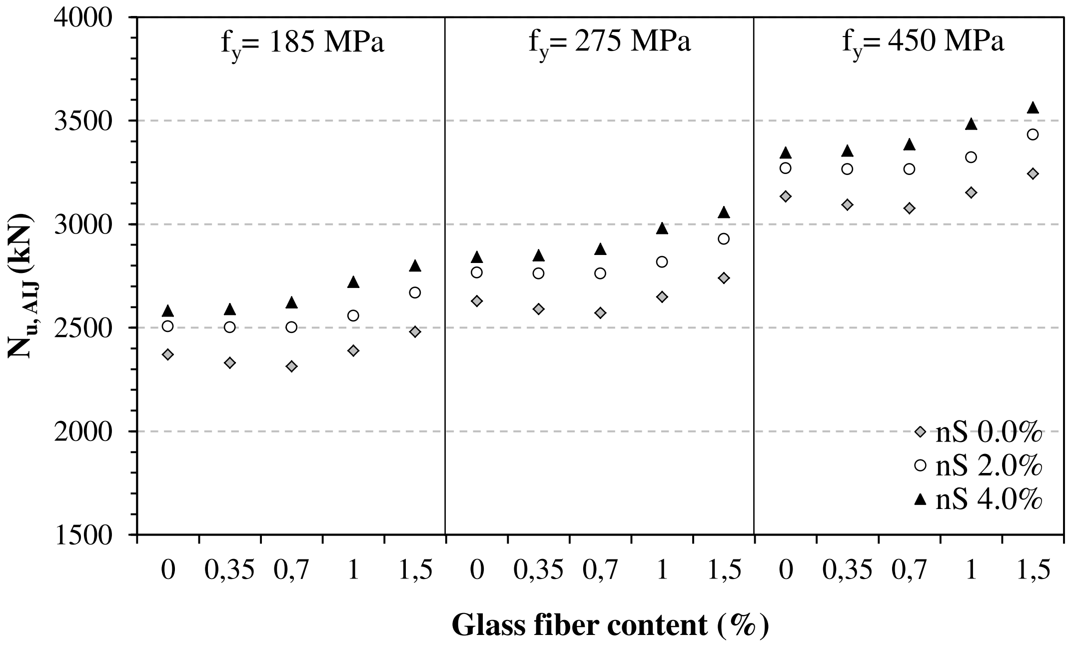

fy= 185 MPa
fy= 275 MPa
fy= 450 MPa
Nu,AIJ (kN)
Glass fiber content (%)
nS 0.0%
nS 2.0%
nS 4.0%

b)

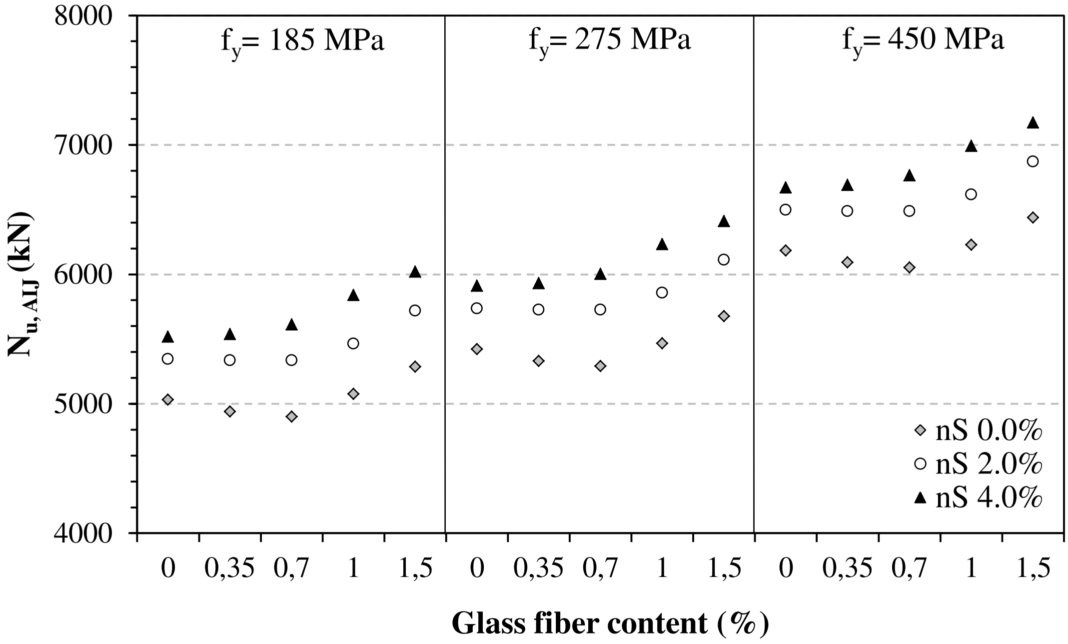

c)

Figure 5.6 AIJ based axial capacity of the CFST columns having SCCs at 90 days in accordance with GF content for the steel tube D/t ratio of a) 30, b) 60 and c) 90

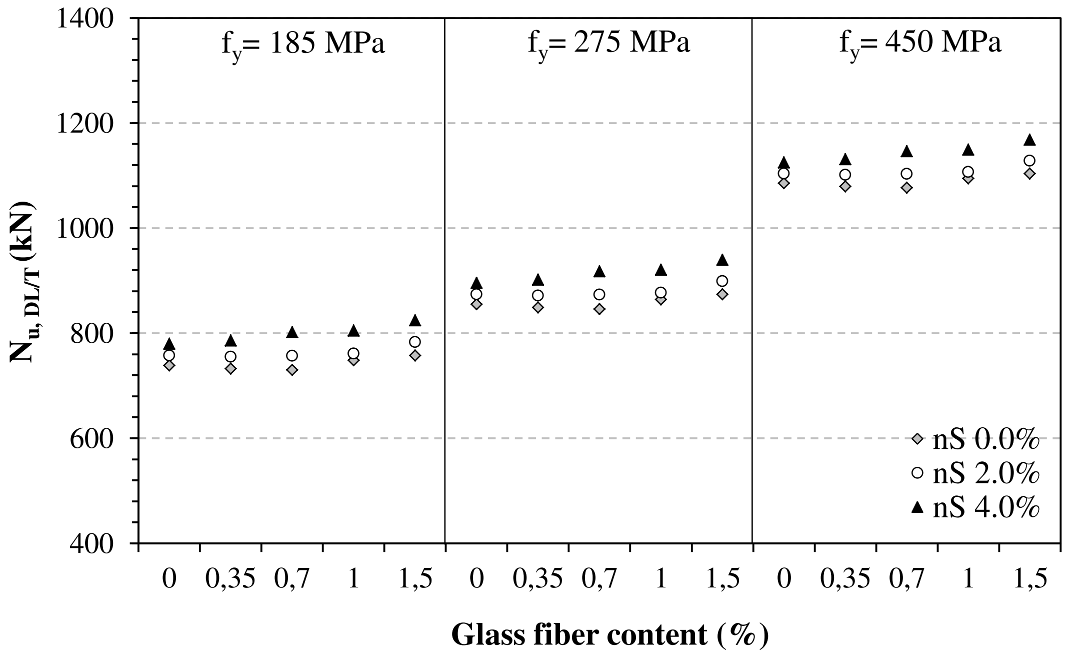

a)

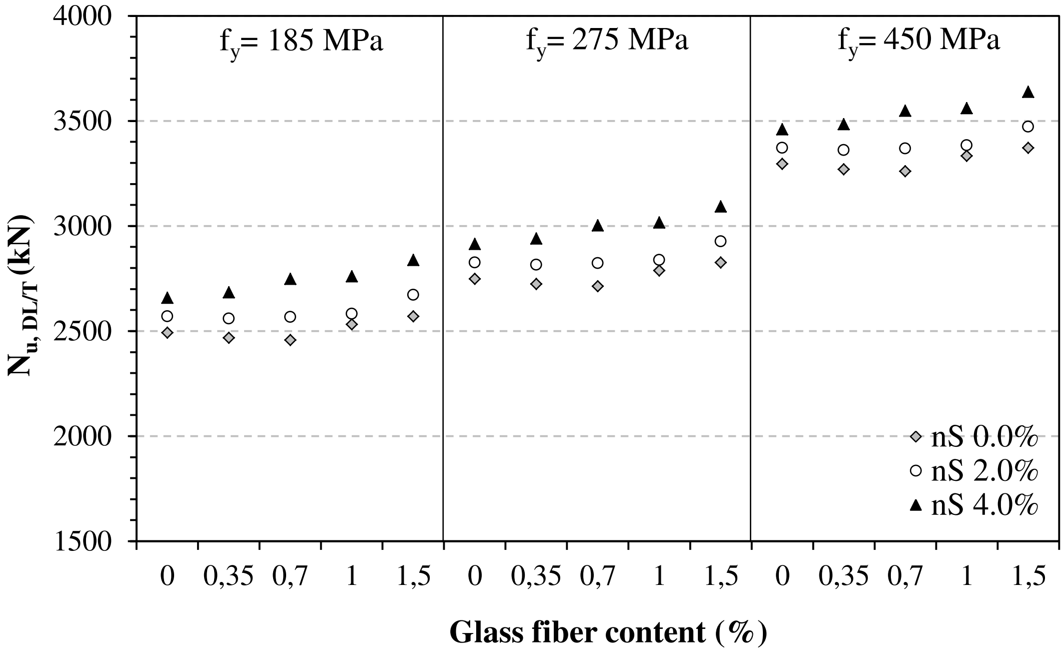

b)

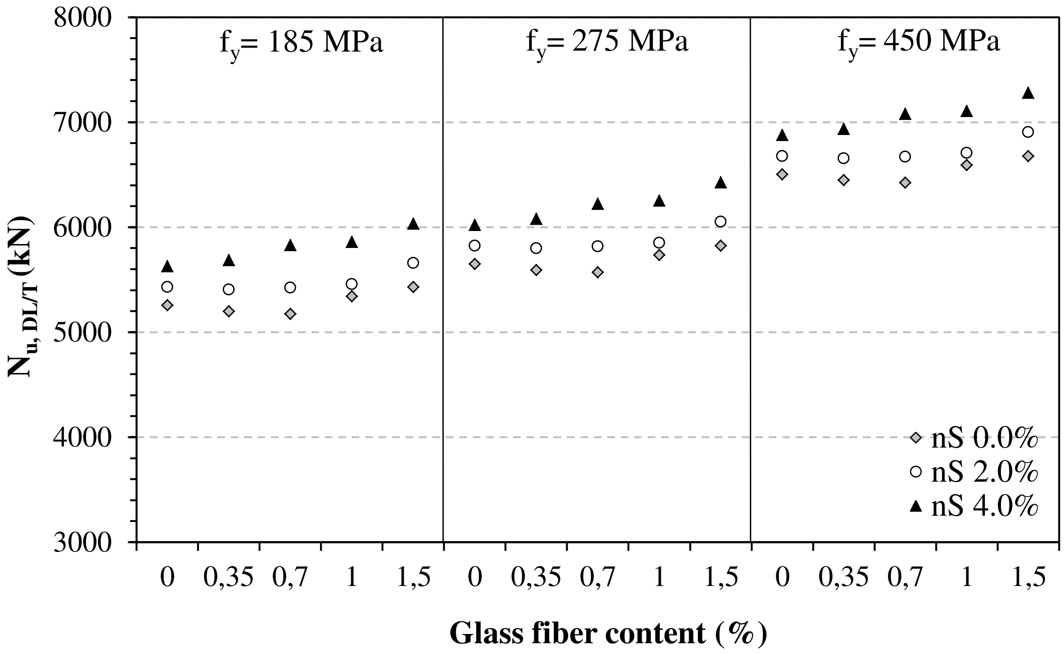

c)

Figure 5.7 DL/T based axial capacity of the CFST columns having SCCs at 28 days in accordance with GF content for the steel tube D/t ratio of a) 30, b) 60 and c) 90

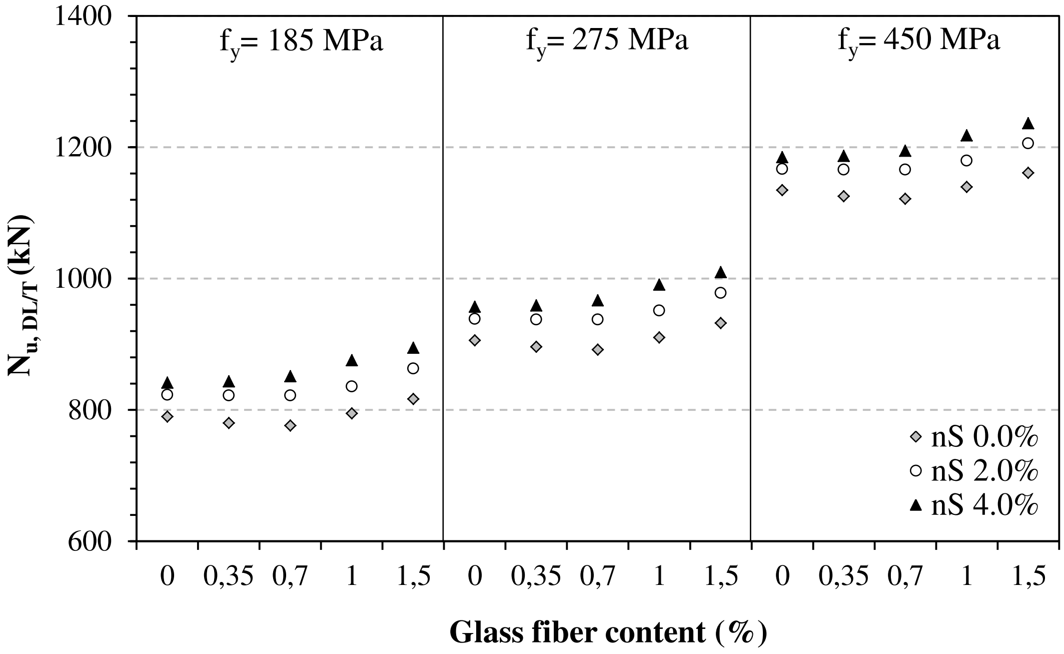

fy= 185 MPa
fy= 275 MPa
fy= 450 MPa
1400
1200
1000
800
600
Nu, DL/T (kN)
0
0,35
0,7
1
1,5
Glass fiber content (%)
nS 0.0%
nS 2.0%
nS 4.0%

a)

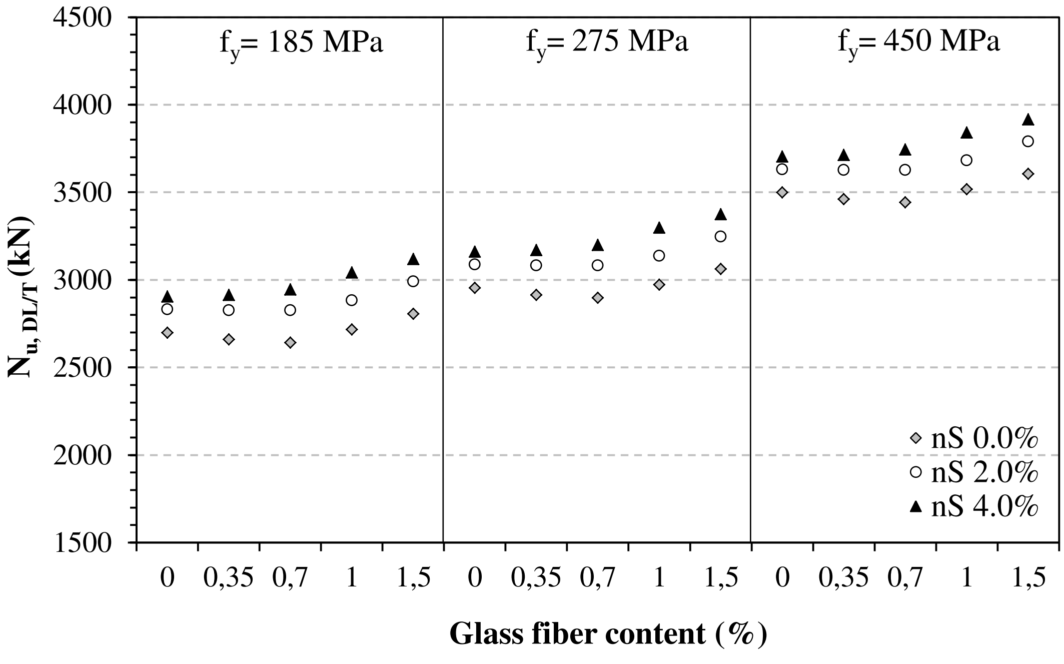

fy= 185 MPa
fy= 275 MPa
fy= 450 MPa
4500
4000
3500
3000
2500
2000
1500
Nu, DL/T (kN)
0
0,35
0,7
1
1,5
Glass fiber content (%)
nS 0.0%
nS 2.0%
nS 4.0%

b)

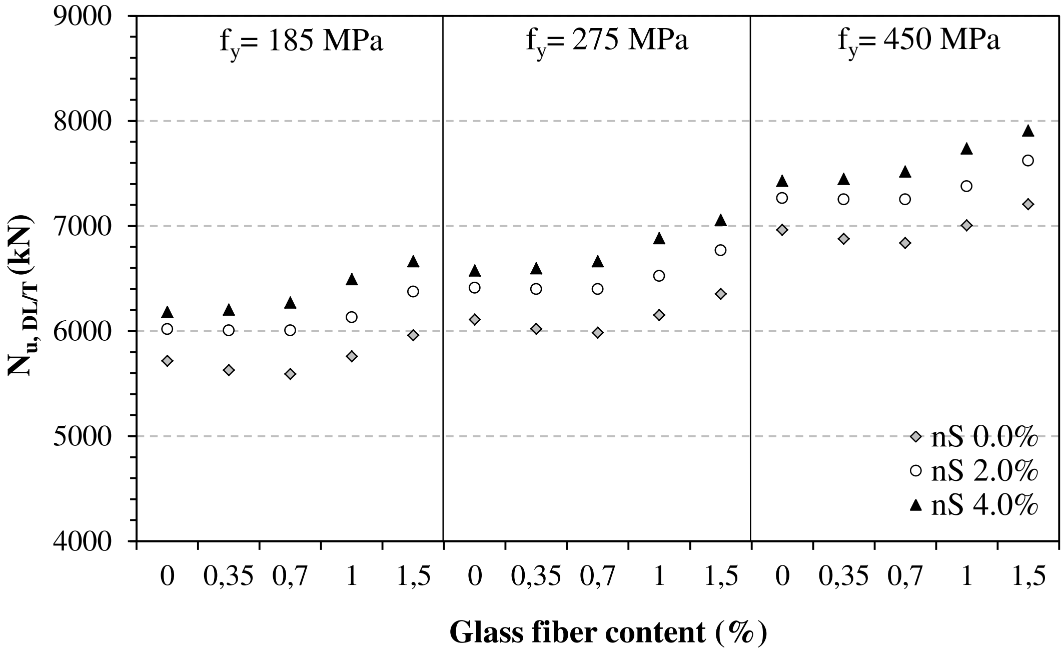

c)

Figure 5.8 DL/T based axial capacity of the CFST columns having SCCs at 90 days in accordance with GF content for the steel tube D/t ratio of a) 30, b) 60 and c) 90

5.1.1 Testing age

The influence of age of curing on the ultimate axial capacity of GFRSCC filled steel tube circular short columns was assessed as the axial load carrying capacity at 90 days divided by the axial load carrying capacity at 28 days. In general the overall $N_{u, 90}$ to $N_{u, 28}$ ratios indicate that the longer curing period the higher N_u value for all the design codes mentioned earlier, Table 5.2. Another indication from Table 5.2 is that that the high D/t ratio tends to increase the effect of age intensity in comparison to low D/t ratio. For example it can be seen from Table 5.2 the age effect intensity of Eurocde 4 computed for CFST column has D/t ratio of 30 varies between 103% to 110% whilst it is between 105% to 115% with respect to column has D/t ratio of 90. This is related to the increase of concrete diameter while using the same steel thickness in all calculations cause to yield higher concrete diameter - higher concrete cross section - consequently, the ultimate axial capacity enhances with increasing of D/t ratio.

Figures 5.9, 5.10, 5.11 and 5.12 depict the effect of curing period on the axial capacity evaluated by provided formulas of Eurocode 4 (2004), ACI-318R (2005), AIJ (2001) and DL/T (1999), respectively. These figures reveal that the incorporation of 0.35% and 0.7% GF caused to slightly decrease the 90 days enhancement in comparison to 1% and 1.5% GF CFST column. Moreover, the contribution of concrete made with 2.0% nS and steel grade of S185 yielded higher improvement in ultimate axial capacities – the ratio between $N_{u, 90}$ and $N_{u, 28}$ - regardless the GF volume fractions and the provision code used, whilst the lower age enhancements resulted for CFST column produced by using concrete free of nS and steel grade of S450.

Finally, the effect of steel grade on the ratio between the ultimate axial capacity of 28 and 90 days are also illustrated in Figures 5.9, 5.10, 5.11 and 5.12. It can be seen that, for the same parameters (GF content, D/t ratio and incorporation dosage of nS) the higher the yield strength the lower ratio of $N_{u, 90/} N_{u, 28}$. As an example, Figure 5.10 shows that the at GF of 0.7% and D/t= 90, the use of steel yield strength of 185, 275 and 450 MPa resulted age ratio of 107.8%, 106.8% and 106 % for SCC free of nS, 113%, 112% and 110.8% for SCC incorporated 2% nS and 109.2%, 108.7% and 107.8% for those made with 4% nS, respectively.

Table 5.2 Testing age effect on axial capacity of CFST short circular columns

Approaches	**D/t ratio**	**Age effect intensity (%)**
Eurocode 4 (2004)	30	103 – 110
	60	104 – 115
	90	105 – 115
ACI 318R (2005)	30	104 – 112
	60	105 – 115
	90	106 – 116
AIJ (2001)	30	103 – 111
	60	105 – 114
	90	106 – 115
DL/T (1999)	30	104 – 110
	60	106 – 112
	90	106 – 113

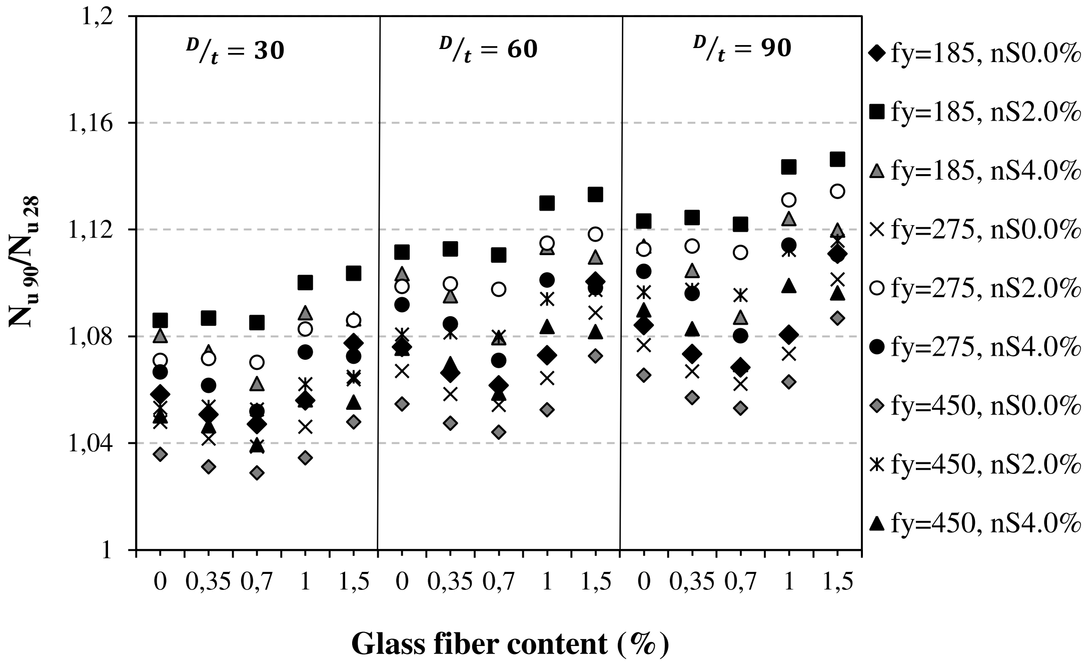

Figure 5.9 Effect of curing period on the predicted axial capacity calculated via Eurocode 4 with respect to GF content

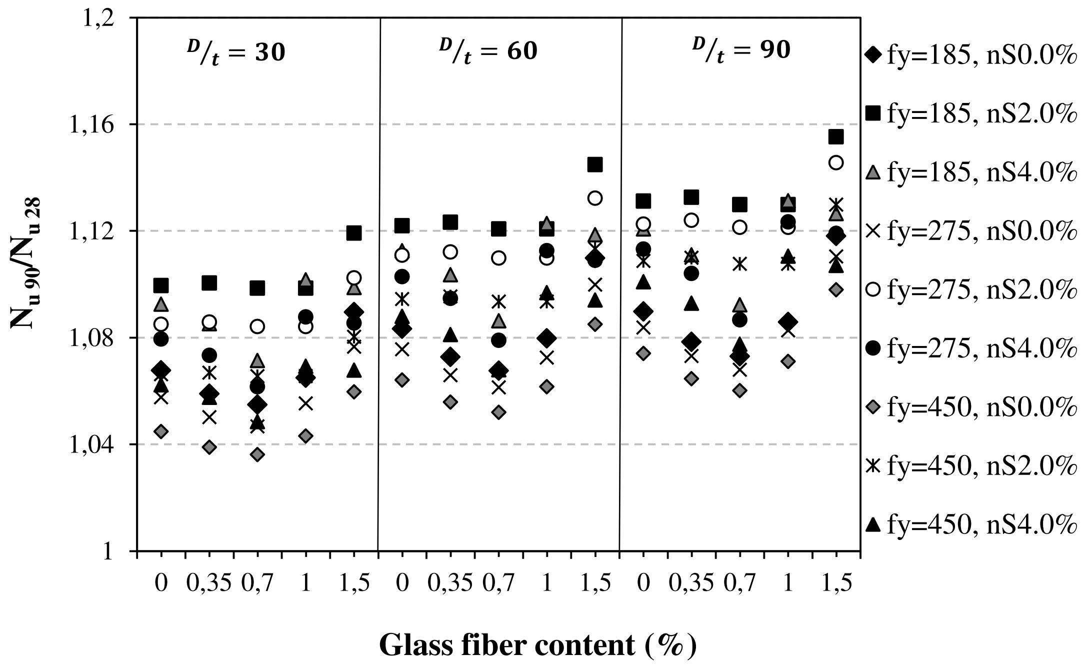

Figure 5.10 Effect of curing period on the predicted axial capacity calculated via ACI 318 with respect to GF content

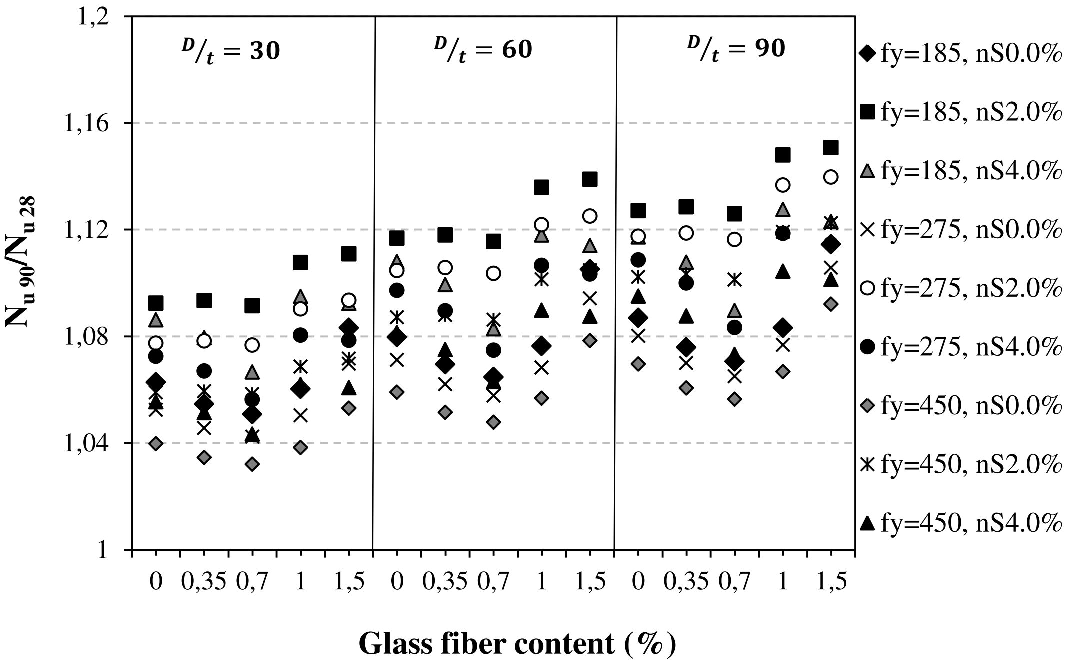

Figure 5.11 Effect of curing period on the predicted axial capacity calculated via AIJ with respect to GF content

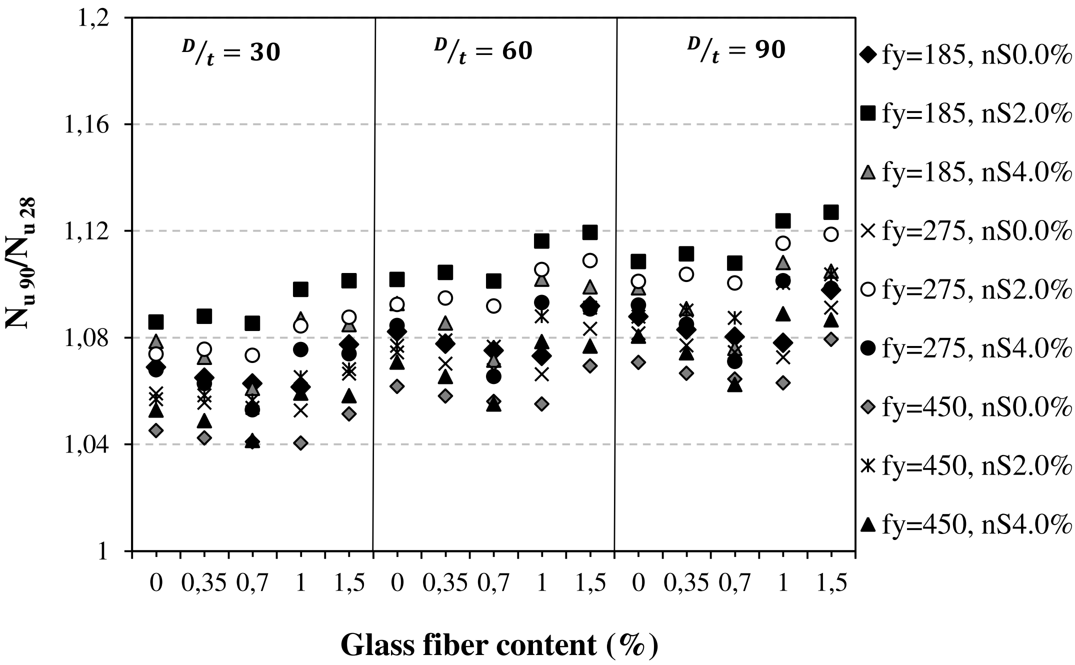

Figure 5.12 Effect of curing period on the predicted axial capacity calculated via DL/T with respect to GF content

5.1.2 Effect of using glass fiber

In this study, the use of five different contents of GF significantly affected the properties of SCC in terms of fresh and hardened properties as mentioned in chapter four. This section presents the effect of GF on structural behaviour of CFST circular short columns. To this aim, the axial capacity of columns infilled with plain concrete was divided by that of infilled with concrete incorporating GF. Figures 5.13 to 5.20 illustrated the effect of using GF on the axial capacity of CFST columns having different SCC mixtures.

Figures 5.13, 5.15, 5.17 and 5.19 simulate the influence of GF on the 28 days axial capacity calculated by using Eurocode4, ACI, AIJ and DL/T, respectively. From these figures, it can be clearly shown that the use of 2% nS and 0.35% or 0.7% or 1.0% GF had no influence on the axial capacity as the ratio between $N_{u,\ plain}$ and $N_{u,\ GF}$ equal or close to 1. Regarding the longer curing period used in this study, the incorporation of 2% nS with 0.35% or 0.7% GF and 4% nS with GF content of 0.35% had no effect on the behaviour of CFST column, Figures 5.14, 5.16, 5.18 and 5.20. Moreover, the overall behaviour of CFST columns reveals that the use of concrete free of nS and GF content of 0.35% or 0.7% caused to slightly decrease axial capacity of CFST column in comparison to column infilled with plain concrete, Figure 5.13 to Figure 5.20. On the other side, the interaction between the utilization of different D/t ratios and GF efficiency presents two different behaviours. The first one is accompanied the columns infilled with concrete made with 0.7% GF and free of nS. It can be seen that the reduction effect of using such concrete increases as the D/t ratio increases. Whereas, the second behaviour is resulted for columns made with concrete incorporated maximum replacement level of nS and higher volume fraction of GF. It can be shown that the enhancement effect due to the use of GF increases with the increase in D/t ratio from 30 to 90, Figure 5.13 to Figure 5.20.

Table 5.3 illustrates the maximum enhancement and maximum reduction percent of different CFST column axial capacity. As presented in the table, the ranges of reduction in axial capacity due to the use of GF did not pass 3% which is revealed there is insignificant effect of GF when the reduction behavior is considered. Moreover, the minimum enhancement due to the utilization of GF as can be seen in

Table 5.3 is 6%. Therefore it is easy to say that the GF efficiency seems to be more important when the enhancement effect is considered.

Table 5.3 GF efficiency

Code	**Age**	**Maximum reduction (%)**	**Maximum enhancement (%)**
Eurocode 4	28	101	107
	90	103	107
ACI	28	101	107
	90	103	108
AIJ	28	101	107
	90	103	108
DL/T	28	102	106
	90	102	106

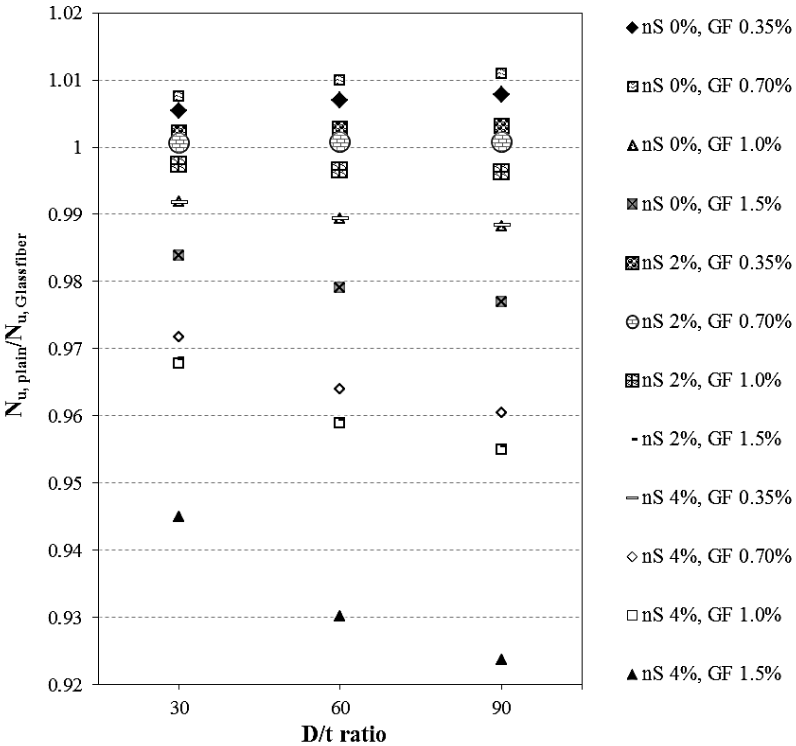

1.02
1.01
1
0.99
0.98
0.97
0.96
0.95
0.94
0.93
0.92
$N_{u, plain}/N_{u, Glassfiber}$
30
60
90
D/t ratio
nS 0%, GF 0.35%
nS 0%, GF 0.70%
nS 0%, GF 1.0%
nS 0%, GF 1.5%
nS 2%, GF 0.35%
nS 2%, GF 0.70%
nS 2%, GF 1.0%
nS 2%, GF 1.5%
nS 4%, GF 0.35%
nS 4%, GF 0.70%
nS 4%, GF 1.0%
nS 4%, GF 1.5%

a)

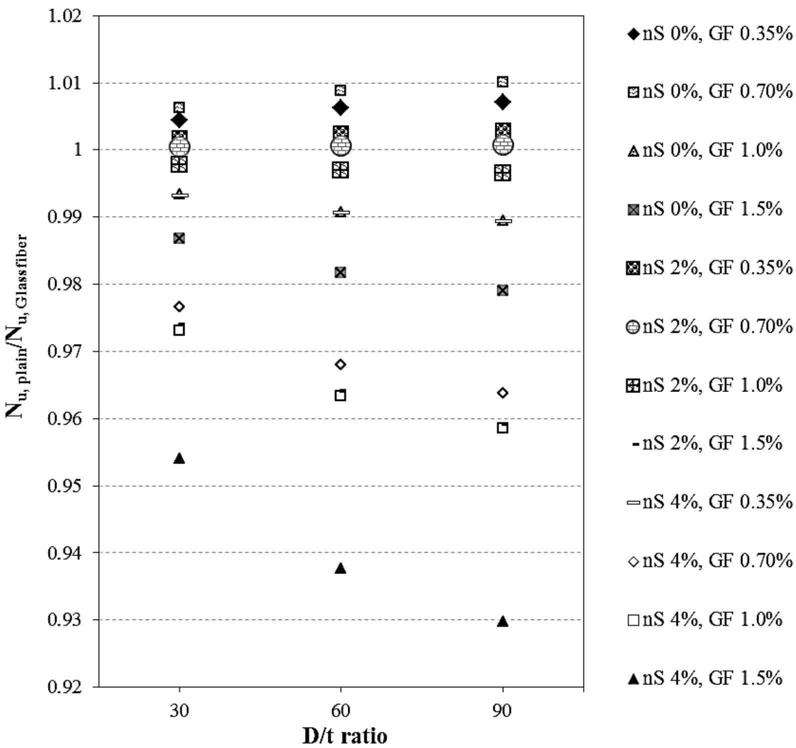

1.02
1.01
1
0.99
0.98
0.97
0.96
0.95
0.94
0.93
0.92
$N_{u, plain}/N_{u, Glassfiber}$
30
60
90
D/t ratio
nS 0%, GF 0.35%
nS 0%, GF 0.70%
nS 0%, GF 1.0%
nS 0%, GF 1.5%
nS 2%, GF 0.35%
nS 2%, GF 0.70%
nS 2%, GF 1.0%
nS 2%, GF 1.5%
nS 4%, GF 0.35%
nS 4%, GF 0.70%
nS 4%, GF 1.0%
nS 4%, GF 1.5%

b)

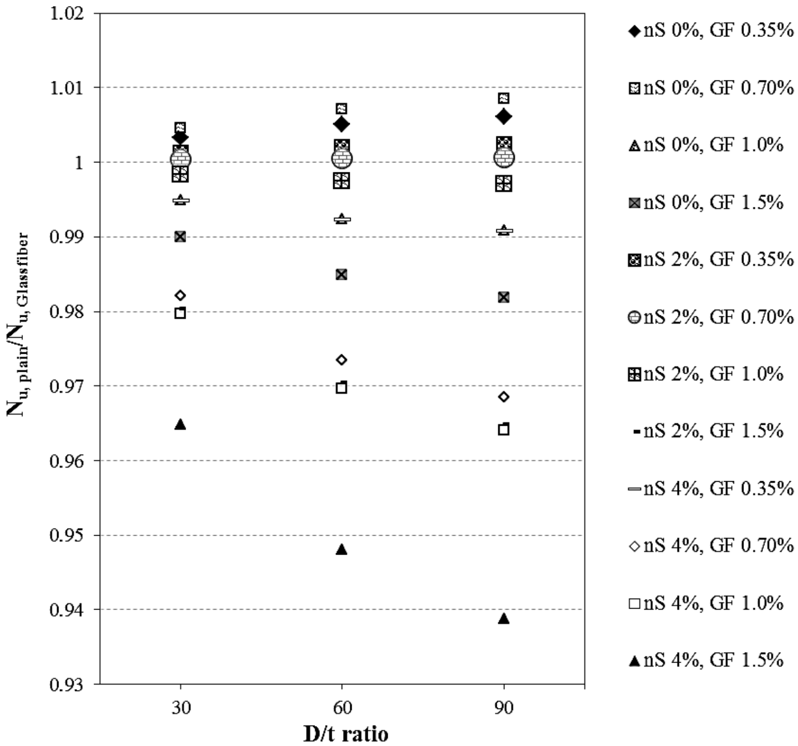

c)

Figure 5.13 Effect of using GF on $N_{u, EC4}$ of the composite columns tested at 28 days for f_y of a) 185 MPa, b) 275 MPa and c) 450 MPa

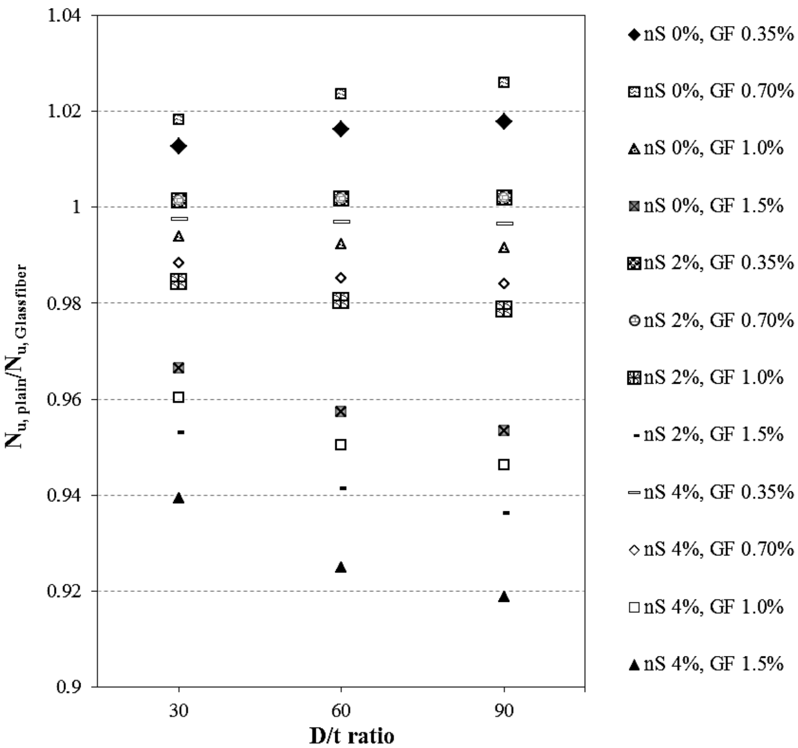

a)

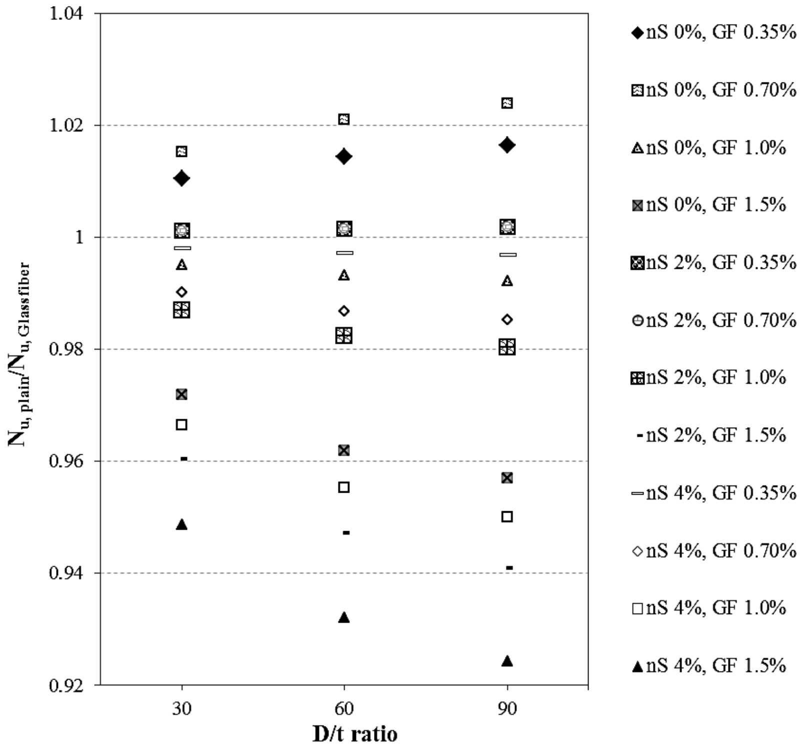

b)

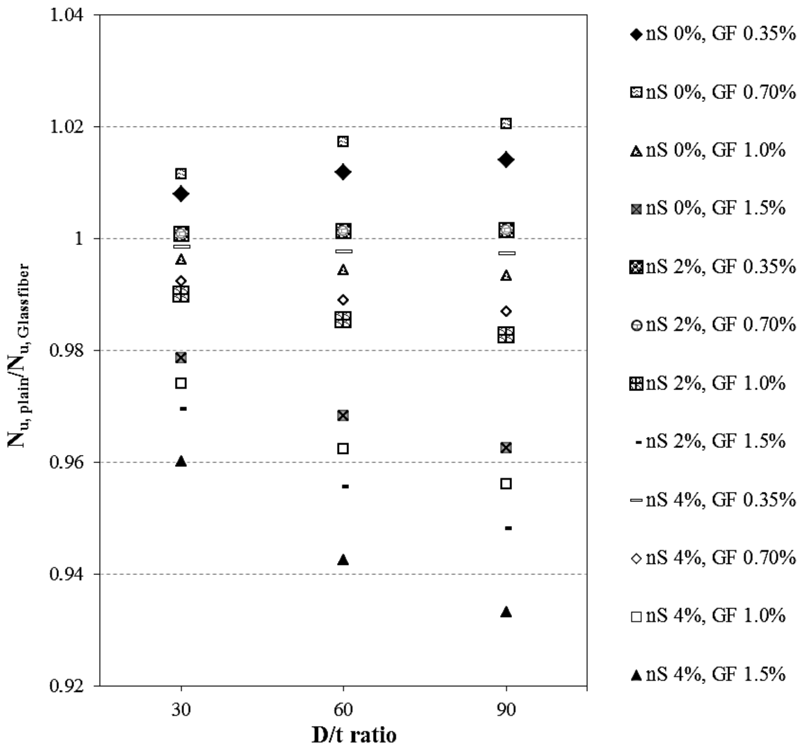

c)

Figure 5.14 Effect of using GF on $N_{u, EC4}$ of the composite columns tested at 90 days for f_y of a) 185 MPa, b) 275 MPa and c) 450 MPa

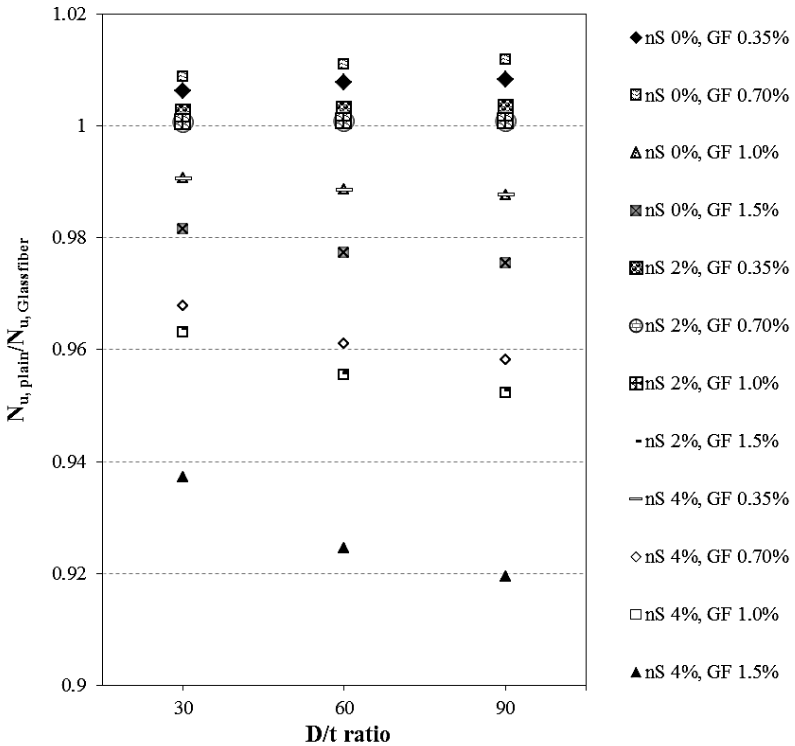
1.02
1
0.98
0.96
0.94
0.92
0.9
30
60
90
D/t ratio
$N_{u, plain}/N_{u, Glass fiber}$
nS 0%, GF 0.35%
nS 0%, GF 0.70%
nS 0%, GF 1.0%
nS 0%, GF 1.5%
nS 2%, GF 0.35%
nS 2%, GF 0.70%
nS 2%, GF 1.0%
nS 2%, GF 1.5%
nS 4%, GF 0.35%
nS 4%, GF 0.70%
nS 4%, GF 1.0%
nS 4%, GF 1.5%

a)

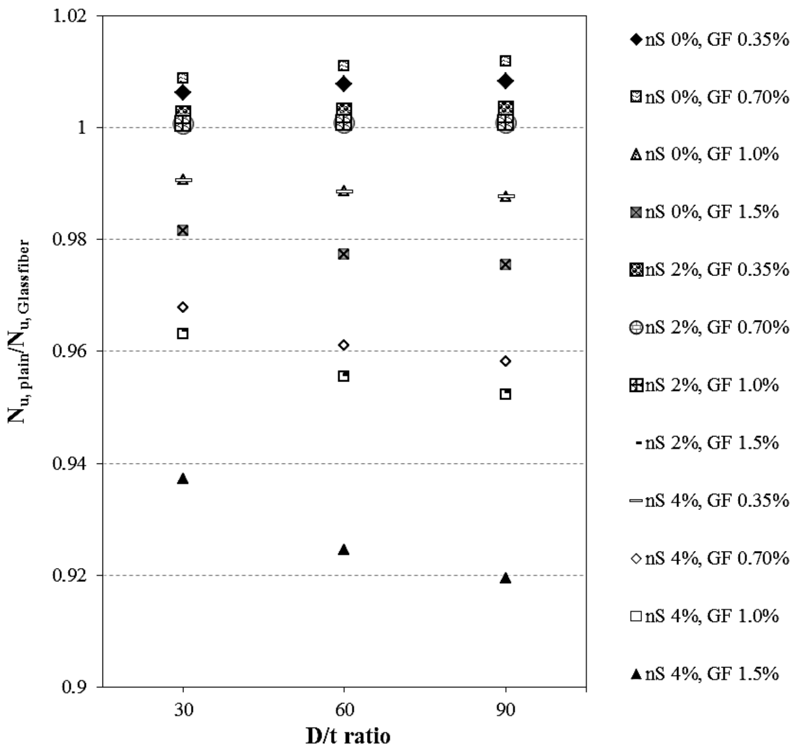
1.02
1
0.98
0.96
0.94
0.92
0.9
30
60
90
D/t ratio
$N_{u, plain}/N_{u, Glass fiber}$
nS 0%, GF 0.35%
nS 0%, GF 0.70%
nS 0%, GF 1.0%
nS 0%, GF 1.5%
nS 2%, GF 0.35%
nS 2%, GF 0.70%
nS 2%, GF 1.0%
nS 2%, GF 1.5%
nS 4%, GF 0.35%
nS 4%, GF 0.70%
nS 4%, GF 1.0%
nS 4%, GF 1.5%

b)

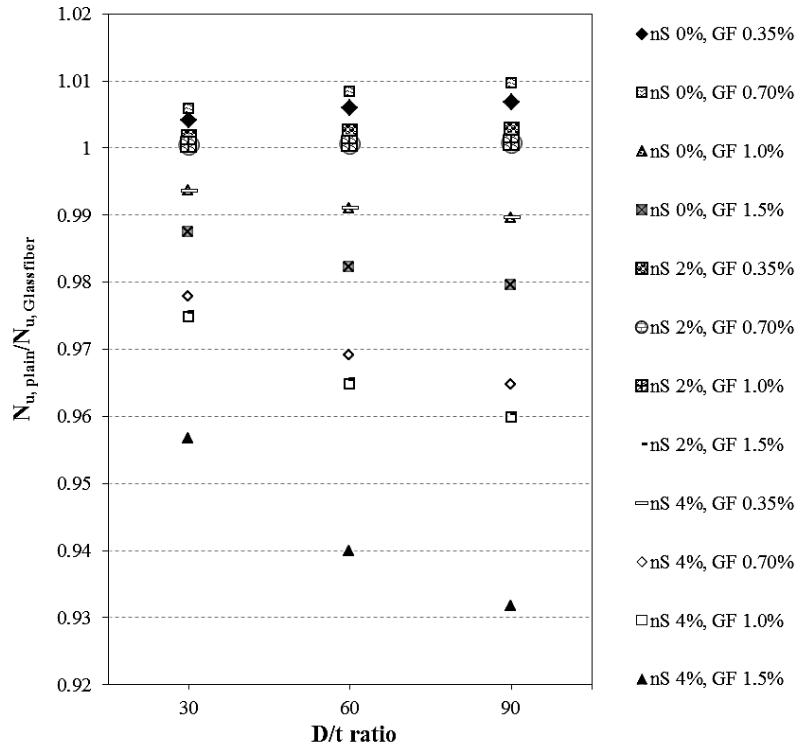

c)

Figure 5.15 Effect of using GF on $N_{u, ACI}$ of the composite columns tested at 28 days for f_y of a) 185 MPa, b) 275 MPa and c) 450 MPa

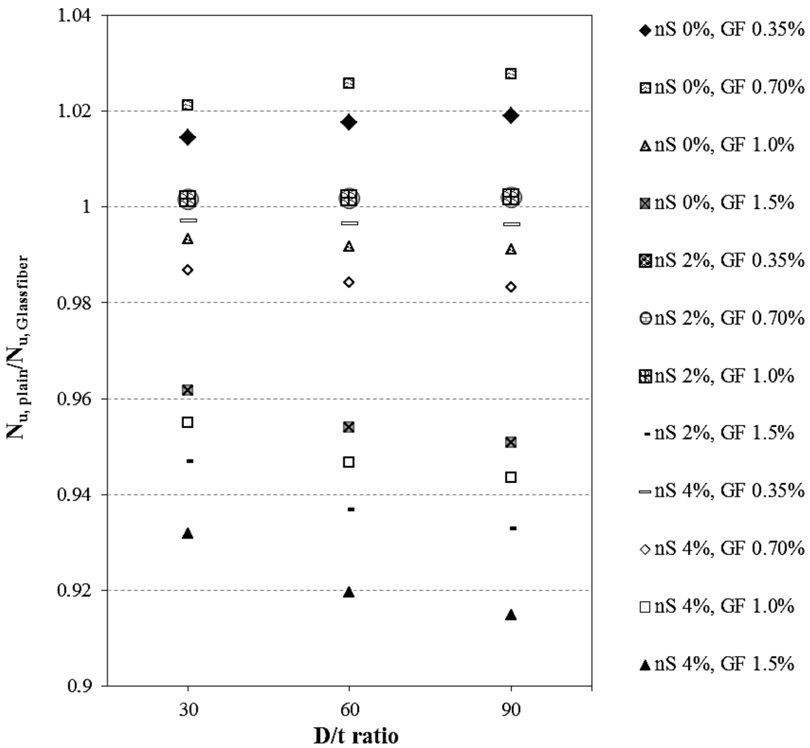

a)

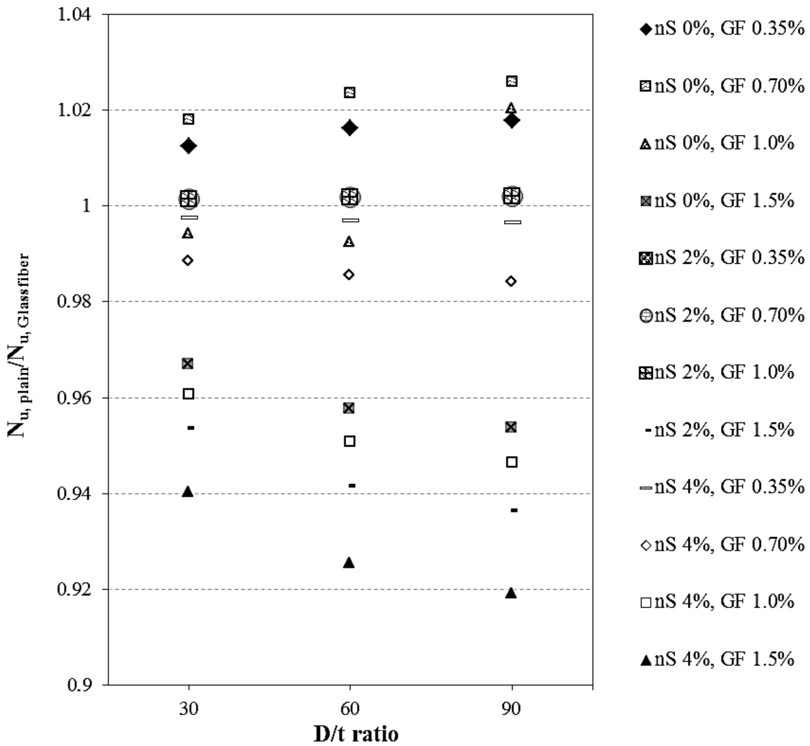

b)

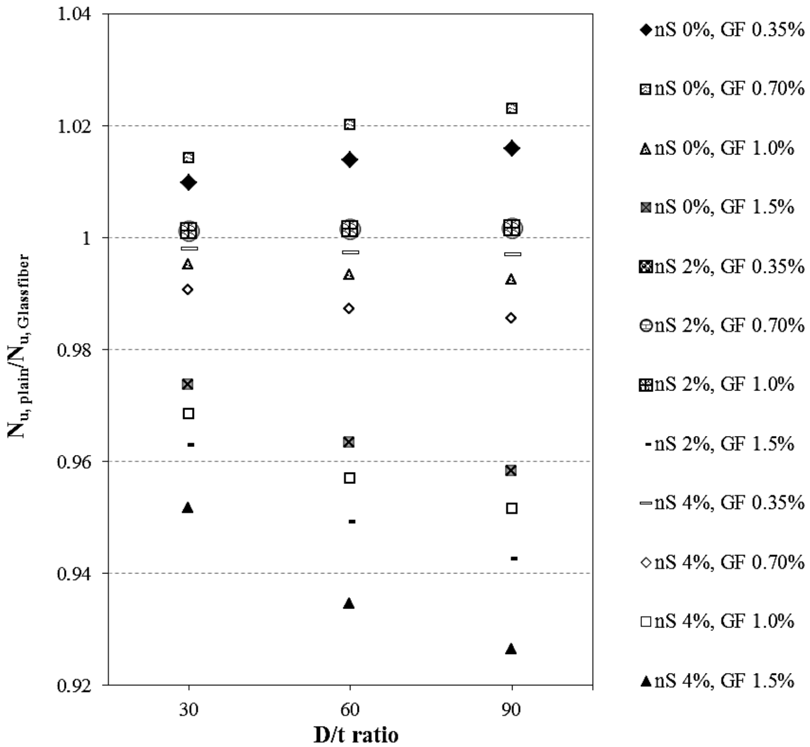

c)

Figure 5.16 Effect of using GF on $N_{u,\,ACI}$ of the composite columns tested at 90 days for f_y of a) 185 MPa, b) 275 MPa and c) 450 MPa

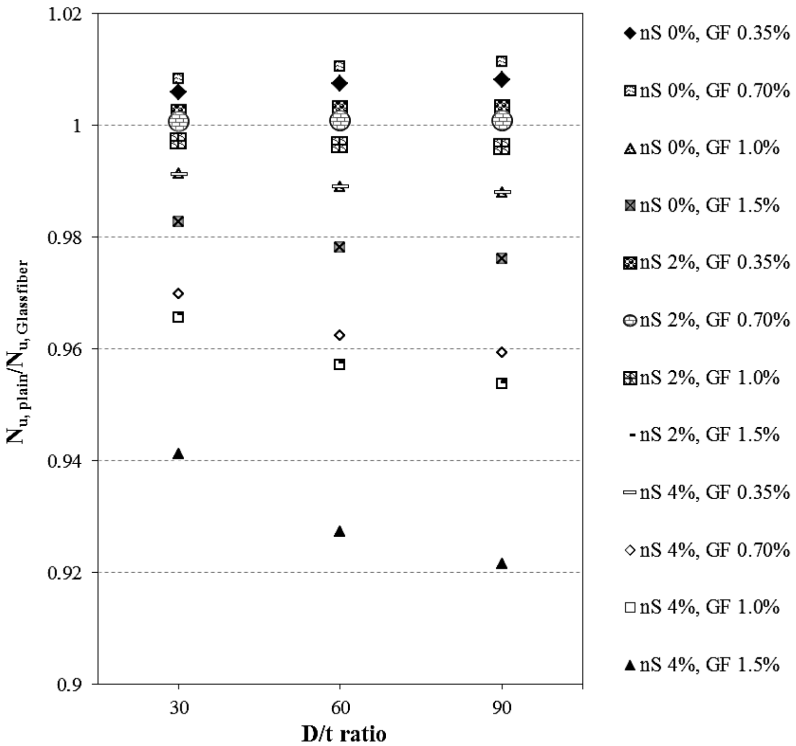
1.02
1
0.98
0.96
0.94
0.92
0.9
$N_{u, plain}/N_{u, Glassfiber}$
30
60
90
D/t ratio
nS 0%, GF 0.35%
nS 0%, GF 0.70%
nS 0%, GF 1.0%
nS 0%, GF 1.5%
nS 2%, GF 0.35%
nS 2%, GF 0.70%
nS 2%, GF 1.0%
nS 2%, GF 1.5%
nS 4%, GF 0.35%
nS 4%, GF 0.70%
nS 4%, GF 1.0%
nS 4%, GF 1.5%

a)

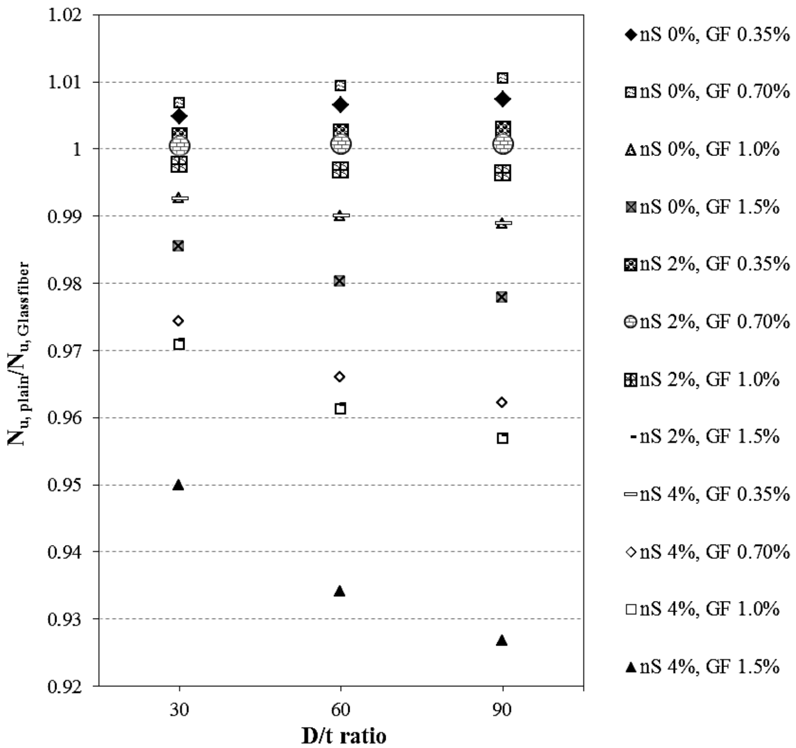
1.02
1.01
1
0.99
0.98
0.97
0.96
0.95
0.94
0.93
0.92
$N_{u, plain}/N_{u, Glassfiber}$
30
60
90
D/t ratio
nS 0%, GF 0.35%
nS 0%, GF 0.70%
nS 0%, GF 1.0%
nS 0%, GF 1.5%
nS 2%, GF 0.35%
nS 2%, GF 0.70%
nS 2%, GF 1.0%
nS 2%, GF 1.5%
nS 4%, GF 0.35%
nS 4%, GF 0.70%
nS 4%, GF 1.0%
nS 4%, GF 1.5%

b)

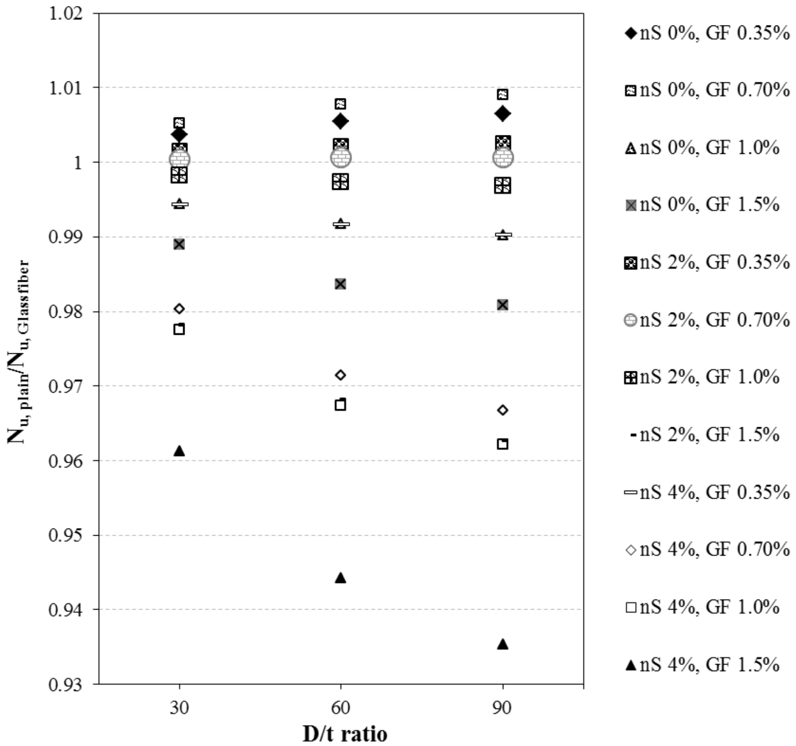

c)

Figure 5.17 Effect of using GF on $N_{u, AIJ}$ of the composite columns tested at 28 days for f_y of a) 185 MPa, b) 275 MPa and c) 450 MPa

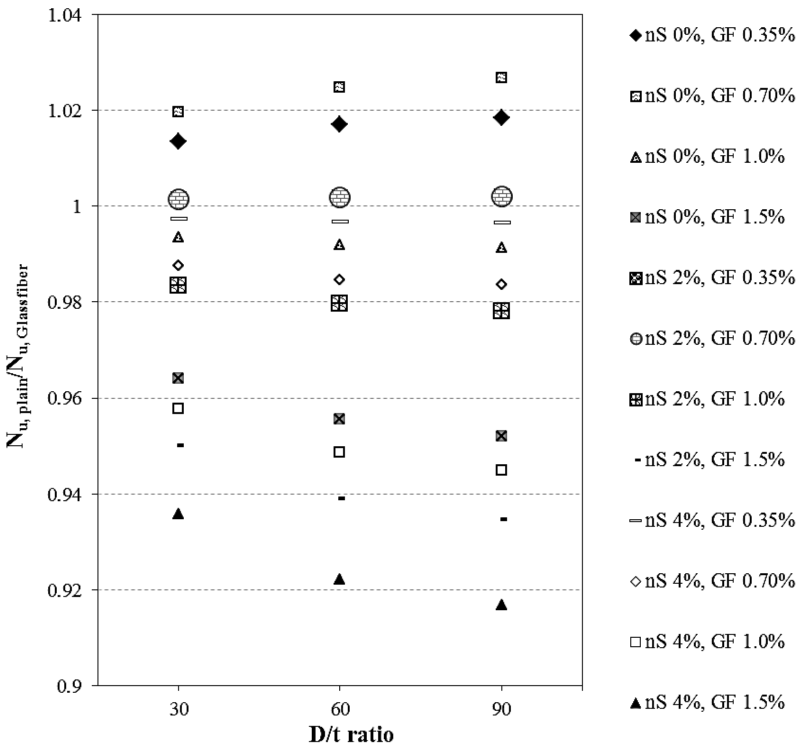

a)

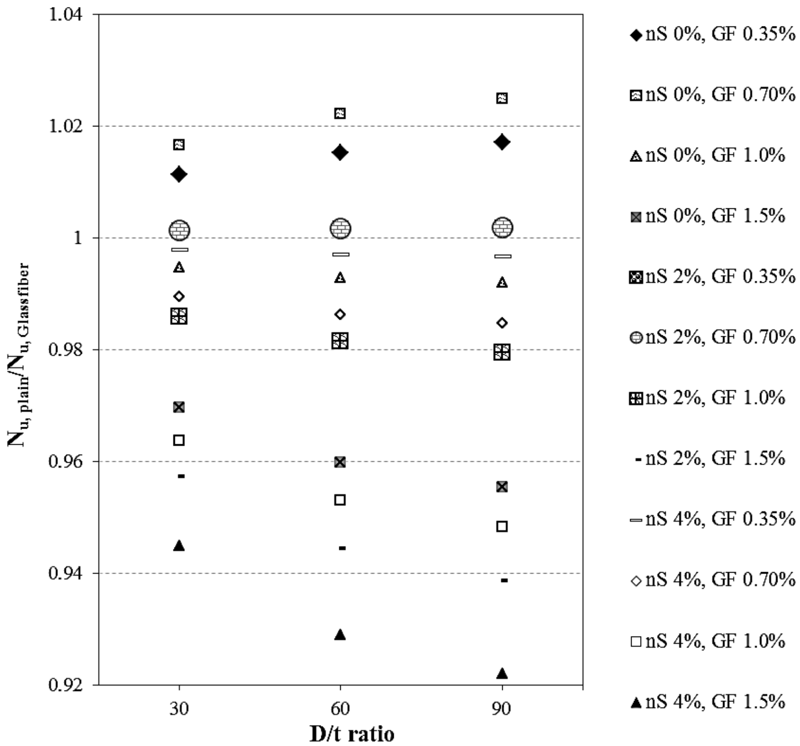

b)

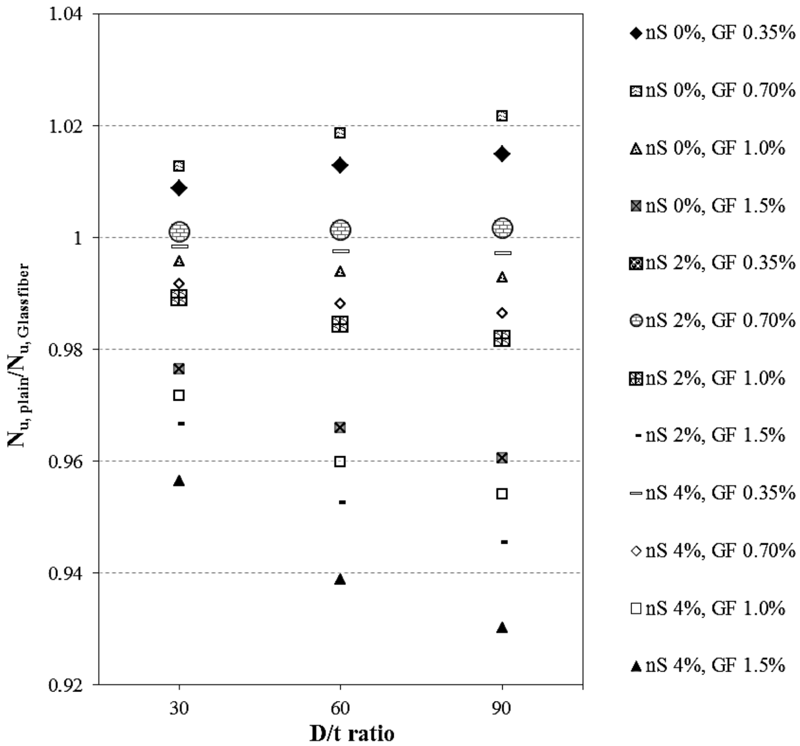

c)

Figure 5.18 Effect of using GF on $N_{u, AIJ}$ of the composite columns tested at 90 days for f_y of a) 185 MPa, b) 275 MPa and c) 450 MPa

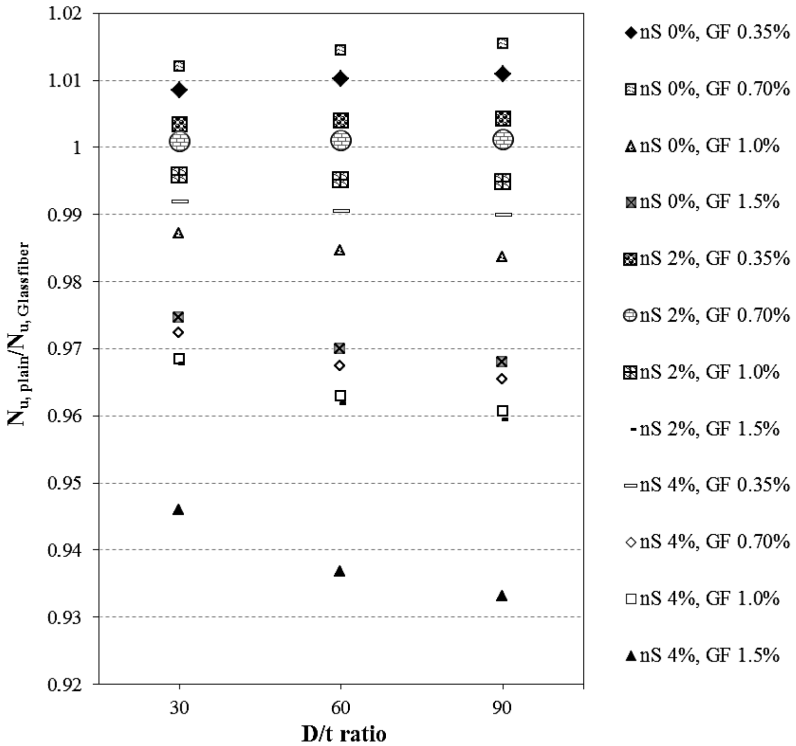
1.02
1.01
1
0.99
0.98
0.97
0.96
0.95
0.94
0.93
0.92
Nu, plain/Nu, Glassfiber
30
60
90
D/t ratio
nS 0%, GF 0.35%
nS 0%, GF 0.70%
nS 0%, GF 1.0%
nS 0%, GF 1.5%
nS 2%, GF 0.35%
nS 2%, GF 0.70%
nS 2%, GF 1.0%
nS 2%, GF 1.5%
nS 4%, GF 0.35%
nS 4%, GF 0.70%
nS 4%, GF 1.0%
nS 4%, GF 1.5%

a)

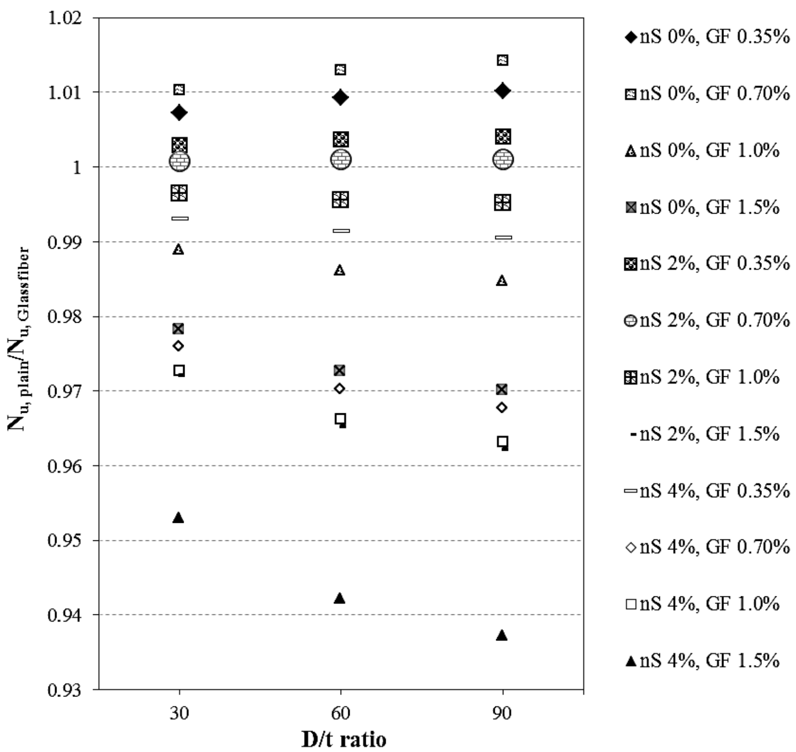
1.02
1.01
1
0.99
0.98
0.97
0.96
0.95
0.94
0.93
Nu, plain/Nu, Glassfiber
30
60
90
D/t ratio
nS 0%, GF 0.35%
nS 0%, GF 0.70%
nS 0%, GF 1.0%
nS 0%, GF 1.5%
nS 2%, GF 0.35%
nS 2%, GF 0.70%
nS 2%, GF 1.0%
nS 2%, GF 1.5%
nS 4%, GF 0.35%
nS 4%, GF 0.70%
nS 4%, GF 1.0%
nS 4%, GF 1.5%

b)

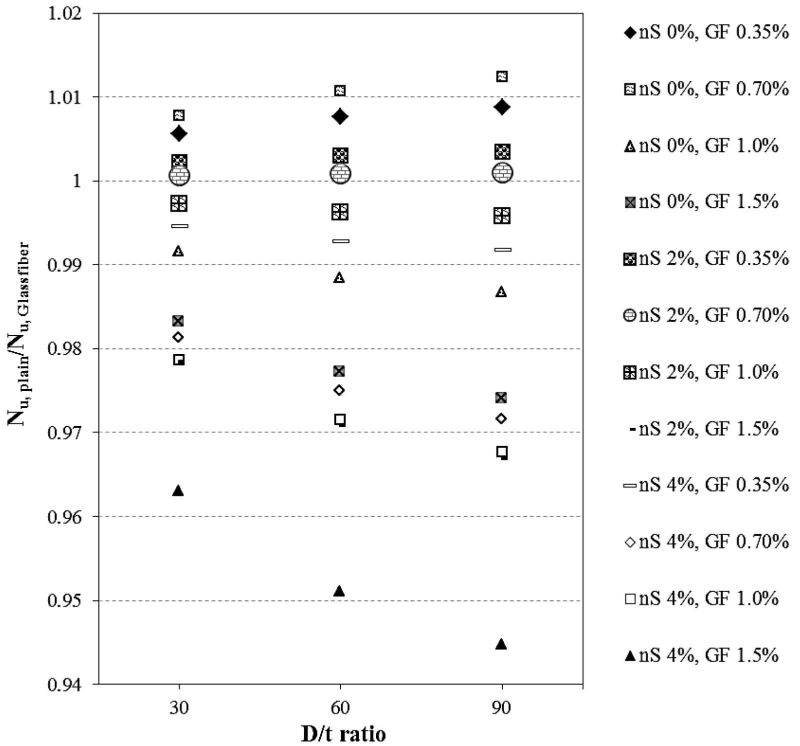

c)

Figure 5.19 Effect of using GF on $N_{u,\ DL/T}$ of the composite columns tested at 28 days for f_y of a) 185 MPa, b) 275 MPa and c) 450 MPa

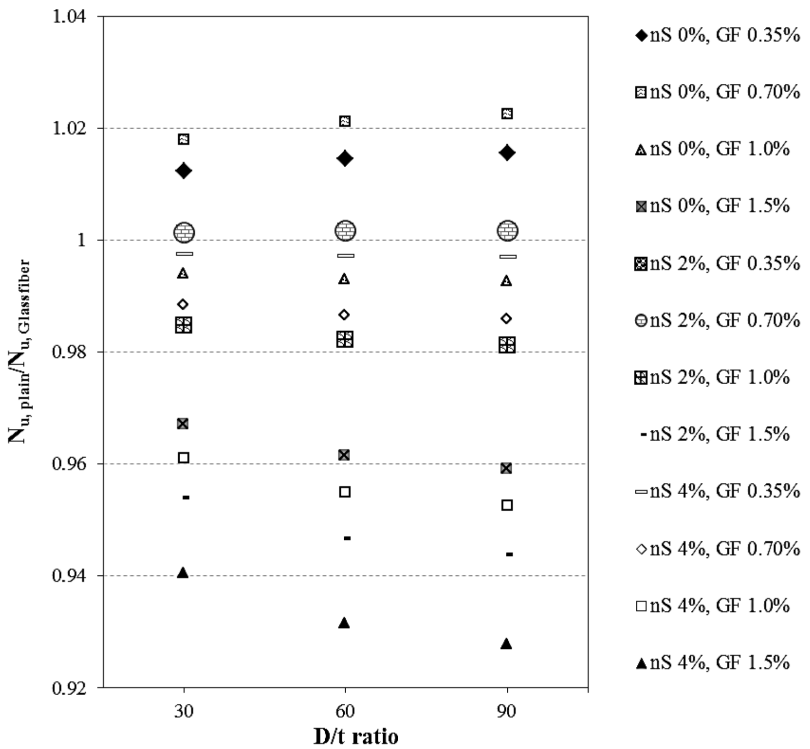

a)

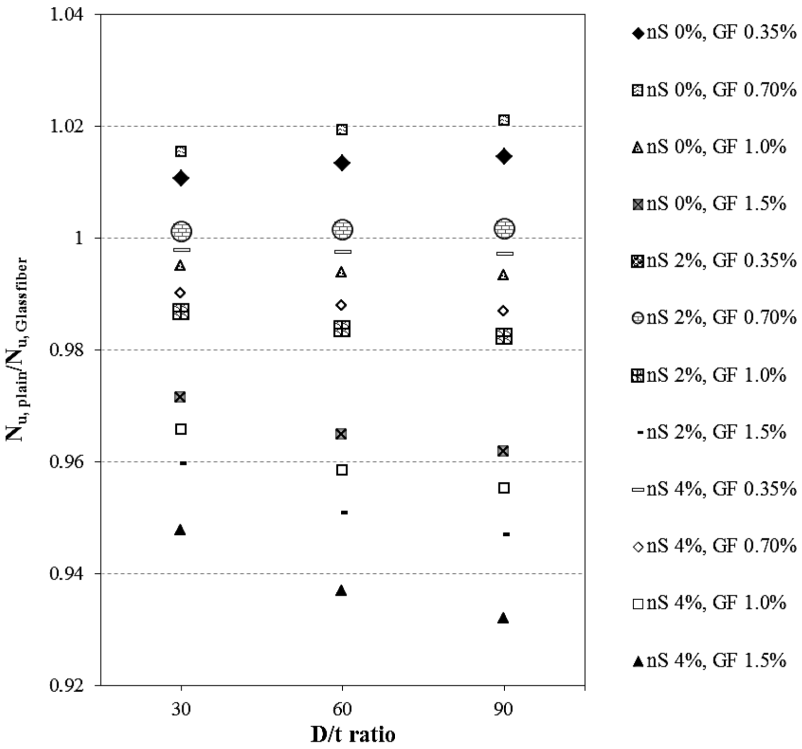

b)

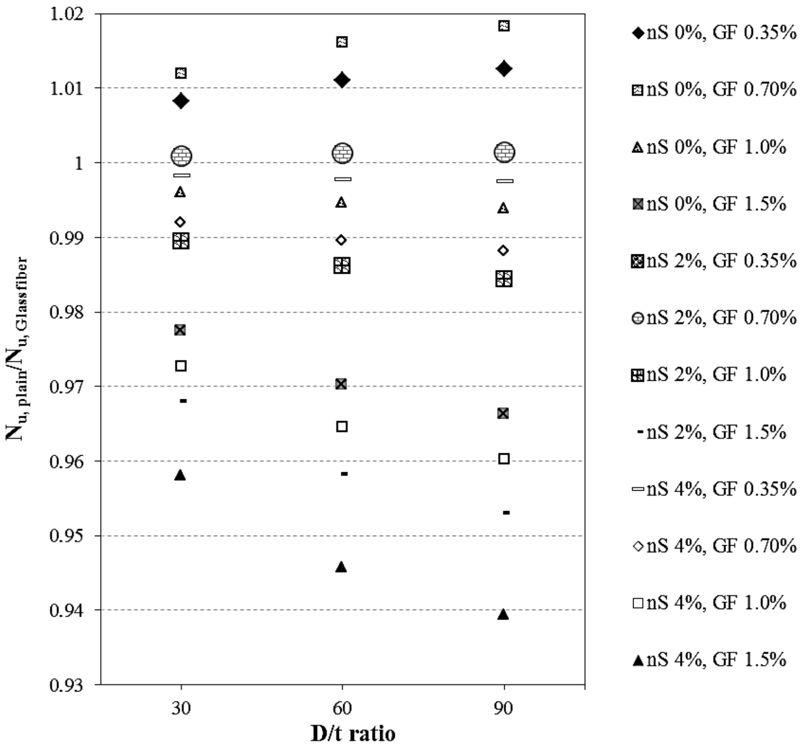

c)

Figure 5.20 Effect of using GF on $N_{u, DL/T}$ of the composite columns tested at 90 days for f_y of a) 185 MPa, b) 275 MPa and c) 450 MPa

5.1.3 Analysis of design codes

As it is expected, in this study the use of four codes namely Eurocode 4 (2004), ACI-318R (2005), AIJ (2001) and DL/T (1999) yielded different axial capacities due to the differences of analysing CFST column structural behaviour of between these codes. However, to understand the overall behaviour of predicted data in terms of type of design code, special approached was adopted. The first one was accomplished by comparing the codes with each other with respect to number of specimen, whereas the second one was performed by developing regression model for predicting ultimate axial capacities between each two codes. For these purposes the first and second approaches are finalized graphically as presented in Figures 5.21 to 5.29.

Figures 5.21, 5.22, 5.23, 5.24, 5.25 and 5.26 present the comparison of the 28 and 90 days axial capacity of CFST column evaluated by Eurocode 4 and ACI, AIJ and Eurocode 4, DL/T and Eurocode 4, respectively. On the other hand, each figure involved a and b because the comparison study analysed predicted axial capacity in terms of number of specimens and Eurocode 4 predicted axial capacity values. As can be clearly seen in Figures 5.21 and Figure 5.22, there are slight differences between the overall behaviour of 28 and 90 days. In general, these two figures indicate that the use of nS in concrete tends to reduce the differences between the Eurocode 4 and ACI results regardless steel grade and D/t ratio. The effect of steel grade can also be found from the same two figures, that is when the same D/t ratio used the increase in steel yield strength caused to increase the differences between the axial capacity of ACI and Eurocode 4. At the same line, when the same steel yield strength used the differences between axial capacity of ACI and Eurocode 4 reduced as the D/t ratio increased.

Figures 5.23 and 5.24 present the comparison between AIJ and Eurocode 4 axial capacity calculated for 28 and 90 days, respectively. It can be seen that the general behaviour seems to be similar to that resulted between ACI and Eurocode 4 which have been maintained in the previous section. Although, Figure 5.23 and 5.24 reveal that the main difference in overall behaviour occurred with CFST columns having D/t ratio of 30 and steel yield strength of 450 MPa.

In the comparison between axial capacity of DL/T and Eurocode 4, the use of nS does not exist with same behaviour as illustrated earlier, Figure 5.25 and 5.26. For instance, Figure 5.26a indicates that the lower differences between the two codes seem to be with columns infilled with concrete free of nS. Such results may be due to the DL/T treats the composite section as one material (Lu and Zhao, 2010).

Figures 5.21 to 5.26 also show that the higher differences were found to be between the predicted axial capacities of ACI and Eurocode 4 in comparison to AIJ and DL/T. This is mainly due to the fact that the composite action between the steel tube and the concrete core was not considered in ACI-318R (2005) (Lu and Zhao, 2010; Jamaluddin et al., 2013). Moreover, the lower differences were resulted between DL/T and Eurocode 4. Wang (2014) adopted the design guidelines specified by Eurocode 4 (2004) and Chinese code DL/T (1999) provisions to determine the test strength for the CFST column. It was also directed that Eurocode 4 (2004) and Chinese code DL/T (1999) were closer to the test column strength than those by the other design guidelines.

Regarding regression analysis, it can be observed that there were considerably high relationship between the predicted values of Eurocode 4 (2004) and ACI-318R (2005), (Figure 5.27a and 5.27b), Eurocode 4 (2004) and AIJ (2001), (Figure 5.28a and 5.28b) and Eurocode 4 (2004) and Chinese code DL/T (1999), (Figure 5.29a and 5.29b), respectively, so that a regression analysis provided correlation coefficient (R^2) of 0.99 and higher for all codes and ages. Within the predicted axial capacity results by using the different provisions of this study, all models appeared to be well close to each other and provided higher prediction.

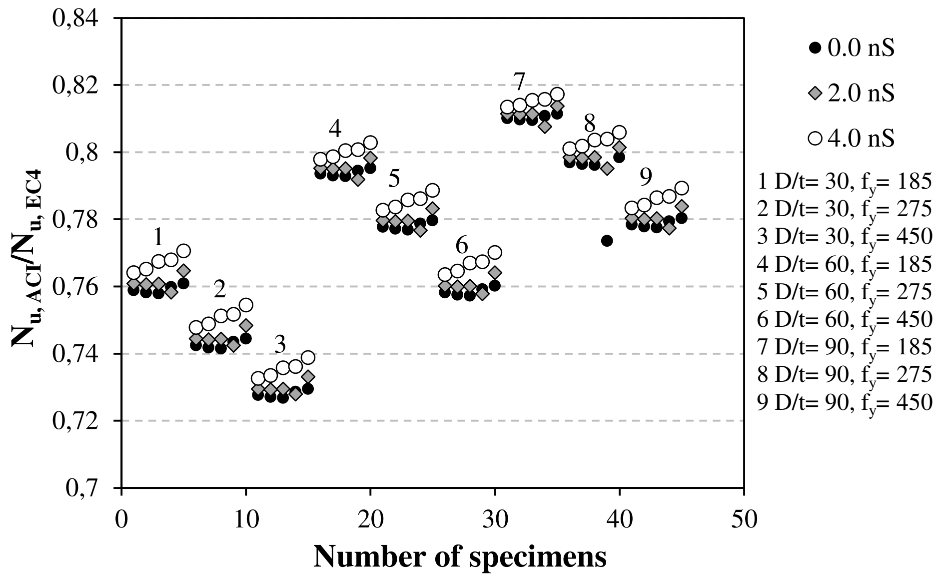

a)

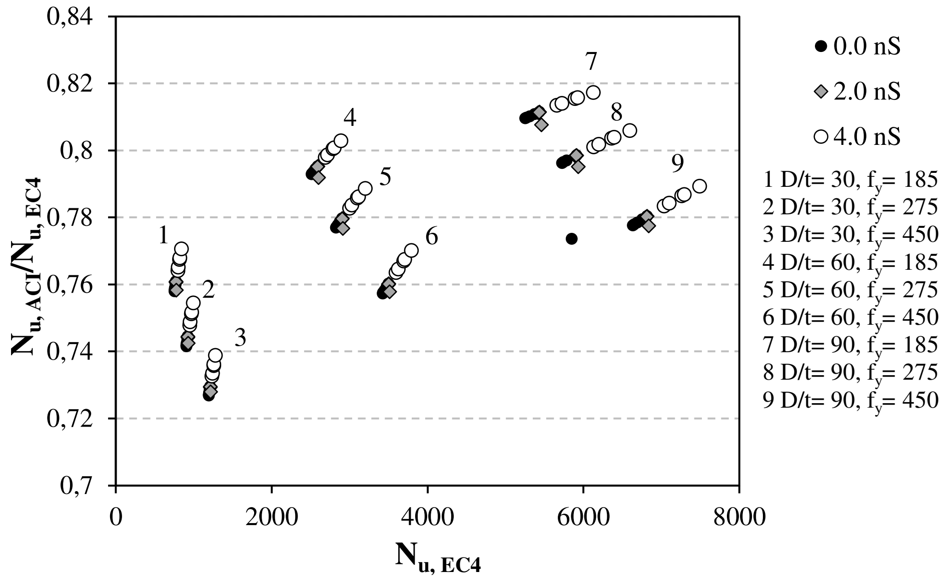

b)

Figure 5.21 Comparison of the 28 day axial capacity of the column computed by Eurocode 4 and ACI

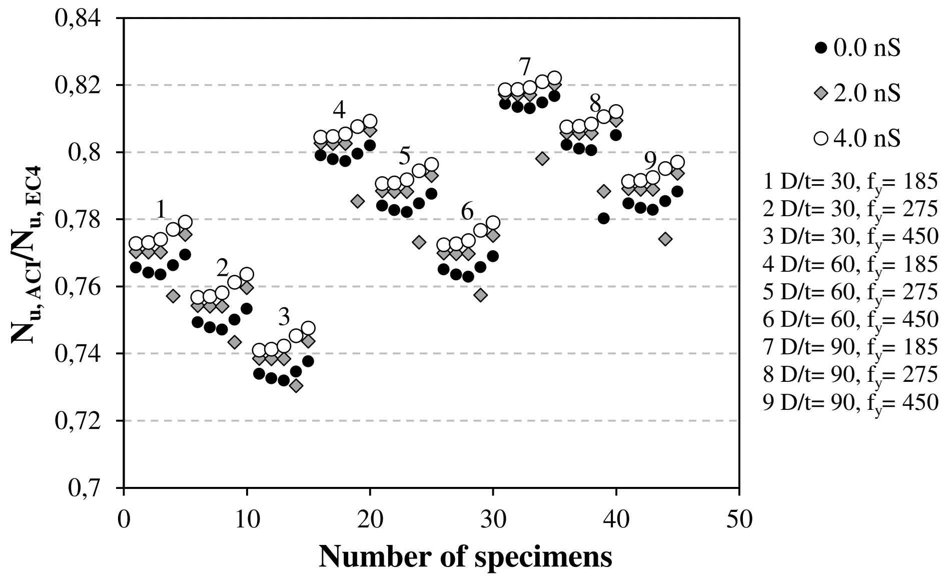

a)

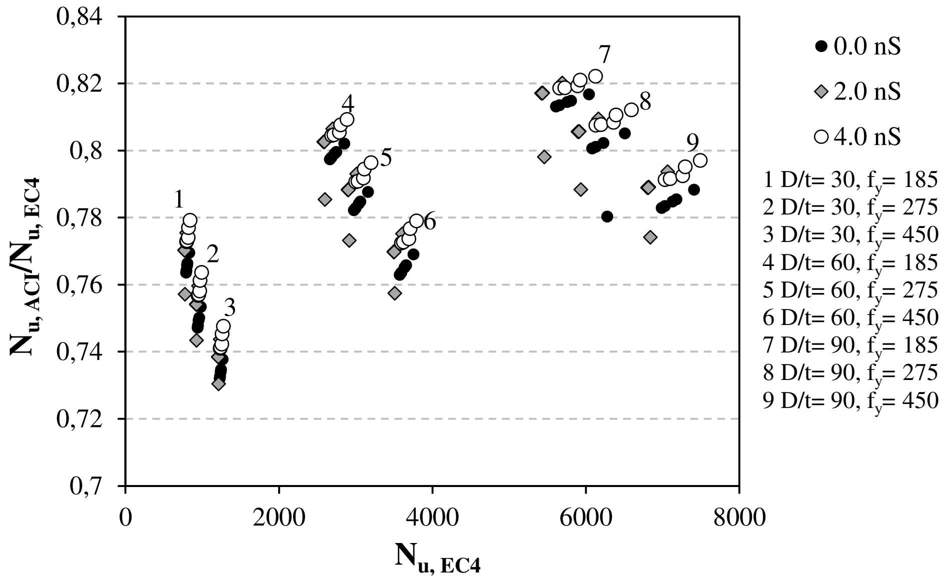

b)

Figure 5.22 Comparison of the 90 day axial capacity of the column computed by Eurocode 4 and ACI

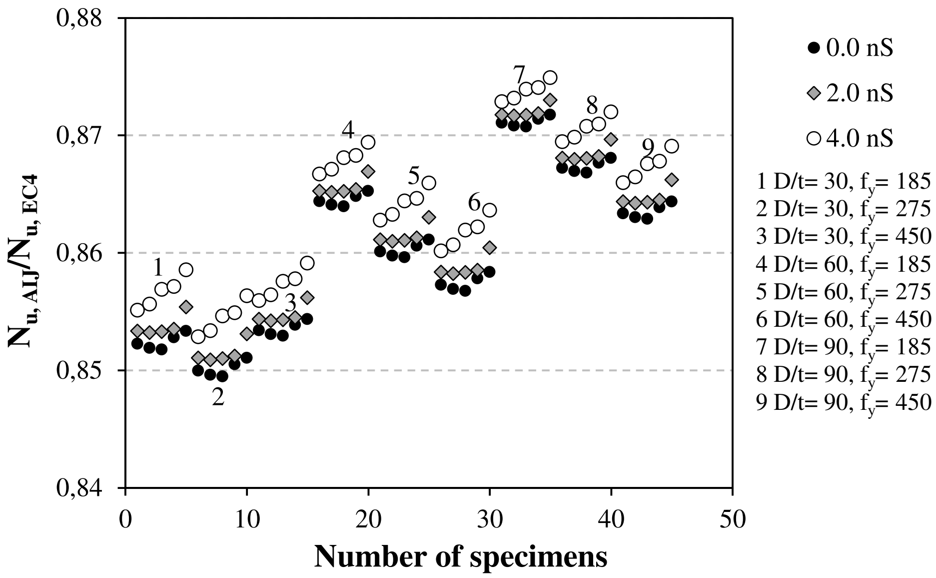

a)

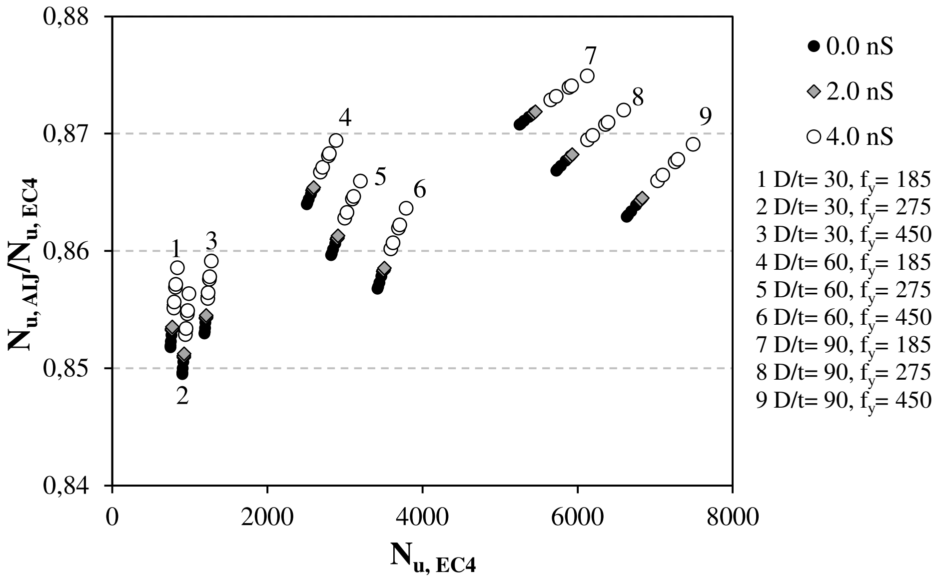

b)

Figure 5.23 Comparison of the 28 day axial capacity of the column computed by Eurocode 4 and AIJ

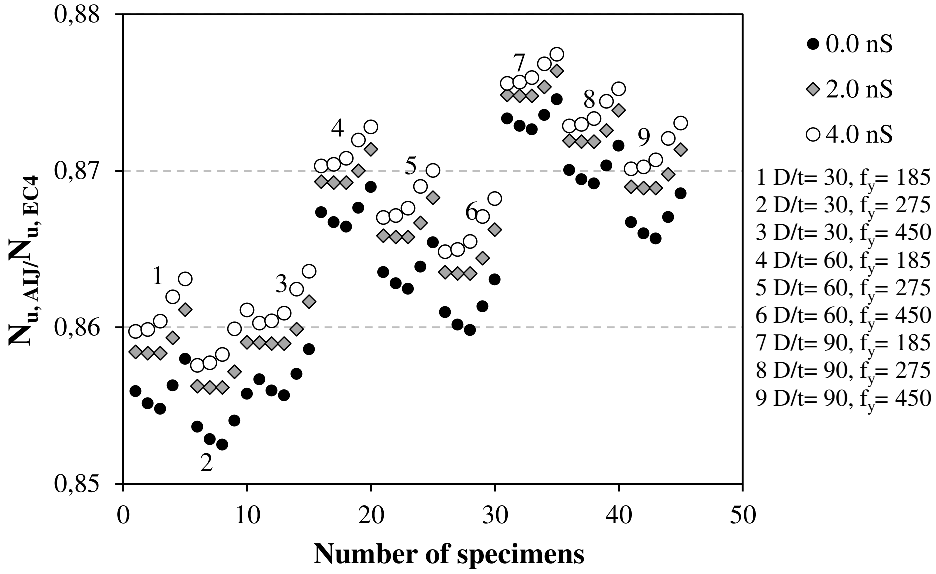

a)

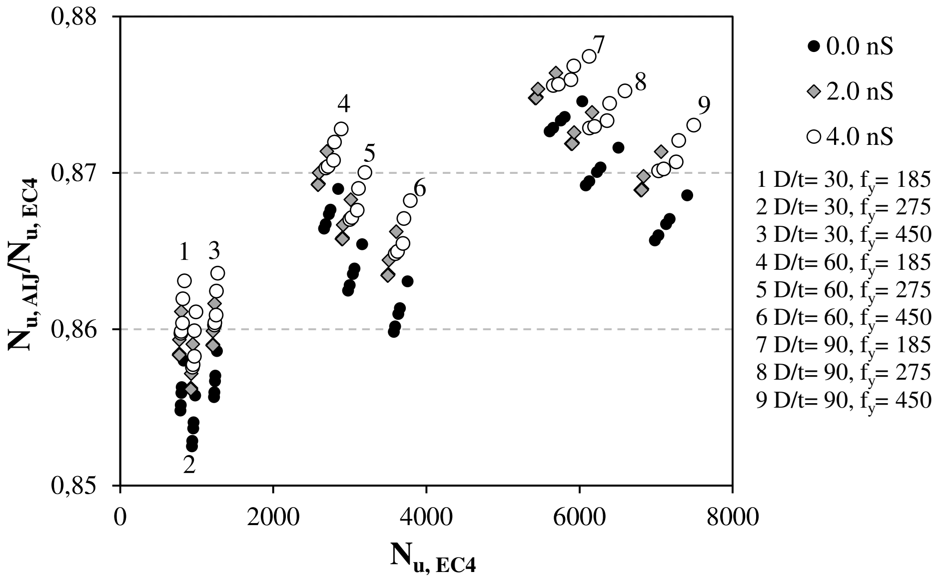

b)

Figure 5.24 Comparison of the 90 day axial capacity of the column computed by Eurocode 4 and AIJ

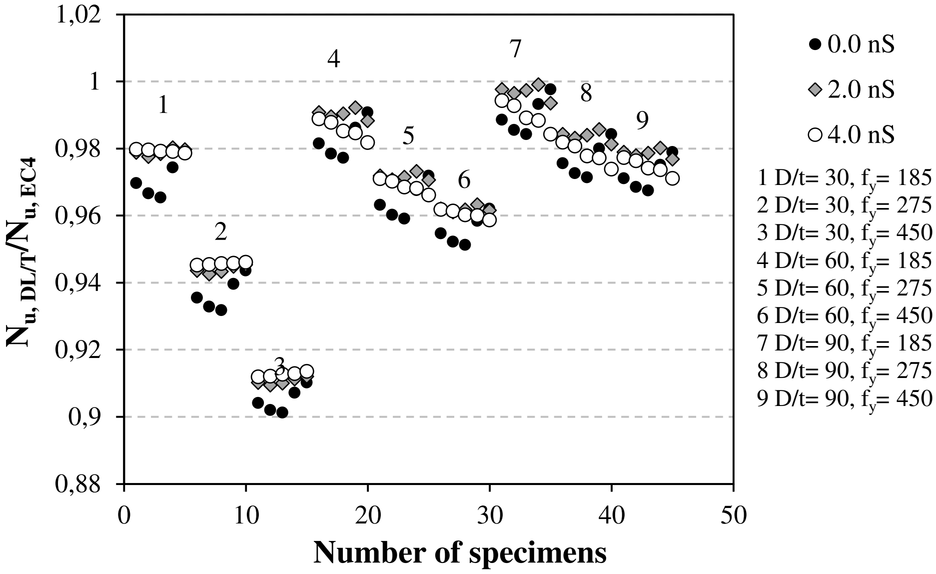

a)

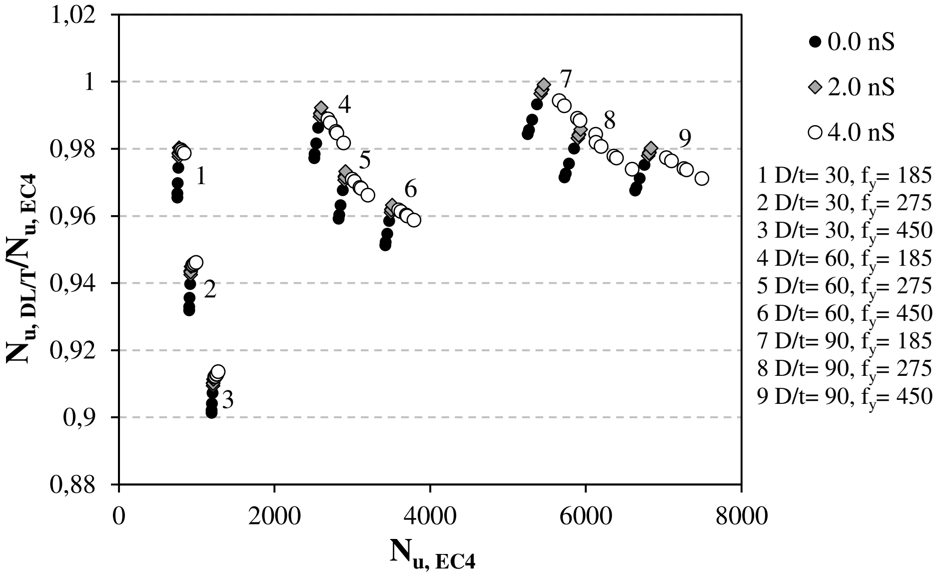

b)

Figure 5.25 Comparison of the 28 day axial capacity of the column computed by Eurocode 4 and DL/T

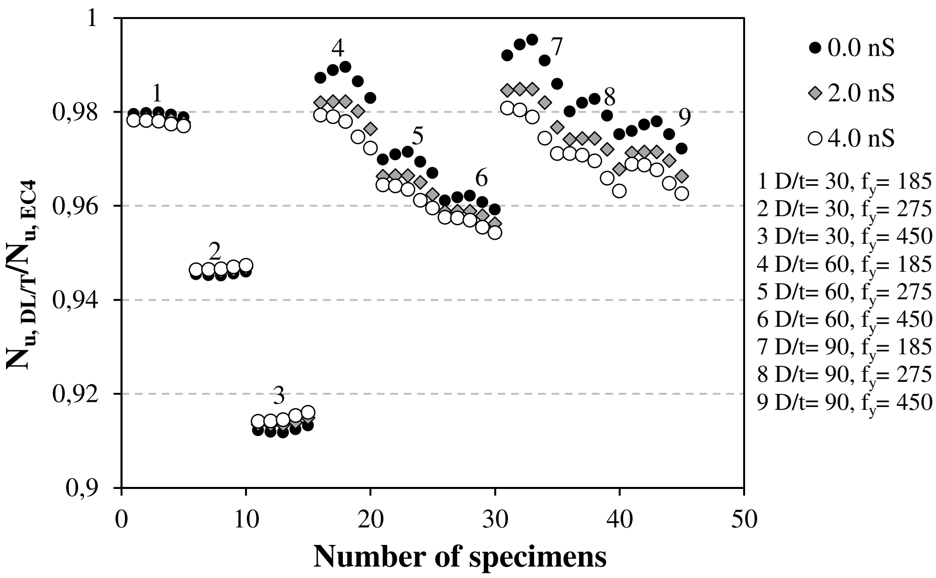

a)

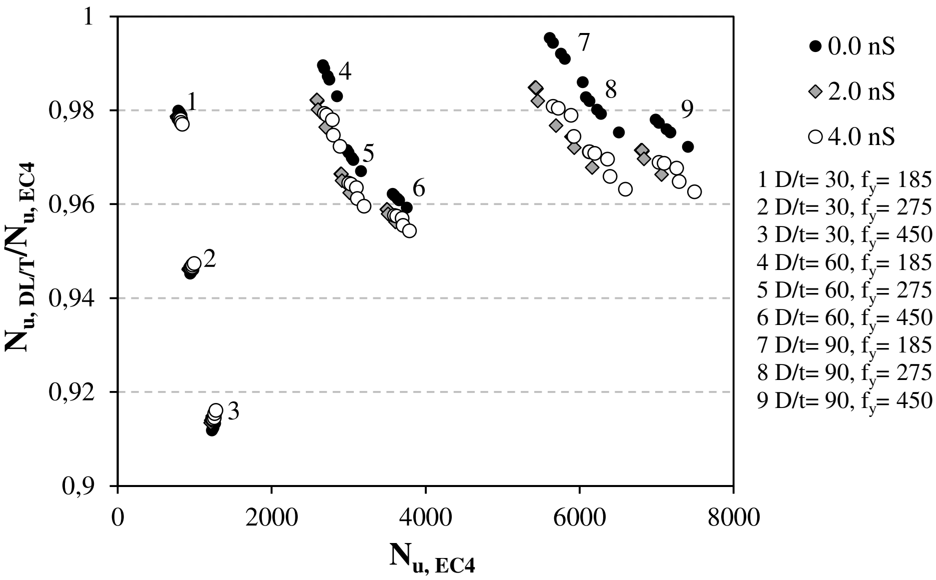

b)

Figure 5.26 Comparison of the 90 day axial capacity of the column computed by Eurocode 4 and DL/T

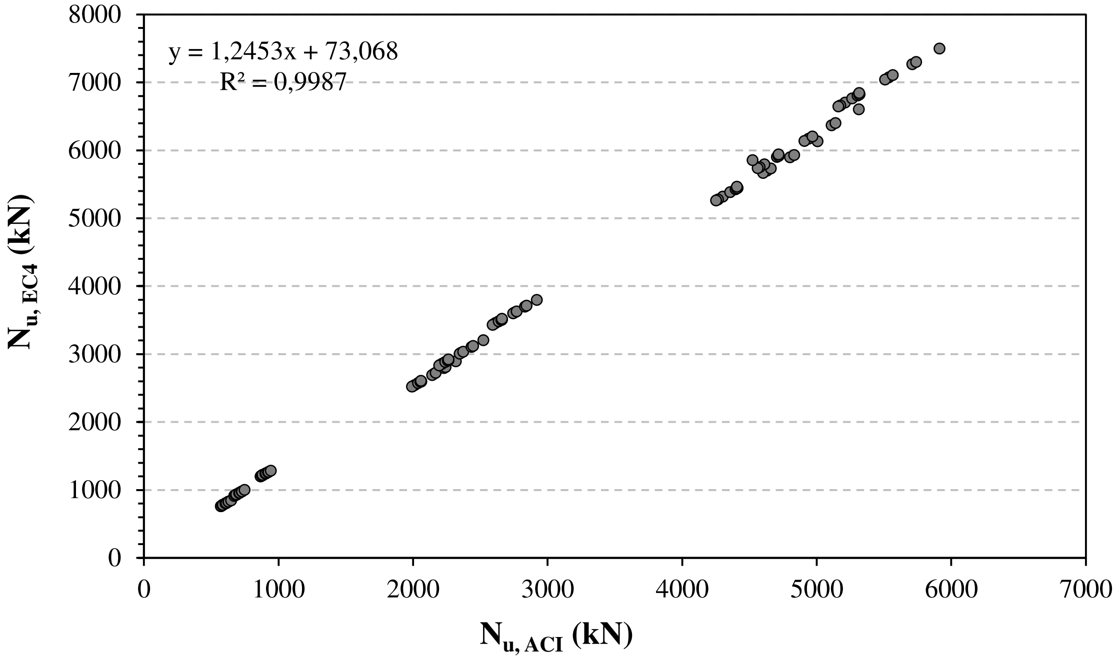

a)

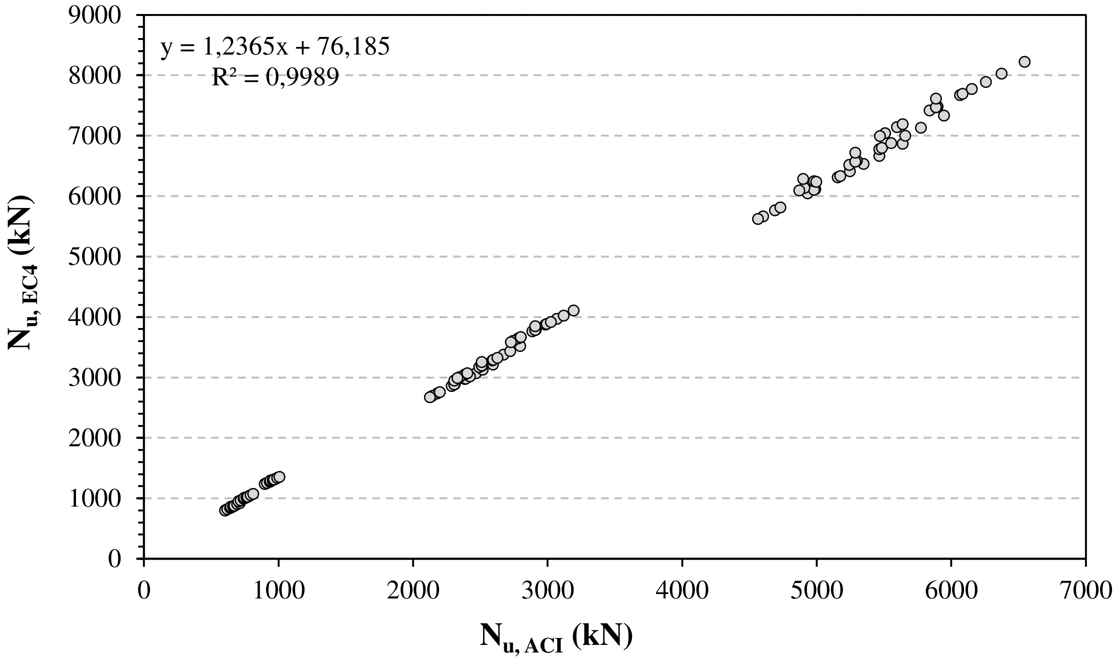

b)

Figure 5.27 Eurocode 4 and ACI regression model of axial capacity of the composite columns; a) for 28 days and b) for 90 days

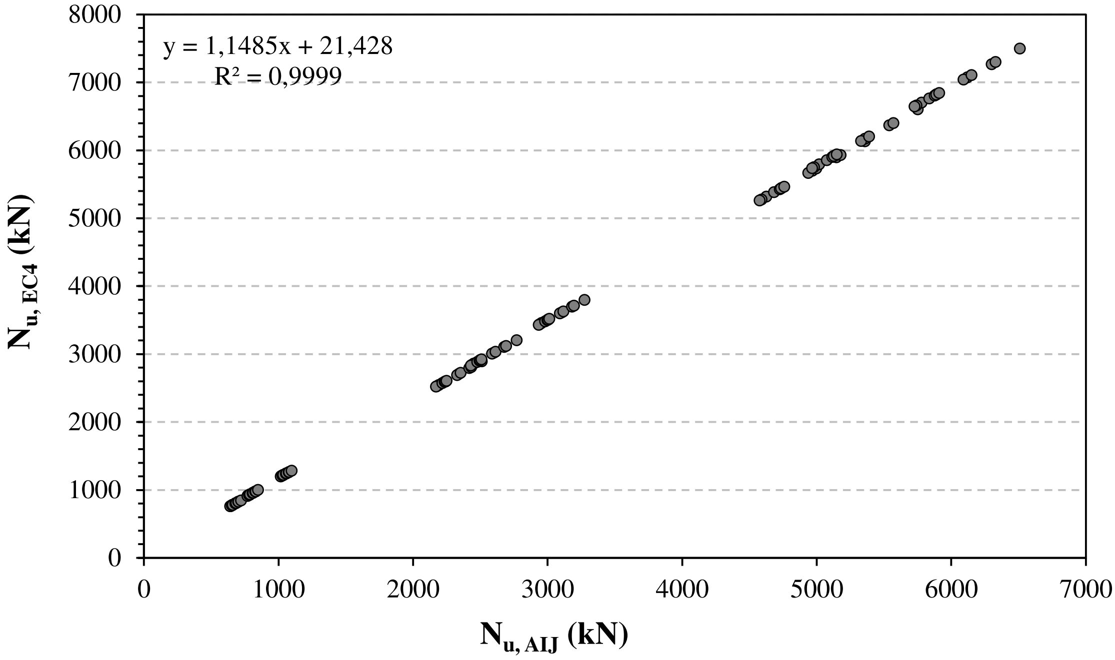

a)

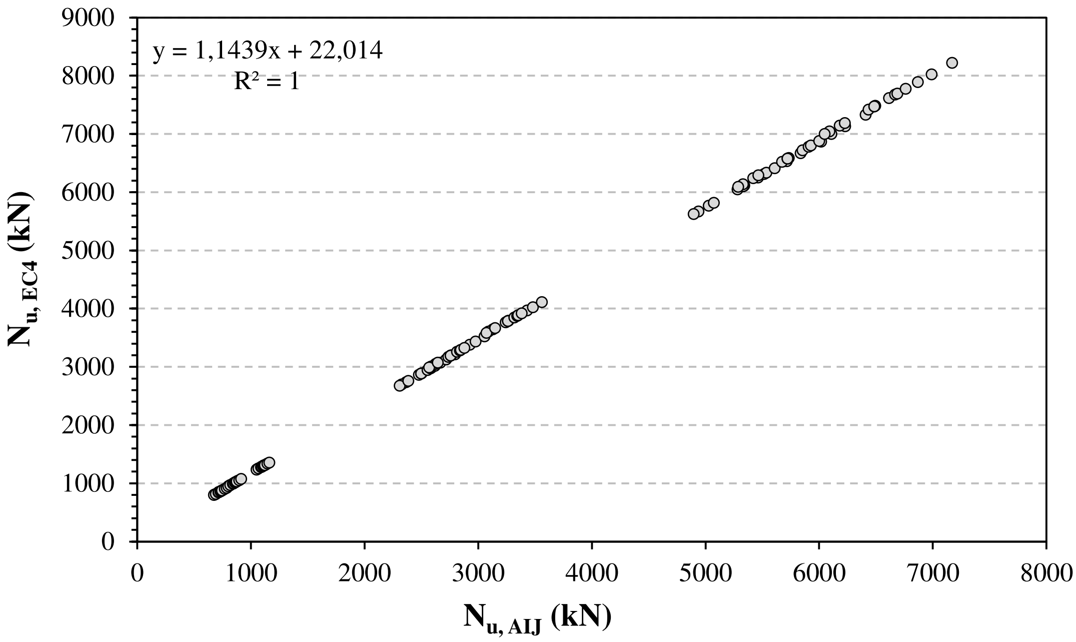

b)

Figure 5.28 Eurocode 4 and AIJ regression model of axial capacity of the composite columns; a) for 28 days and b) for 90 days

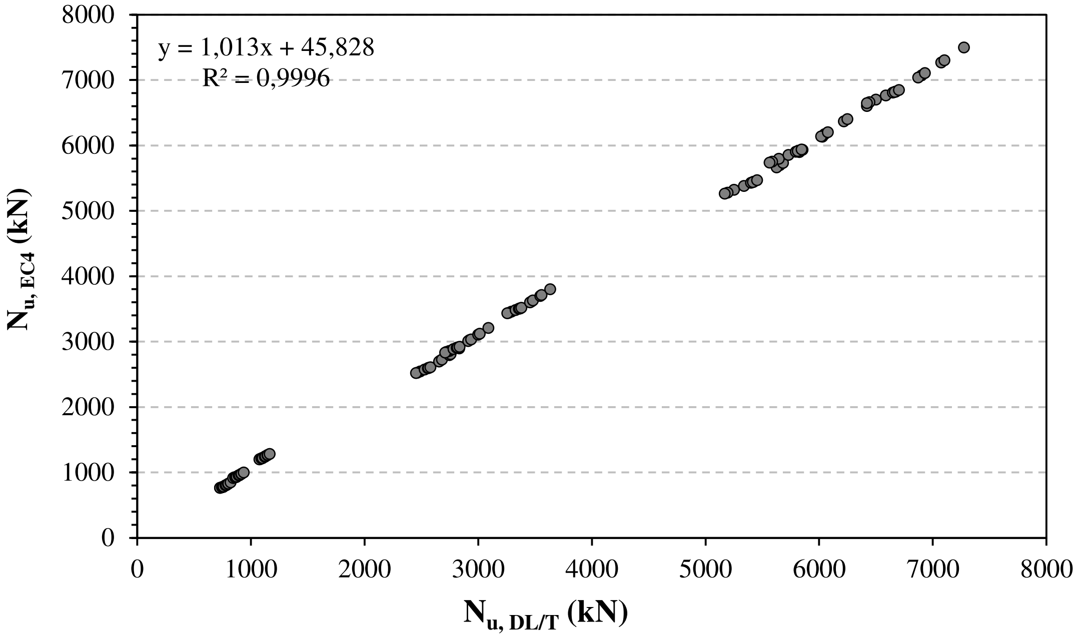

a)

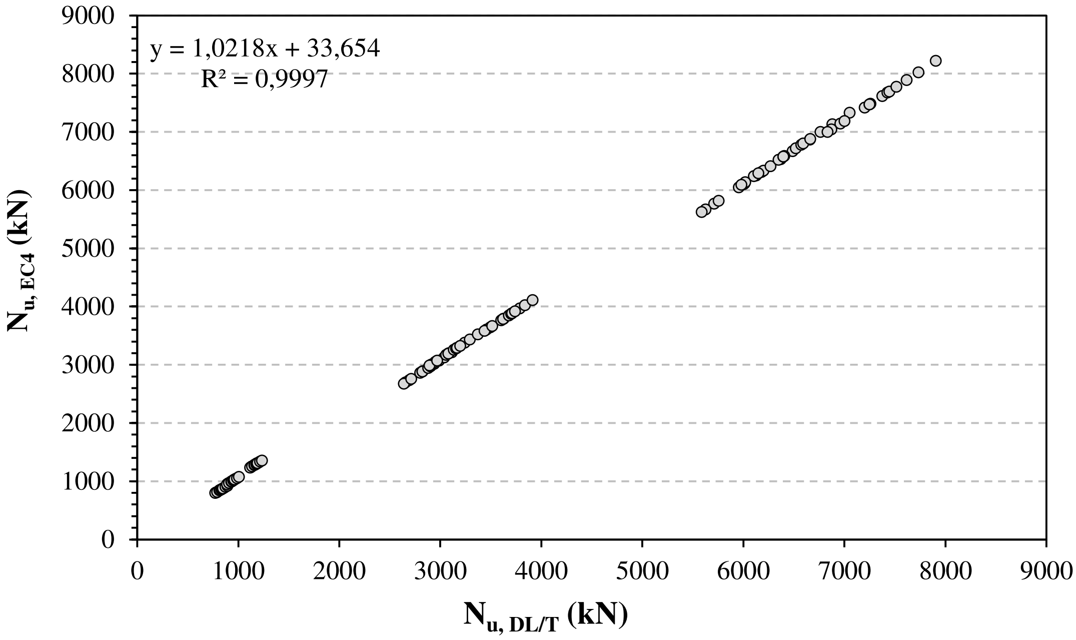

b)

Figure 5.29 Eurocode 4 and DL/T regression model of axial capacity of the composite columns; a) for 28 days and b) for 90 days

CHAPTER 6

CONCLUSIONS

In the experimental study (first part) of this thesis which was adopted to investigate and improve the properties of glass fiber (GF) reinforced self-compacting concrete (GFRSCC) with nano silica (nS) have been utilized to achieve the purposes of our investigation. For this end, producing and testing of fifteen mixtures were accomplished in an ideal laboratory conditions. The second part of the current thesis covers the structural performance of GFRSCC filled steel tube circular short columns having different diameter and steel yield strength. To this aim, an analytical study depending on the experimented compressive strength and available worldwide trustworthy provisions was performed. Based on the a comprehensive experimental program and the analytical study presented in this thesis, the following conclusions can be drawn:

- In the terms of slump flow diameter, GFRSCC mixes were satisfied the first and second classes of EFNARC (2005) limitation. The most of the mixtures made with 0, 2, and 4% nS and GF up to 0.7% were classified as SF2. On the other hand, the mixtures out of the aforementioned cases (made with 1 and 1.5% GF and nS content of 2% and/or 4%) were classified as SF2.
- The time required to reach 500 mm ($T_{500\ mm}$) increased from 3.7 to 7.9 s due to the increase of nS and GF from 0% to the maximum amount employed in the stage of production. A similar trend was also observed in the V-funnel flow times. The produced GFRSCC can be classified as VS2/VF2.
- All GFRSCC mixtures had blocking ratio between 0.8 and 1.0, therefore they were classified as PA2 in terms of passing ability class.
- According to the rheometer test results, an increment in the GF volume fraction caused to rise torque values of SCC. The torque values were also

observed to increase with increasing nS content. In all mixtures, shear stress increases with the addition of nS and GF.

- In this thesis, high strength GFRSCC had been produced. The highest compressive strength was 94 MPa, whist 71 MPa is the lowest one. Compressive and splitting tensile strengths of different SCC increased due to the use of nS and GF and increasing of curing period.
- The improvements of strength (compressive and splitting) were detected up to 4% of nS and 1.5% GF such that the maximum enhancement in strength of 34% was observed within 90 day splitting tensile strength of nS4%GF150 compared to that of the plain concrete.
- The use of nS and GF provided an excellent enhancement in the static elastic modulus of SCC compared to those free of nS and GF and those modified with 0.35 and 0.70% GF. The key role of GF in improving elastic modulus of concrete increased the efficiency of incorporated nS.
- The flexural strength increased with increasing GF volume fraction. This is probably due to the fact that after cracking of the matrix, the fibres will resist the load until the loss of the interfacial bond between the fibres and the matrix.
- Through work of fracture method, the fracture energy absorption capacity of SCC free of GF increases from 98 to 126 N/m and from 134 to 168 N/m for those of 1.5% GF as the nS content increased from 0% to 4%, respectively. Considering characteristics length, the incorporation of nS and GF lead to make SCC more ductile.
- The analytical study of this thesis clearly showed that nS and GF can be used beside concrete constituents to enhance the structural performance of steel tube in-filled with SCC.
- Increasing period of curing upgraded the predicted resistance of CFST column under axial compression. In this regard, the highest axial capacity with respect to Eurocode 4 (2004), ACI 318R (2005), AIJ (2001) and DL/T (1999) were found to be as 8215, 6547, 7172 and 7907 kN, respectively.
- The analysis of the results indicated that the composite column made with high strength steel tube and greater diameter to thickness (D/t) ratio

provided higher compression resistance. Similarly, the increasing the amount of nS in GFRSCC caused more compressive strength which in turn high load carrying capacity for the columns.

- Comparisons between the predictions of ultimate axial capacity of circular CFST short columns showed that the ACI 318R (2005), AIJ (2001) and DL/T (1999) provide lower predictions with respect to Eurocode 4. This is due to the fact that Eurocode 4 takes account mainly the composite action between the tube and the core of the concrete. Lower differences resulted for those computed via Eurocode 4 and DL/T.
- It was noted that the axial capacity ratio obtained from ACI to Eurocode varied from 0.72 to 0.82 while this variation was observed from 0.85 to 0.88 and from 0.90 to 1.0 between AIJ and Eurocode 4; DL/T and Eurocode 4, respectively.
- Although different parameters for each design code had been used to calculate the ultimate axial capacity of CFST column by following different strategies, significantly high coefficient and positive correlation between the Eurocode 4 and the others (ACI, AIJ and DL/T) were observed.

REFERENCES

ACI Manual of Concrete Practice (1996). A state-of-the-art report on fiber reinforced concrete. ACI Committee 544.1R-1996.

ACI. American Concrete Institute. (2005). Building code requirements for structural concrete and commentary. *Manual of Concrete Practice*. ACI committee 318R, Farmington Hills, Michigan, U.S.A.

ACI. American Concrete Institute. (2007). Self-consolidating concrete, ACI 237R-07. Manual of Concrete Practice. Farmington Hills, Michigan, USA.

Aggarwal, P., Siddique, R., Aggarwal, Y., Gupta, S.M. (2008). Self-compacting concrete -procedure for mix design. *Leonardo electronic journal of practices and technologies*. **12**, 15-24.

Ahmad, J., Dixit, R. B., Singh, R. (2015). To study the properties of self compacting concrete using recycled aggregate and polypropylene fiber. *International Journal of Recent Research in Civil and Mechanical Engineering*. **2(1)**, 173-177.

Ahmed, S., Umar, A., Masood, A. (2017). Properties of normal concrete, self-compacting concrete and glass fiber-reinforced self-compacting concrete: an experimental study. *Procedia Engineering*. **173**, 807-813.

AIJ. Recommendations for design and construction of concrete filled steel tubular structures. (1997). *Japan: Architectural Institute of Japan.* Tokyo, Japan (in Japanese).

AIJ. Standards for structural calculation of steel reinforced concrete structures. (2001). 5^{th} edition. *Architectural Institute of Japan.* Tokyo, Japan (in Japanese).

AISC 360-10. (2005). Specification for structural steel buildings. Chicago, USA: American Institute of Steel Construction (AISC).

Alonso, M.C. Sánchez, M., Rodriguez, C., Barragán, B. (2008). Durability of SCC reinforced with polymeric fibers: interaction with environment and behaviour against high temperatures. *11th International inorganic bonded fiber Composite Conference*. 227-235.

ASTM. American Society for Testing and Materials. (2011). Tensile strength of cylindrical concrete specimens (C496). *Annual book of ASTM standards,* **vol. 04.02**. West Conshohocken, Pennsylvania, USA.

ASTM. American Society for Testing and Materials. (2012). Standard test method for compressive strength of cylindrical concrete specimens (C39). *Annual book of ASTM standards,* **vol. 04.02**. West Conshohocken, Pennsylvania, USA.

ASTM. American Society for Testing and Materials. (2012).Standard specification for coal fly ash and raw or calcined natural pozzolan for use in concrete (C618). *Annual book of ASTM standards*, **vol. 04.02.** West Conshohocken, Pennsylvania, USA.

ASTM. American Society for Testing and Materials. (2014). Standard Test Method for Static Modulus of Elasticity and Poisson's Ratio of Concrete in Compression (C469). *Annual book of ASTM standards,* **vol. 04.02**. West Conshohocken, Pennsylvania, USA.

Aveston, J., Cooper, G.A., Kelly, A. (1971). Single and multiple fracture. In: Proceedings of properties of fiber composites, National Physical Laboratory. Guildford (UK): IPC Science and Technology Press, pp 15-24.

Aydin, A.C. (2007). Self compactability of high volume hybrid fiber reinforced concrete. *Construction and Building Materials*. **21**, 1149-1154.

B.S EN 450. (2005). Fly ash for concrete- definition, specifications, and conformity criteria. British standards Institution, London, U.K.

Barbhuiya, S. (2011). Effects of fly ash and dolomite powder on the properties of self-compacting concrete. *Construction and Building Materials*. **25(8)**, 3301-3305.

Barfield, M., Ghafoori, N. (2012). Air-entrained self-consolidating concrete: A study of admixture sources. *Construction and Building Materials*. **26**, 490-496.

Barluenga, G., Hernández-Olivares, F. (2007). Cracking control of concretes modified with short AR-glass fibers at early age. Experimental results on standard concrete and SCC. *Cement and Concrete Research*. **37(12)**, 1624-1638.

Basheerudeen, A., Anandan, S. (2015). Simplified Mix Design Procedures for Steel Fibre Reinforced Self Compacting Concrete. *Engineering Journal*. **19(1)**, 21-36.

Beigi, M.H., Berenjian, J., Omran, O.L., Nik, A.S., Nikbin, I.M. (2013). An experimental survey on combined effects of fibers and nanosilica on the mechanical, rheological, and durability properties of self-compacting concrete. *Materials & Design*. **50**, 1019-1029.

Beissel, R., Lim, H. (2001). Self-compacting concrete : modern concrete and admixture technology. *26th Conference on Our World in Concrete & Structures*. 27 - 28 August.

Bentur, A., Igarashi, S., Kovler, K. (2001). Prevention of autogenous shrinkage in high-strength concrete by internal curing using wet lightweight aggregates. *Cement and Concrete Research*. **31**, 1587-1591.

Bergmann, R., Matsui, C., Meinsma, C., Dutta, D. (1995). Design guide for concrete filled hollow section columns under static and seismic loading. CIDECT, Construction with hollow steel sections. Verlag TÜV Rheinland.

Beygi, M., Kazemi, M. T., Amiri, J. V., Nikbin, I. M., Rabbanifar, S., Rahmani, E. (2014). Evaluation of the effect of maximum aggregate size on fracture behavior of self compacting concrete. *Construction and Building Materials*. **55**, 202-211.

Bilodeau, A., Sivasundaram, V., Painter, K.E., Malhotra, V.M. (1994). Durability of concrete incorporating high volumes of fly ash from sources in the U.S.A. *ACI Materials Journal*. **91(1)**, 3-12.

Bingöl, A.F., Tohumcu, I. (2013). Effects of different curing regimes on the compressive strength properties of self compacting concrete incorporating fly ash and silica fume. *Material and Design*. **51**, 12-18.

Blontrock, H., Taerwe, L. (2002). Exploratory spalling tests on self compacting concrete. In: Proceedings of 6th international symposium on utilization of high performance concrete. p. 659-666.

Boukendakdji, O., Kadri, H., Kenai, S. (2012). Effects of granulated blast furnace slag and superplasticizer type on the fresh properties and compressive strength of self-compacting concrete. *Cement & Concrete Composites*. **34**, 583-590.

BS EN 12620. (2002) Aggregates for concrete including those for use in roads and pavements. British standards Institution, London, U.K.

Cao, C., Sun, W., Qin, H. (2000). The analysis on strength and fly ash effect of roller-compacted concrete with high volume fly ash. *Cement and Concrete Research*. **30(1)**, 71-75.

Chang, X., Lei, F., Zhao H.B., Zhang, Y.B. (2013). Behaviors of axially loaded circular concrete-filled steel tube (cft) stub columns with notch in steel tubes. *Thin-Walled Structures*. **73**, 273-280.

Choolaei, M., Rashidi, A. M., Ardjmand, M., Yadegari, A., Soltanian, H. (2012). The effect of nanosilica on the physical properties of oil well cement. *Materials Science and Engineering A*. **538**, 288-294.

Corinaldesi, V., Moriconi, G. (2004). Durable fiber reinforced self-compacting concrete. *Cement and Concrete Research*. **34(2)**, 249-254.

Corinaldesi, V., Moriconi, G. (2009). Influence of mineral additions on the performance of 100% recycled aggregate concrete. *Construction and Building Materials*. **23(8)**, 2869-2876.

Dehn, F., Holschemacher, K., Weiße, D. (2000). Self-compacting concrete (SCC) time development of the material properties and the bond behavior. https://www.schmitzmix.com/press/pdfs/scc.pdf.

Dinakar, P., Kartik Reddy, M., Sharma, M. (2013). Behaviour of self compacting concrete using Portland pozzolana cement with different levels of fly ash. *Materilas and Design*. **46**, 609-616.

Ding, Y., Liu, S., Zhang, Y., Thomas, A. (2008). The investigation of workability of fiber cocktail reinforced self-compacting high performance concrete. *Construction and Building Materials*. **22**, 1462-1470.

DL/T. Chinese design code for steel-concrete composite structures. (1999). In: DL/T 5085-1999. *Chinese Electricity Press*. Beijing, China (in Chinese).

EFNARC. European Federation of National Associations Representing for Concrete. (2005). Specification and guidelines for self-compacting concrete. UK: EFNARC.

Ellobody, E. (2013). Nonlinear behavior of eccentrically loaded FR concrete-filled stainless steel tubular columns. *Journal of Constructional Steel Research*. **90**, 1-12.

Ellobody, E., Young, B., Lam, D. (2006). Behaviour of normal and high strength concrete-filled compact steel tube circular stub columns. *Journal of Constructional Steel Research*. **62**, 706-715.

Elremaily, A., Azizinamini, A. (2002). Behavior and strength of circular concrete-filled tube columns. *Journal of Constructional Steel Research*. **58**, 1567-1591.

EN 1994-1-1. (2004). Eurocode 4: design of composite steel and concrete structures - Part 1-1. General rules and rules for buildings. European Committee for Standardization: British Standards Institution.

Eramma, H., Niranjan, B.R. (2012). Experimental behaviour of self compacting concrete filled steel rectangular fluted columns for concentric load. *IOSR Journal of Mechanical and Civil Engineering*. **3(2)**, 41-49.

Eurocode 2. European Committee for Standardization: British Standards Institution. (2004). Design of concrete structures. Part 1-1: General rules and rules for buildings.

Eurocode 4. (1994). Design of composite steel and concrete structures - Part 1-2: General rules - Structural fire design. European Committee for Standardization: British Standards Institution.

Eurocode 4. European Committee for Standardization: British Standards Institution. (2004). Design of composite steel and concrete structures. Part 1.1, General rules and rules for buildings.

Fanella, D.A., Naaman, A.E. (1985). Stress-strain properties of fiber reinforced mortar in compression. American Concrete Institute. **82(4)**, 475-483.

Fard, A.R.T. (2016). Combined Effect of glass fiber and polypropylene fiber on mechanical property of self-compacting concrete. *Global Advanced Research Journal of Engineering*. **5(4)**, 57-68.

Ferguson, J., Kembłowski, Z. (1991). Applied fluid rheology. Elsevier Applied Science.

Feys, D., Verhoeven, R., De Schutter, G. (2007). Evaluation of time independent rheological models applicable to fresh self-compacting concrete. *Applied Rheology*. **17(5)**, 1-10.

Fraay, A.L.A., Bijen, J.M., de Haan, Y.M. (1989). The reaction of fly ash in concrete a critical examination. *Cement and Concrete Research*. **19(2)**, 235-246.

Fujimoto, T., Mukai, A., Nishiyama, I. (2004). Behavior of eccentrically loaded concrete-filled steel tubular columns. *Journal of Structural Engineering*. **130(2)**, 203-212.

Furlong, R.W. (1967). Strength of steel-encased concrete beam columns. *Journal of Structural Division, ASCE*. **93(ST5)**, 113-124.

Gao, J., Suqa, W., Morino, K. (1997). Mechanical properties of steel fiber-reinforced, high strength, lightweight concrete. *Cement and Concrete Composite*. 19, 307-313.

Gesoğlu, M., Güneyisi, E. (2011). Permeability properties of self-compacting rubberized concretes. *Construction and Building Materials*. **25**, 3319-3326.

Gesoğlu, M., Güneyisi, E., Kocabağ, M. E., Bayram, V., Mermerdaş, K. (2012). Fresh and hardened characteristics of self compacting concretes made with combined use of marble powder, limestone filler, and fly ash. *Construction and Building Materials*. **37**, 160-170.

Ghafari, E., Costa, H., Júlio, E., Portugal, A., Durães, L. (2014). The effect of nanosilica addition on flowability, strength and transport properties of ultra high performance concrete. *Materials & Design*. **59**, 1-9.

Giakoumelis, G., Lam, D. (2004). Axial capacity of circular concrete-filled tube columns. *Journal of Constructional Steel Research*. **60(7)**, 1049-1068.

Giovanni Muciaccia, G., Giussani, F., Rosati, G., Mola, F. (2011). Response of self-compacting concrete filled tubes under eccentric compression. *Journal of Constructional Steel Research*. **67**, 904-916.

Güneyisi, E., Gesoğlu, M. (2008). Properties of self-compacting mortars with binary and ternary cementitious blends of fly ash and metakaolin. *Materials and Structures.* **41(9)**, 1519-1531.

Güneyisi, E., Gesoğlu, M., Algin, Z., Mermerdaş, K. (2014). Optimization of concrete mixture with hybrid blends of metakaolin and fly ash using response surface method. *Composite: Part B Engineering*. **60**, 707-715.

Güneyisi, E., Gesoglu, M., Al-Goody, A., İpek, S. (2015b). Fresh and rheological behavior of nano-silica and fly ash blended self-compacting concrete. *Construction and Building Materials*. **95**, 29-44.

Güneyisi, E., Gesoğlu, M., AZEZ, O.A., Öz, H.Ö. (2016b). Effect of nano silica on the workability of self-compacting concretes having untreated and surface treated lightweight aggregates. *Construction and Building Materials*. **115**, 371-380.

Güneyisi, E., Gesoğlu, M., Booya, E. (2012). Fresh properties of self-compacting cold bonded fly ash lightweight aggregate concrete with different mineral admixtures. *Construction and Building Materials*. **45**, 1849-1859.

Güneyisi, E., Gesoğlu, M., Özturan, T., İpek, S. (2015a). Fracture behavior and mechanical properties of concrete with artificial lightweight aggregate and steel fiber. *Construction and Building Materials.* **84**, 156-168.

Güneyisi, E.M., Gültekin A., Mermerdaş K. (2016a). Ultimate capacity prediction of axially loaded. *International Journal of Steel Streuctures*. **16(1)**, 99-114.

Guru Jawahar, J., Sashidhar, C., Reddy, I.V.R., Peter, J.A. (2013). Micro and macrolevel properties of fly ash blended self compacting concrete. *Materials and Design*. **46**, 696-705.

Han, L.H, Yao, G.H., Zhao, X.L. (2005). Tests and calculations for hollow structural steel (HSS) stub columns filled with self-consolidating concrete (SCC). *Journal of Constructional Steel Research*. **61**, 1241-1269.

Han, L.H., Li, W., Bjorhovde, R. (2014). Developments and advanced applications of concrete-filled steel tubular (CFST) structures: Members. *Journal of Constructional Steel Research*. **100**, 211-228.

Han, L.H., Yang, Y.F., Li, Y.J., Feng, B. (2005). Hydration heat and shrinkage of HSS columns filled with self-consolidating concrete. Proceedings of the Fourth International Conference on Advances in Steel Structures, Shanghai, China. **1**, 647-52.

Heikal, M., Ali, A.I., Ismail, M.N., Ibrahim, S.A.N.S. (2014). Behavior of composite cement pastes containing silica nano-particles at elevated temperature. *Construction and Building Materials*. **70**, 339-350.

Helmuth, R. (1987). Fly ash in cement and concrete. Portland Cement Association, USA.

Ho, D.W.S., Sheinn, A.M.M., Ng, C.C., Lim, W.B., Tam, C.T. 2001. Self-compacting concrete for singapore. 26th Conference on Our World in Concrete & Structures, Singapore, 293-300.

Hosseini, P., Booshehrian, A., Farshchi, S. (2010). Influence of nano-SiO2 addition on microstructure and mechanical properties of cement mortars for ferrocement. *Journal of the Transportation Research Board*. **2141**, 15-20.

Hou, P., Kawashima, S., Kong, D., Corr, D. J., Qian, J., Shah, S.P. (2013). Modification effects of colloidal nanoSiO_2 on cement hydration and its gel property. *Composites: Part B*. **45**, 440-448.

Hou, P., Kawashima, S., Wang, K., Corr, D., Qian, J., Shah, S.P. (2013). Effects of colloidal nanosilica on rheological and mechanical properties of fly ash-cement mortar. *Cement and Concrete Composites*. **35**, 12-22.

Hu, C., De Larrard, F., Gjørv, O. E. (1995). Rheological testing and modelling of fresh high performance concrete. *Materials and Structures.* **28(1)**, 1-7.

Hughes, B.P., Dougill, N.I. (1975). Fibre bond strength in cement and concrete. *Magazin of Concrete Research.* **27(92)**, 161-166.

Jalal, M., Mansouri, E., Sharifipour, M., Pouladkhan, A.R. (2012). Mechanical, rheological, durability and microstructural properties of high performance self-compacting concrete containing SiO_2 micro and nanoparticles. *Materials & Design*. **34**, 389-400.

Jamaluddin, N., Lam, D., Dai, X.H., Ye, J. (2013). An experimental study on elliptical concrete filled columns under axial compression. *Journal of Constructional Steel Research*. 87, 6-16.

Jiang, L.H., Malhotra, V. M. (2000). Reduction in water demand of non-air-entrained concrete incorporating large volumes of fly ash. *Cement and Concrete Research*. **30(11)**, 1785-1789.

Jonckbloedt, R.C.L. (1997). The Dissolution of Olivine in Acid, a Cost Effective Process for the Elimination of Waste Acids. *PhD Thesis*, Utrecht University, Utrecht.

Kamal, M.M., Safan, M.A., Etman, Z.A., Kasem, B.M. (2014). Mechanical properties of self-compacted fiber concrete mixes. *HBRC Journal*. **10(1)**, 25-34.

Kang, S.T., Lee, Y., Park, Y.D., Kim, J.K. (2010). Tensile fracture properties of an Ultra High Performance Fiber Reinforced Concrete (UHPFRC) with steel fiber. *Composite Structures*. **92(1)**, 61-71.

Kayali, O., Haque, M. N., Zhu, B. (2003). Some characteristics of high strength fiber reinforced lightweight aggregate concrete. *Cement and Concrete Composites*. **25**, 207-213.

Khairallah, F. (2013). Mechanical behavior of confined self-compacting reinforced concrete circular columns under concentric axial loading. *Ain Shams Engineering Journal*. **4**, 641–649.

Khaleel, O.R., Al-Mishhadani, S.A., Abdual Razak, H. (2011). The effect of coarse aggregate on fresh and hardened properties of self-compacting concrete (SCC). *Procedia Engineering*. **14**, 805-813.

Khaleel, O.R., Al-Mishhadani, S.A., Abdul Razak, H. (2011). The effect of coarse aggregate on fresh and hardened properties of self-compacting concrete (SCC). *Procedia Engineering*. 14, 805-813.

Khatib, J.M. (2008). Performance of self-compacting concrete containing fly ash. *Construction and Building Materials*. **22(9)**, 1963-1971.

Kılıç, A., AtiĢ, C. D., YaĢar, E., Özcan, F. (2003). High-strength lightweight concrete made with scoria aggregate containing mineral admixtures. *Cement and*

Concrete Research. **33**, 1595-1599.

Kim, Y. J., Choi, Y. W., Lachemi, M. (2010). Characteristics of self-consolidating concrete using two types of lightweight coarse aggregates. *Construction and Building Materials*. **24**, 11-16.

Knowles, R.B., Park, R. (1970). Axial load design for concrete filled steel tubes. *Journal of the Structural Division, ASCE*. **96(ST10)**, 2125-2153.

Kodur, V., McGrath, R. (2003). Fire endurance of high strength concrete columns. *Fire Technology*. **39(1)**, 73-87.

Kodur, V.K.R. (1998). Design equations for evaluating fire resistance of SFRC-Filled HSS columns. *Journal of Structural Engineering, ASCE*. **124(6)**, 671-677.

Kodur, V.K.R. (1999). Performance-based fire resistance design of concrete-filled steel columns. *Journal of Constructional Steel Research*. **51(1)**, 21-36.

Kodur, V.K.R., Lie, T.T. (1996). Fire resistance of circular steel columns filled with steel fiber-reinforced concrete. *Journal of Structural Engineering, ASCE*. **122(7)**,776-782.

Koehler, E. P., Fowler, D. W. (2004). Development of a portable rheometer for fresh portland cement concrete. *Aggregates foundation for technology, research and education* (AFTRE).

Kurtz, S., Balaguru, P. (2000). Postcrack creep of polymeric fiber-reinforced concrete in flexure. *Cement and Concrete Research*. **30(2)**, 183-190.

Li, G. (2004). Properties of high-volume fly ash concrete incorporating nano-SiO_2. *Cement and Concrete Research*. **34(6)**, 1043-1049.

Liang, Q.Q., Fragomeni, S. (2009). Nonlinear analysis of circular concrete-filled steel tubular short columns under axial loading. *Journal of Constructional Steel Research*. **65(12)**, 2186-2196.

Liew, J.Y.R., Xiong M.X. (2015). Design guide for concrete filled tubular members with high strength materials - an extension of Eurocode 4 method to C90/105 concrete and S550 steel. Research Publishing Singapore.

Liu, M. (2009). Wider application of additions in self-compacting concrete. *Ph.d*

Thesis. Department of Civil, Environmental and Geomatic Engineering University College London.

Lo, T., Tang, P., Cui, H., Nadeem, A. (2007). Comparison of workability and mechanical properties of self-compacting lightweight concrete and normal self-compacting concrete. *Materials Research Innovations*. **11(1)**, 45-50.

Lu, H., Han, L.H., Zhao, X.L. (2010). Fire performance of self-consolidating concrete filled double skin steel tubular columns: Experiments. Fire Safety Journal. **45**, 106-115.

Lu, Y., Li, N., Li, S. (2014). Behavior of FRP-confined concrete-filled steel tube columns. *Polymers*. 1333-1349.

Lu, Y., Li, N., Li, S., Liang, H. (2015). Behavior of steel fiber reinforced concrete-filled steel tube columns under axial compression. *Construction and Building Materials*. **95**, 74-85.

Lu, Z-H., Zhao, Y.G. (2010). Suggested empirical models for the axial capacity of circular CFT stub columns. *Journal of Constructional Steel Research*. **66(6)**, 850-862.

Macosko, C. W. (1994). Rheology: principles, measurements and applications Wiley-VCH.

Madandoust, R., Mohseni, E., Mousavi, S. Y., Namnevis, M. (2015). An experimental investigation on the durability of self-compacting mortar containing nano-SiO_2, nano-Fe2O3 and nano-CuO. *Construction and Building Materials*. **86**, 44-50.

Majumdar, A.J. (1974). The role of the interface in glass fibre reinforced cement. *Cement and Concrete Research*. **4(2)**, 247-268.

Manz, O.E. (1999). Coal fly ash: a retrospective and future look. Fuel. **78(2)**, 133-136.

McGraw-Hill Concise Encyclopedia of Engineering. (2002). McGraw-Hill Companies, Inc. Retrieved Novamber 1, 2014, from http://encyclopedia2.thefreedictionary.com/composite+beam">composite beam.

Mehta, P. K, Monteiro, P. J. M. (2006). Microstructure, properties and materials. 3rd edn. McGraw-Hill, London.

Mirza, F.A., Soroushian, P. (2002). Effects of alkali-resistant glass fiber reinforcement on crack and temperature resistance of lightweight concrete. *Cement and Concrete Composites*. **24(2)**, 223-227.

Mohamed, H.A. (2011). Effect of fly ash and silica fume on compressive strength of self-compacting concrete under different curing conditions. *Ain Shams Engineering Journal*. **2(2)**, 79-86.

Mohammed, M.K., Dawson, A.R., Thom, N.H. (2013). Production, microstructure and hydration of sustainable self-compacting concrete with different types of filler. *Construction and Building Materials*. **49**, 84-92.

Muciaccia, G., Giussani, F., Rosati, G., Mola, F. (2011). Response of self-compacting concrete filled tubes under eccentric compression. *Journal of Constructional Steel Research.* **67**, 904-916.

Mukharjee, B.B., Barai, S.V. (2014). Influence of nano-silica on the properties of recycled aggregate concrete. *Construction and Building Materials*. **55**, 29-37.

Naik, B.T.R., Chun, Y., Kumar, R., Ramme, B.W. (2004). Development of high-strength self-consolidating concrete. *Center for By-Products Utilization*. Report No. CBU-2003-14. March, 2004.

Naik, T., Singh, S., Hassaballah, A. (1992). Effects of water to cementitious ratio on compressive strength of cement mortar containing fly ash. CANMET-EPRI Sponsored Fourth International Conference on Fly Ash, Silica Fume, Slag and Natural Pozzolans in Concrete, Istanbul, Turkey.

Naik, T.R., Kumar, R., Ramme, B.W.F. Canpolat, F. (2012). Development of high-strength, economical self-consolidating concrete. *Construction and Building Materials*. **30**, 463–469.

Najigivi, A., Khaloo, A., Zad, A.I., Rashid, S.A. (2013). Investigating the effects of using different types of SiO_2 nanoparticles on the mechanical properties of binary blended concrete. *Composites Part B: Engineering*. **54**, 52-58.

Nazari, A., Riahi, S. (2011a). The effects of SiO_2 nanoparticles on physical and mechanical properties of high strength compacting concrete. *Composites Part B: Engineering*. **42(3)**, 570-578.

Nazari, A., Riahi, S. (2011b). Abrasion resistance of concrete containing SiO_2 and Al2O3 nanoparticles in different curing media. *Energy and Buildings*. **43**, 2939-2946.

Nehdi, M., Rahman, M. A. (2004). Effect of geometry and surface friction of test accessory on oscillatory rheological properties of cement pastes. *ACI Materials Journal*. **101(5)**, 416-424.

Neville, A. (1995). Properties of Concrete. Longman, London.

Niewiadomski, P., Cwirzeń, A., Hoła, J. (2015). The influence of an additive in the form of selected nanoparticles on the physical and mechanical characteristics of self-compacting concrete. *Procedia Engineering*. **111**, 601-606.

Nik, A.S., Omran, O.L. (2013). Estimation of compressive strength of self-compacted concrete with fibers consisting nano-SiO_2 using ultrasonic pulse velocity. *Construction and Building Materials*. **44**, 654-662.

Nili, M., Ehsani, A. (2015). Investigating the effect of the cement paste and transition zone on strength development of concrete containing nanosilica and silica fume. *Material and Design*. **75**, 174-183.

Nili, M., Ehsani, A., Shabani, K. (2010). Influence of Nano-SiO_2 and Microsilica on Concrete Performance. Proc. Second International Conference on Sustainable Construction and Building Materials and Technologies.

Noumowe, A., Carre, H., Daoud, A., Toutanji, H. (2006). High-strength self-compacting concrete exposed to fire test. *Journal of Materials in Civil Engineering*. **18(6)**, 754-808.

Oh, B. H., Cha, S. W., Jang, B. S., Jang, S. Y. (2002). Development of high-performance concrete having high resistance to chloride penetration. *Nuclear Engineering and Design*. **212**, 221-231.

Okamura, H, Ouchi, M. 1997. Self-compacting high-performance concrete. *Concrete International*. **19(7)**, 50-54.

Okamura, H., Ouchi, M. (2003). Self-Compacting Concrete. *Journal of Advanced Concrete Technology*. **1(1)**, 5-15.

Owsiak, Z., Grzmil, W. (2015). The evaluation of the influence of mineral additives on the durability of self-compacting concretes. *KSCE J Civil Engineering*. **19(4)**, 1002-1008.

Öz, H.Ö. (2014). Properties of self-compacting concretes made with cold bonded fly ash lightweight aggregates. *Ph.D Thesis*. Gaziantep University, Turkey.

Park, S.H., Kim, D.J., Ryu, G.S., Koh, K.T. (2012). Tensile behavior of Ultra High Performance Hybrid Fiber Reinforced Concrete. *Cement and Concrete Composites*. **34(2)**, 172-184.

Patel, V. I., Liang, Q. Q., Hadi, M. N. S. (2014). Behavior of biaxially-loaded rectangular concrete-filled steel tubular slender beam-columns with preload effects. *Thin-Walled Structures.* **79**, 166-177.

Pathak, N., Siddique, R. (2012). Effects of elevated temperatures on properties of self-compacting-concrete containing fly ash and spent foundry sand. *Construction and Building Materials*. **34**,512-521.

Perea, T. (2010). Analytical and experimental study on slender concrete-filled steel tube columns and beam-columns. *Ph.D Thesis.* Georgia Institute of Technology.

Pereira, E.N.B., Barros, J.A.O., Ribeiro, A.F., Camões, A. (2004). Post-cracking behaviour of selfcompacting steel fibre reinforced concrete. *International RILEM symposium on fibre reinforced concrete, 6, Varenna*. 1-10.

Persson, B. (2004). Fire resistance of self-compacting concrete. *Material and Structures*. **37(273)**, 575-584.

Qing, Y., Zenan, Z., Deyu, K., Rongshen, C. (2007). Influence of nano-SiO2 addition on properties of hardened cement paste as compared with silica fume. *Construction and Building Materials*. **21(3)**, 539-545.

Quercia, G., Brouwers, H. J. H. (2010). Application of nano-silica (nS) in concrete mixtures. *8th fib PhD Symp*. 431-436.

Quercia, G., Hüsken, G., Brouwers, H.J.H. (2012). Water demand of amorphous nano silica and its impact on the workability of cement paste. *Cement and Concrete Research*. **42**, 344-357.

Qureshi, L.A, Ahmed, A. (2013). An investigation on strength properties of glass fiber reinforced concrete. *International Journal of Engineering Research and Technology*. **2(4)**, 2567-2572.

Reddy, L.R.P., Munireddy, M.G., Prasad, M.L.V. (2013). Effect of glass fiber on mechanical properties of vibrated concrete and self-compacting concrete. *International Journal of Engineering & Science Research*. **4(10)**, 760-765.

Reinhardt, H.W., Stegmaier, M. (2006). Self-consolidating concrete in fire. *ACI Materials Journal*. **103(2)**, 130-135.

Richard Liew, J.Y., Xiong, M., Xiong, D. (2016). Design of concrete filled tubular beam-columns with high strength steel and concrete. *Structures.* **8**, 213-226.

RILEM 50-FMC. Committee of fracture mechanics of concrete. (1985). Determination of fracture energy of mortar and concrete by means of three-point bend tests on notched beams. *Materials and Structures.* **18(106)**, 285-290.

RILEM TC 162-TDF. (2002). Test and design methods for steel fibre reinforced concrete: Bending test. *Materials and Structures*. **35**, 579-582.

RILEM TC 188-CSC. (2006). Casting of self compacting concrete. *Materials and Structures*. **39(10)**, 937-954.

Roik, K., Bergmann, R. (1989). Report on Eurocode 4, clause 4.8 and 4.9. Composite columns harmonization of European construction codes. Minister fur Raumordnung, Bauwesen und Stadtebau der Bundesrepublik Deutschland, Bochum, Germany.

Rui, X., Zhean, L., Zhigang, R., Chunguang, H. (2012). Experimental research on the performance of microexpansion and self-compacting concrete-filled steel tubular short column under axial compression. Procedia *Earth and Planetary Science 5*. 19-24.

Saak, A. W., Jennings, H. M., Shah, S. P. (2001a). The influence of wall slip on yield stress and viscoelastic measurements of cement paste. *Cement and Concrete Research*. **31(2)**, 205-212.

Saak, A. W., Jennings, H. M., Surendra, P. S. (2001b). New methodology for designing self-compacting concrete. *ACI Materials Journal*. **98(6)**, 429-439.

Şamhâl, E. (2005). Lecture 1.1: Composite Construction. http://web.itu.edu.tr/~haluk/COMPOSITE%201.pdf.

Sanchez, F., Sobolev, K. (2010). Nanotechnology in concrete - A review. *Construction and Building Materials*. **24(11)**, 2060-2071.

Schneider, S.P. (1998). Axially loaded concrete-filled steel tubes. *Journal of Structural Engineering*. **124(10)**, 1125-1138.

Sear, L. K. Dundee University Conference-Global Construction-Ultimate Concrete Opportunities 5 to 7 July 2005 Should you be using more PFA.

Senff, L., Labrincha, J.A, Ferreira, V.M, Hotza, D., Repette, W.L. (2009). Effect of nano-silica on rheology and fresh properties of cement pastes and mortars. *Construction and Building Materials*. **23**, 2487-2491.

Shanmugam, N.E., Swaddiwudhipong, S. (1988). Strength of fibre reinforced concrete deep beams containing openings. *International Journal of Cement Composites and Lightweight Concrete*. **10(1)**, 53-60.

Shi, C. (2004). Effect of mixing proportions of concrete on its electrical conductivity and the rapid chloride permeability test (ASTM C1202 or ASSHTO T277) results. *Cement and Concrete Research*. **34**, 537-545.

Siddique, R. (2004). Performance characteristics of high-volume Class F fly ash concrete. *Cement and Concrete Research*. **34(3)**, 487-493.

Singh, L.P., Karade, S.R., Bhattacharyya, S. K., Yousuf, M. M., Ahalawat, S. (2013). Beneficial role of nanosilica in cement based materials - A review. *Construction and Building Materials*. **47**, 1069-1077.

Skarendahl, A., Petersson, O. (1999). International Union of Testing and Research Laboratories for Materials and Structures., and Y. SHIMOVAMA, 1st International

RILEM Symposium on Self-Compacting Concrete : Stockholm, Sweden, September. RILEM Publications.

Sonebi, M., García-Taengua, E., Hossain, K.M.A., Khatib, J., Lachemi, M. (2015). Effect of nanosilica addition on the fresh properties and shrinkage of mortars with fly ash and superplasticizer. Construction and Building Materials. **84**, 269-276.

Tangpagasit, J., Cheerarot, R., Jaturapitakkul, C., Kiattikomol, K. (2005). Packing effect and pozzolanic reaction of fly ash in mortar. Cement and Concrete Research. **35(6)**, 1145-1151.

Tao, Z., Han, L.H. (2006). Behaviour of concrete-filled double skin rectangular steel tubular beam–columns. *Journal of Constructional Steel Research*. **62**, 631-664.

Tao, Z., Han, L.H., Wang, D.Y. (2008). Strength and ductility of stiffened thin-walled hollow steel structural stub columns filled with concrete. Thin-Walled Structures. **10(46)**, 1113-1128.

Tao, Z., Uy, B., Han, L.H., Wang, Z.B. (2009). Analysis and design of concrete-filled stiffened thin-walled steel tubular columns under axial compression. *Thin-Walled Structures*. **47(12)**, 1544-1556.

Tassew, S.T., Lubell, A.S. (2014). Mechanical properties of glass fiber reinforced ceramic concrete. *Construction and Building Materials*. **51**, 215-224.

Tavakoli, H. R., Omran, O. L., Kutanaei, S. S., Shiade, M. F. (2014). Predication of energy absorption capability in fiber reinforced self-compacting concrete containing nano-silica particles using artificial neural network. *Latin American Journal of Solids and Structures*. **11**, 966-979.

Thomas, M.D.A., Matthews,J.D. (2004). Performance of pfa concrete in a marine environment-10- year results. *Cement and Concrete Research*. **26(1)**, 5-20.

Turk, K. (2012). Viscosity and hardened properties of self-compacting mortars with binary and ternary cementitious blends of fly ash and silica fume. *Construction and Building Materials*. **37**, 326-334.

Uy, B., Das, S. (1999). Bracing of thin walled steel box columns during pumping of wet concrete in tall buildings. *Thin-Walled Structures*. **33(2)**, 127-154.

Uysal, M., Sumer, M. (2011). Performance of self-compacting concrete containing different mineral admixtures. *Construction and Building Materials*. **25(11)**, 4112-4120.

Uysal, M., Yilmaz, K. (2011). Effect of mineral admixtures on properties of self-compacting concrete. *Cement and Concrete Composites*. **33(7)**, 771-776.

Wallevick, J. E. (2003). Rheology of particle suspension: fresh concrete, mortar and cement paste with various types of lignosulfates. *Ph.D Thesis*. The Norwegian University of Science and Technology (NTNU), Trondheim, Norway.

Wang, Y. C. (2003). Composite columns. Edited by Nethercot, DA, Spon Press, 2003.

Wang, Y., Chen, J., Geng, Y. (2015). Testing and analysis of axially loaded normal-strength recycled aggregate concrete filled steel tubular stub columns. *Engineering Structures*. **86**, 192-212.

Wang, Y.C. (2014). Design guide for concrete filled hot finished structural hollow section (SHS) columns. www.steelconstruction.info/File:CFT_Design_Guide_March_2014.pdf? internal_link

Xie, Y.B., Liu, B., Yin, J., Zhou, S. (2002). Optimum mix parameters of high-strength self-compacting concrete with ultrapulverized fly ash. *Cement and Concrete Research*. **32(3)**, 477-480.

Yazıcı, H. (2008). The effect of silica fume and high-volume class C fly ash on mechanical properties, chloride penetration and freeze–thaw resistance of self-compacting concrete. *Construction and Building Materials*. **22(4)**, 456-462.

Yu, K., Yu, J., Lu, Z., Chen, Q. (2016). Fracture properties of high-strength/high-performance concrete (HSC/HPC) exposed to high temperature. *Materials and Structures*. **49(11)**, 4517-4532.

Yuan, W.B, and Yang J.J. (2013). Experimental and numerical studies of short concrete-filled double skin composite tube columns under axially compressive loads. *Journal of Constructional Steel Research*. **80**, 23-31.

Zeghiche, J., Chaoui, K. (2005). An experimental behaviour of concrete-filled steel tubular columns. *Journal of Constructional Steel Research*. **61(1)**, 53-66.

Zhang, M. H., Islam, J., Peethamparan, S. (2012). Use of nano-silica to increase early strength and reduce setting time of concretes with high volumes of slag. *Cement and Concrete Composites*. **34(5)**, 650-662.

Zhu, M., Liu, J., Wang, Q., Feng, X. (2010). Experimental research on square steel tubular columns filled with steel-reinforced self-consolidating high-strength concrete under axial load. *Engineering Structures*. **32**, 2278-2286.

PERSONAL INFORMATION

Full name: Yahya Resan ATEWI

Nationality: Iraqi

Birth place and date: Thi-Qar , 1976

Marital status: Married, 3 children

Phone number: 5395677735

Email: yahya.atewi@mail2.gantep.edu.tr, yahyaresan976@gmail.com

EDUCATION

Degree	**Graduate school**	**Year**
Master	Civil Engineering Dep., Al-Mustansiriya University, Baghdad, Iraq	2007
Bachelor	Civil Engineering Dep., Al-Mustansiriya University, Baghdad, Iraq	1998
High school	Alshatrah for boys	1994

WORK EXPERIENCE

2003-2007	Engineer	Thi-Qar University Presidency, Thi-Qar, Iraq
2007-Present	Assistant lecturer	Thi-Qar University Presidency, Thi-Qar, Iraq

FOREIGN LANGUAGE

Arabic (Mother language), English

HOBBIES

Traveling, Reading